

Dissertation zur Erlangung des Doktorgrades
der Fakultät für Chemie und Pharmazie
der Ludwig-Maximilians-Universität München

**Subversion of Toll-like receptor 7/9 signaling
by Measles virus – V holds the key**



Christian Karl Pfaller

aus

Berching

2009

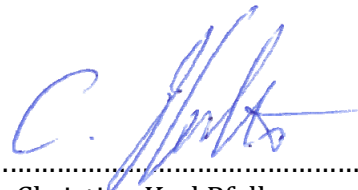
Erklärung

Diese Dissertation wurde im Sinne von § 13 Abs. 4 der Promotionsordnung vom 29. Januar 1998 von Herrn Professor Dr. Karl-Klaus Conzelmann und von Herrn Professor Dr. Karl-Peter Hopfner vor der Fakultät für Chemie und Pharmazie vertreten.

Ehrenwörtliche Versicherung

Diese Dissertation wurde selbständig, ohne unerlaubte Hilfe erarbeitet.

München, am 22.12.2009



.....
Christian Karl Pfaller

Dissertation eingereicht am:	22.12.2009
1. Gutachter:	Prof. Dr. Karl-Klaus Conzelmann
2. Gutachter:	Prof. Dr. Karl-Peter Hopfner
Mündliche Prüfung am:	25.02.2010

"Thought alone is without profit;

It is much better to study."

Chinesisches Sprichwort

Danksagung

Allen voran danke ich Herrn Prof. Dr. Karl-Klaus Conzelmann, in dessen Labor diese Arbeit entstanden ist. Er hat es in jeder Situation verstanden, mich und diese Arbeit zum Ziel zu führen und hat mir stets Gelegenheit zur persönlichen Entfaltung gegeben.

Ganz herzlich danke ich Herrn Prof. Dr. Karl-Peter Hopfner, der sich ohne zu zögern bereit erklärt hat, diese Arbeit vor der Fakultät zu vertreten und als Zweitgutachter aufzutreten.

Ich danke den Herren Prof. Dr. Roland Beckmann, Prof. Dr. Klaus Förstemann, Prof. Dr. Patrick Cramer und Dr. Dietmar Martin für ihre Bereitschaft, die Promotionskommission zu bilden.

Ich danke meiner Arbeitsgruppe für die aufregenden vier Jahre zwischen Humor und Wahnsinn. Laetitia, hab' Dank für die exzellente Zusammenarbeit im Autophagie-Projekt und die schönen Stunden mit „Wein und Käse“ aus Frankreich. *Merci bien!* Anika, dir danke ich für die erbaulichen Busfahrdiskussionen, die mich immer wieder aufgerichtet haben, wenn's mal nicht so gut war. Nadin, dir danke ich für deine unersetzliche Kompetenz im Tollwut-Rescue und die viele Hilfe, die du mir geboten hast. Alex, Kerstin, Lisa und Martina danke ich für die schöne Atmosphäre im Labor. Ich danke auch allen, die uns in der Zwischenzeit verlassen haben: Kris, Yvonne und Christine; sowie Adriane, die in der Zeit des Paper- und Zusammenschreibens meine Leidensgenossin war. Dank auch an meine „Praktikanten“ Konstantin und Dominik Z., die wichtige Teile zu dieser Arbeit während ihrer Bachelorarbeit bzw. ihrem Praktikum beigetragen haben.

Ich danke den Jungs meiner DSA-Runde, Daniel, Ben, Benno und Konstantin, die mich immer zur richtigen Zeit auf andere Gedanken gebracht haben. Besonders du, Daniel, hast dich in den letzten Jahren zu einem wichtigen Freund entwickelt.

Schließlich danke ich meiner Mutter Elfriede, meinem Bruder Michael, sowie Horst dafür, dass sie während der langen Zeit des Studiums bis heute immer für mich da waren, mich allzeit unterstützt haben und stets ein offenes Ohr für meine Probleme hatten, aber auch mit mir meine Freude geteilt haben.

Contents

List of publications	viii
List of abbreviations	ix
List of figures and tables	xii
1 Introduction	1
1.1 Measles virus.....	1
1.1.1 Taxonomy and molecular basics of measles virus.....	1
1.1.2 Pathogenicity and control of measles virus.....	5
1.2 Immune response to measles virus infection	7
1.2.1 The Interferon system of the innate immune response.....	7
1.2.2 MV specific adaptive immune response.....	13
1.2.3 Immunosuppression and immune antagonistic functions of MV	15
1.3 Aims of this thesis.....	16
2 Materials and Methods	17
2.1 Materials	17
2.1.1 Chemicals.....	17
2.1.2 Kits.....	19
2.1.3 Enzymes	20
2.1.4 Recombinant proteins and peptides.....	20
2.1.5 Antibodies	20
2.1.6 Oligonucleotides.....	21
2.1.7 Cell lines and media	24
2.1.8 Viruses	25
2.1.9 Plasmids and bacteria	26
2.1.10 Buffers and solutions.....	29
2.1.11 Equipment.....	33
2.1.12 Miscellaneous	34
2.2 Methods.....	36

2.2.1	Molecular biological methods.....	36
2.2.1.1	Cloning and mutagenesis.....	36
2.2.1.2	Working with bacteria	39
2.2.1.3	Plasmid preparation	40
2.2.1.4	Sequencing	41
2.2.1.5	RNA isolation.....	41
2.2.2	Cell biological and virological methods.....	41
2.2.2.1	Cell culture	41
2.2.2.2	Isolation and cultivation of bone marrow derived cells (BMDCs).....	42
2.2.2.3	Transfection	43
2.2.2.4	Infection assays.....	43
2.2.2.5	Generation of MV stocks	43
2.2.2.6	Generation of RV stocks	44
2.2.2.7	Generation of recombinant RV (helper virus free)	44
2.2.2.8	Titration of virus stocks	45
2.2.3	Biochemical and immunological methods	46
2.2.3.1	Luciferase reporter gene assays	46
2.2.3.2	Co-Immunoprecipitation	46
2.2.3.3	Denaturing Polyacrylamid (PAA)-gel electrophoresis.....	47
2.2.3.4	Western blot (Semi dry method).....	48
2.2.3.5	Immunodetection.....	48
2.2.3.6	Immunofluorescence (IF)	49
2.2.3.7	Enzyme-linked immunosorbent assay (ELISA)	50
2.2.3.8	Expression and Ni-NTA purification of recombinant proteins from bacteria.....	50
2.2.3.9	<i>In vitro</i> kinase assays.....	51
2.2.3.10	<i>In vivo</i> ³² P-labelling	52
2.2.3.11	Northern blot	52
3	Results	54
3.1	Reconstitution of MyD88-dependent induction of IFN α in cell lines and establishment of luciferase reporter gene assays.....	54
3.2	Identification of V as inhibitor of MyD88-dependent induction of IFN α	56
3.3	Identification of interaction partners of V	59
3.4	Identification of the V interaction domain.....	60

3.5	Influence of V on activation of IRF7 by IKK α	62
3.6	Inhibition of both inactive and active IRF7 by V	68
3.7	Infection studies of primary BMDC with recombinant rabies viruses expressing MV P, V, or C	70
3.8	Analysis of V of different strains – search for IFN α -ineffective V mutants.....	74
3.9	Sequential and mutational analysis of <i>paramyxoviral</i> V proteins	79
3.10	MV V peptides	87
3.11	Functions of MV V in NF- κ B activation	88
3.12	Control of autophagy by Measles virus.....	90
4	Discussion	93
4.1	Mechanism of the inhibition of IFN α induction by MV V.....	93
4.2	Interaction of MV with pDCs	97
4.3	MV induced immunosuppression and impact of IFN α inhibition.....	101
4.4	Components of the TLR7/9 signaling complex.....	102
4.5	Inhibition of TLR7/9 signaling by the MV C protein	103
4.6	Future perspectives	104
5	Summary.....	106
5	Zusammenfassung.....	108
6	References.....	111
7	Appendices.....	121
A	Complete sequence alignment of <i>paramyxoviral</i> N proteins.....	121
B	Complete sequence alignment of <i>paramyxoviral</i> V proteins.....	127
8	Curriculum vitae	133

List of publications

Parts of this thesis have been published or will be published in scientific journals in future.

Original articles:

Schuhmann,K, Pfaller,C.K. and Conzelmann,K.K. (2010). A novel function of the measles virus V protein in signaling inhibition (*working title; in preparation*).

Brzózka´,K., Rieder,M., Pfaller,C.K., Cox,J., Stitz,L. and Conzelmann,K.K. (2010). Genetic dissection of IFN antagonistic functions of rabies virus phosphoprotein: Inhibition of IRF3/7 activation is crucial for pathogenicity (*in preparation*).

Pfaller,C.K. and Conzelmann,K.K. (2008). Measles virus V protein is a decoy substrate for I κ B kinase alpha and prevents Toll-like receptor 7/9-mediated interferon induction. *J. Virol.* 82, 12365-12373.

Review article:

Brzózka,K., Pfaller,C., and Conzelmann,K.K. (2007). Signal transduction in the type I interferon system and viral countermeasures. *Signal Transduction* 7, 5-19.

List of abbreviations

Full protein names and names of viruses are written in the text when mentioned first. Abbreviations of protein names and viruses are therefore not included in the list below.

°C	degree Celsius; base of temperature
A	Adenin; one of the four bases of DNA and RNA
A	Ampere; SI base of amperage
aa	amino acids
add.	additional
approx.	approximately
ATP	adenosintriphosphate; a nucleotide
BCA	bicinchoninic acid assay
BMDC(s)	bone marrow derived cell(s)
b(p)	base (pairs); unit for the length of DNA/RNA
BSA	bovine serum albumin
c	centi (10 ⁻²)
C	Cytidin; one of the four bases of DNA and RNA
(Co-)IP	(co-)immunoprecipitation
conc.	concentration
CTL(s)	cytotoxic T-lymphocytes
CTP	cytidintriphosphate; a nucleotide
d	day(s)
Δ	delta; deletion
dd	double distilled (deionized and sterilized)
Da	Dalton; unit for the molecular weight of proteins
DNA	deoxyribonucleic acid
ds	double strand(ed)
ECL	enhanced chemiluminescence
ELISA	Enzyme-Linked Immunosorbent Assay
e.g.	<i>exempli gratia</i> ; for example
Fig.	figure
Fl	FLAG®-epitope tag
g	gram; SI base of weight
g	standard gravity
G	Guanine; one of the four bases of DNA/RNA

GST	glutathione-S-transferase-epitope tag
GTP	guanosintriphosphate; a nucleotide
h	hour(s)
His	hexahistidine (6xHis)-epitope tag
HPLC	high pressure liquid chromatography
HRP	horse raddish peroxidase
i.e.	<i>id est</i> ; that is
IF	immunofluorescence
Ig	immunoglobulin-epitope tag
IU	infectious unit; base for infectivity of a virus
IU	international unit; standardized base for activity of a substance
J	Joule; base of energy
k	kilo (10^3)
L	liter; base of volume
LB	lysogeny broth (growth medium for bacteria)
m	meter; SI base of length
μ	mikro (10^{-6})
m	milli (10^{-3})
M	molar; base of concentration
mDC(s)	myeloid dendritic cell(s)
min	minute(s)
mol	mol; SI base of amount of substance
M Φ (s)	macrophage(s)
MOI	multiplicity of infection (proportion of infectious particles and number of cells)
mRNA	messenger RNA
mut	mutant
MW(s)	molecular weight(s)
n	nano (10^{-9})
nt	nucleotide(s)
ODN	oligodeoxynucleotide
o/n	over night
ORF(s)	open reading frame(s)
p	pico (10^{-12})
PAA	poly acrylamide
PBMC(s)	peripheral blood monocyctic cell(s)
pDC(s)	plasmacytoid dendritic cell(s)
p. i.	post infection
p. tr.	post transfection
RNA	ribonucleic acid
rpm	rotations per minute
rRNA	ribosomal RNA
R.T.	room temperature (approx. 25 °C)
ss	single strand(ed)

T	tymidin; one of the four bases of DNA
Th(1/2)	T-helper cell (type 1 or 2)
TTP	tymidintriphosphate; a nucleotide
U	uridin; one of the four bases or RNA
U	unit(s)
UTP	uridintriphosphate; a nucleotide
V	Volt; SI base of voltage
v/v	volume per volume
WB	Western blot
wt	wild type
w/v	weight per volume

List of figures and tables

Figure 1:	Measles virus, gene expression and replication.	2
Figure 2:	MV P gene and products P, V and C.	4
Figure 3:	Model of MV infectious route.	6
Figure 4:	Pathways of IFN induction and NF- κ B activation by TLRs and RLRs.	9
Figure 5:	Type-I and Type-II IFN signaling pathways.	12
Figure 6:	Immune response to MV infection in vivo.	14
Figure 7:	Reconstitution of the MyD88-dependent signaling complex leading to the induction of IFN α in cell lines.	55
Figure 8:	Identification of the viral antagonist of IFN α induction.	57
Figure 9:	Identification of interaction partners of MV V.	59
Figure 10:	Identification of the MV V interaction domain.	61
Figure 11:	Purification of recombinant proteins from <i>E. coli</i> .	63
Figure 12:	Inhibition of phosphorylation of IRF7 by IKK α in the presence of V.	64
Figure 13:	<i>In vitro</i> kinase assay with truncated MV V and P and kinases IKK α , IKK β , and TBK1.	66
Figure 14:	MV V, but not P is able to inhibit IRF7-phosphorylation <i>in vitro</i> .	67
Figure 15:	Inhibition of active IRF7 by MV V.	68
Figure 16:	Generation and characterization of recombinant rabies viruses expressing MV P, V, or C.	71
Figure 17:	IFN α production in murine bone marrow-derived pDCs.	73
Figure 18:	V protein amino acid sequence comparison of different MV strains.	75
Figure 19:	Analysis of V mutants for their capacity to inhibit IFN α induction and type-I IFN signaling.	77
Figure 20:	Amino acid sequence comparison of V from different <i>Paramyxovirinae</i> .	79
Figure 21:	Sequence comparison of MV V _C and <i>rubulaviral</i> V _C and homology modelling of MV V _C based on the PIV5 V _C structure.	80
Figure 22:	Inhibition of IFN α induction by MV and PIV5 V mutant proteins.	84

Figure 23:	Inhibition of IFN α induction by Box1 and Box2 mutants of MV V	85
Figure 24:	MV V peptides.	86
Figure 25:	Effects of MV V on NF- κ B activation.	89
Figure 26:	Effect of MV infection on the activation of autophagy.	91
Figure 27:	Model of the inhibitory mechanism of MV V.	94
Figure 28:	Model of TLR7/8/9 signaling, JAK/STAT signaling and autophagy.	100
Table 1:	Nucleotide mutations introduced into MV(Schwarz) V to generate specific aa mutants.	76
Table 2:	Nucleotide mutations introduced into MV(Schwarz) V to generate specific <i>rubulavirus</i> analog mutants.	83

1 Introduction

1.1 Measles virus

1.1.1 Taxonomy and molecular basics of measles virus

Measles virus (MV) is a member of the genus *Morbillivirus* in the family of *Paramyxoviridae* (subfamily: *Paramyxovirinae*). It is a virus with a small non-segmented negative ssRNA genome (approx. 16 kb), encoding 6 genes (Fig. 1A). Due to their genomes, viruses from the family of *Paramyxoviridae* and the families of *Rhabdoviridae*, *Bornaviridae*, and *Filoviridae* form the order of *Mononegavirales* (non-segmented negative strand RNA viruses = NNSV).

The genes are arranged in 3' to 5' direction of the genome in the following order: the N gene (approx. 1.7 kb), which encodes for the nucleoprotein (N; 58 kDa), the P gene (approx. 1.7 kb) encoding the phosphoprotein (P; 54 kDa), as well as the two non-structural proteins V (32 kDa) and C (21 kDa), the M gene (approx. 1.5 kb), encoding the matrix protein (M; 38 kDa), the F gene (approx. 2.4 kb), encoding the fusion protein (F; 60 kDa), the H gene (approx. 2.0 kb), encoding the hemagglutinin protein (H; 69 kDa), and the L gene (approx. 6.6 kb), encoding the large protein (L; 247 kDa). The genome is flanked by two small regions encoding the viral promoters called “leader region” (genomic promoter at the 3' end of the genome; 55 nt) and “trailer region” (antigenomic promoter at the 3' end of the antigenome; 37 nt).

MV emerges in eight clades (A, B, C, D, E, F, G, and H) which include up to now 23 genotypes (reviewed in (Rota et al., 2009)). However, all viruses share the same serotype.

The virus forms pleiomorphic and polypliod particles (Fig. 1B and C), consisting of a ribonucleoprotein complex (RNP), which is enwrapped by a lipid envelope.

The RNP is composed of the viral genomic RNA and the N protein, which encloses the RNA (6 nt/ N protein monomer). The genomic RNA strictly follows the “rule of six”, which means that the genome must be of polyhexameric length ($6n+0$; reviewed in (Kolakofsky et al., 2005)). P and L, which together form the viral RNA-dependent RNA polymerase (RdRp) are associated to the RNP. The M protein connects the RNP to the lipid envelope with the two viral transmembrane glycoproteins F and H, which are responsible for viral entry into host cells.

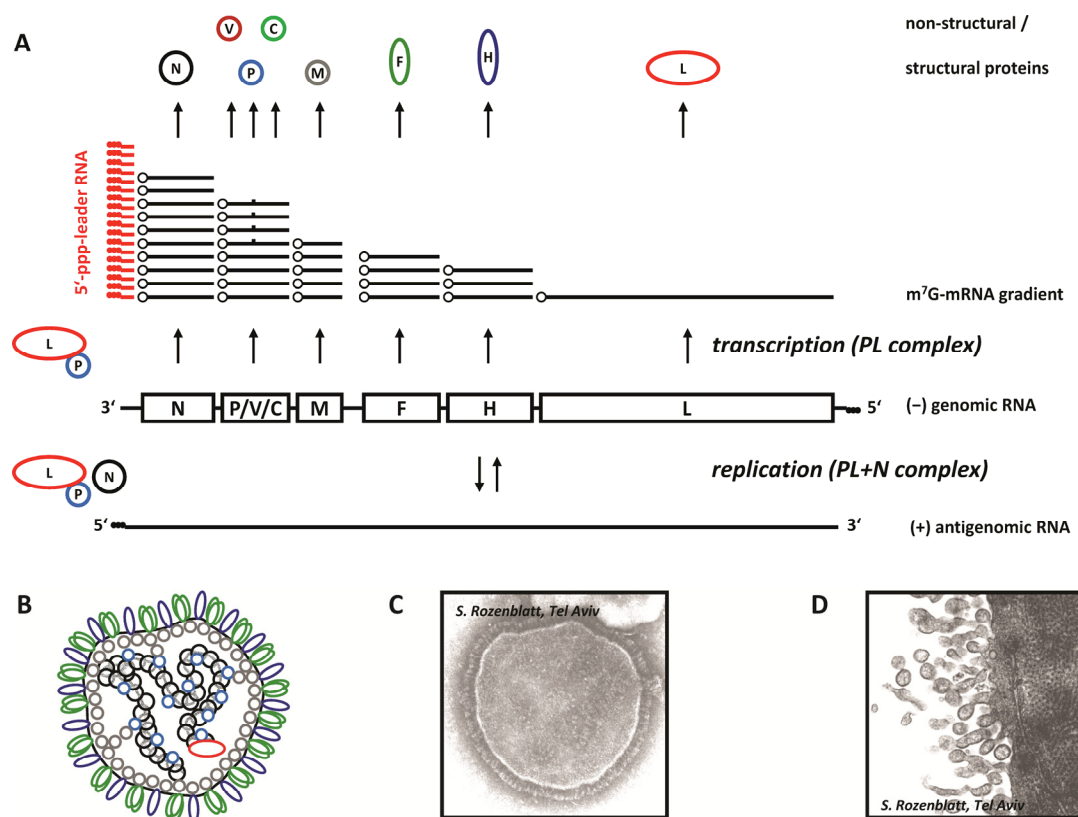


Figure 1: Measles virus, gene expression and replication.

(A) Schematic presentation of the MV genome, mRNA transcription gradient, structural (N, P, M, F, H, and L) and non-structural proteins (V, C) derived from the different genes, and replication cycle with antigenome intermediate. (B) Schematic MV particle. The RNP is composed of genomic RNA and N, and associated with P and L. The lipid envelope harbours homotrimers of F associated with H. M is located at the inner membrane and connects the RNPs to the envelope. (C) Electron micrograph of a MV particle. Published by S. Rozenblatt, Tel Aviv. (D) Electron micrograph of emerging MV particles. Published by S. Rozenblatt, Tel Aviv.

Upon infection, H protein dimers bind to cellular entry receptors. These receptors are, as yet identified, the signaling lymphocytic activation molecule (SLAM; or CD150; (Tatsuo et al., 2000)), or the membrane cofactor protein (MCP; or CD46; (Dörig et al., 1993; Naniche et al., 1993)). Recent publications suggest the existence of a third entry receptor, which is a so far uncharacterized epithelial cell receptor (EpR; (Takeda et al., 2007; Tahara et al., 2008)). The F protein mediates the fusion of cellular and viral membranes in a class I fusion reaction (reviewed in (Kielian and Rey, 2006; Yin et al., 2006)), leading to the release of the RNP into the cytoplasm.

There, viral gene expression and replication take place (reviewed in (Rima and Duprex, 2009)). The P/L polymerase complex first transcribes the viral genes, thereby generating 5'-capped and 3'-polyadenylated mRNAs from each gene (Fig. 1A). In addition, the leader region is transcribed into a 5'-triphosphorylated leader RNA (MV leader). Transcription takes place in a sequential way, meaning that most proximal genes (to the 3' end of the genome) are transcribed to a higher extent than more distal genes, resulting in a mRNA gradient. The mRNAs are translated into proteins by the cellular translation machinery. At one point, that might be determined by the availability of newly synthesized N protein, the P/L complex switches from transcription to replication mode. Full length antigenomic RNA is generated in a continuous polymerization reaction starting with the MV leader. The antigenomic RNA is enwrapped immediately by N and serves again as a template for replication and production of new genomic RNA. The newly synthesized RNPs are transported to the cell membrane. The M protein is thought to mediate this transport and the subsequent virus assembly at sites of the cell membrane, where F and H are incorporated. Finally, the budding process (Fig. 1D) completes the viral replication cycle.

A typical characteristic of MV infection *in vitro* and also *in vivo* is the formation of multi-nucleated giant cells (= syncytia (Bunting, 1950; Black et al., 1956)) which are formed upon fusion of infected cells with non-infected cells in a F and H mediated manner (Wild et al., 1991).

The P gene exhibits a special feature: While all the other genes encode only for a single protein, the P gene encodes for three proteins (Fig. 2A). Two alternative ORFs give rise to the P or to the C protein. These ORFs are translated via ribosomal scanning, where the ribosomes do not necessarily use the first start codon to initiate translation (P protein), but a start codon more downstream (C protein). Furthermore, the viral polymerase is able to perform RNA editing. This function leads to the cotranscriptional insertion of non-coding nucleotides into the mRNA. In case of MV, an additional G is inserted between nt position 748/749 of the P mRNA (Fig. 2B). The insertion leads to a shift in the ORF and gives rise to a modified gene product, called V protein. P and V share a common N-terminal domain, consisting of 231 amino acids. The C-termini of P (276 aa) and V (68 aa) are completely individual. The V C-terminus is highly conserved among the family of *Paramyxoviridae* and forms a unique Zn-binding motif (Liston and Briedis, 1994). All viruses from the subfamily of *Paramyxovirinae* are able to edit the mRNA of the P gene. However, some insert not only one G residue, but two or more (for review see

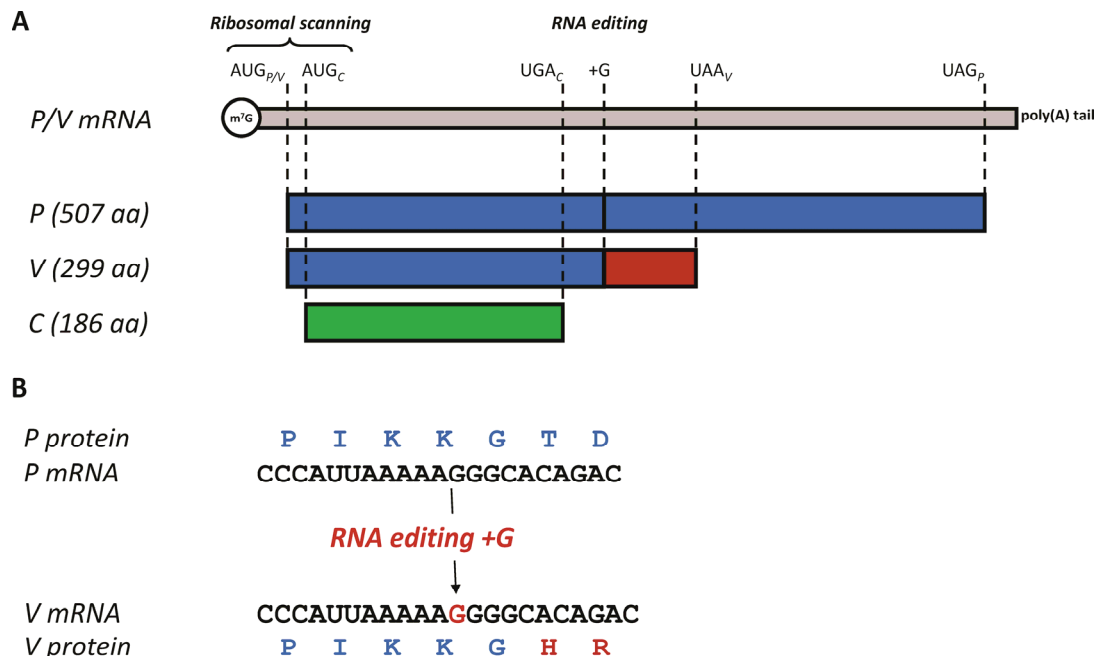


Figure 2: MV P gene and products P, V and C.

(A) Schematic representation of the MV P mRNA and location of start (P/V; C) and stop codons (C; V; P) as well as RNA editing site. (B) Nucleotide sequence (-11 - +10) of the RNA editing site and corresponding amino acid sequences of P (unedited mRNA; blue amino acids) and V (edited mRNA; red amino acids).

(Kolakofsky et al., 2005)). V and C of MV are known as virulence factors and interferon antagonists (Gotoh et al., 2001). They are not incorporated into the virus particle.

1.1.2 Pathogenicity and control of measles virus

Measles virus is a highly contagious pathogen that is restricted almost exclusively to humans and some primate species. It is transferred via respiratory droplets and airborne spray and initially infects mucous membranes of the upper respiratory tract (for review see (Naniche, 2009)). Infection with MV causes a characteristic disease (“measles”) with prodromal symptoms like fever, cough, and conjunctivitis at 10 – 12 d p. i., followed by a characteristic rash and high fever. Clearance of the virus occurs around day 7 – 10 after the onset of the rash.

In former times, measles was a major cause of childhood morbidity and mortality. It caused major epidemics among non-immunized native American tribes in the 16th century, when European immigrants brought the virus to North and South America. Although there is a live attenuated virus vaccine available today (Enders et al., 1962), which provides long-term protection from all MV strains (as they share the same serotype), the virus is still a risk factor in developing countries. Still, more than 20,000,000 acute infections with MV are reported annually, with 197,000 deaths due to measles in 2007 (WHO/UNICEF Joint Statement, 2006). More than 95 % of the deaths occur in developing countries in Africa and Asia.

MV is a hematotropic virus preferably infecting and replicating in lymphocytes. The infectious route of MV is still under discussion, as not all open questions are yet solved. One model proposes the infection of dendritic cells (DCs) at the site of initial infection, either directly or via transmission of the virus from the airway epithelium (Fig. 3A). Another option is the use of attachment receptors like DC-SIGN (de Witte et al., 2006) to attach to the surface of migrating DCs. MV might use these cells to enter local lymphatic tissue, where it is transmitted to B and T cells (Fig. 3B). Replication occurs in these cell types, causing a

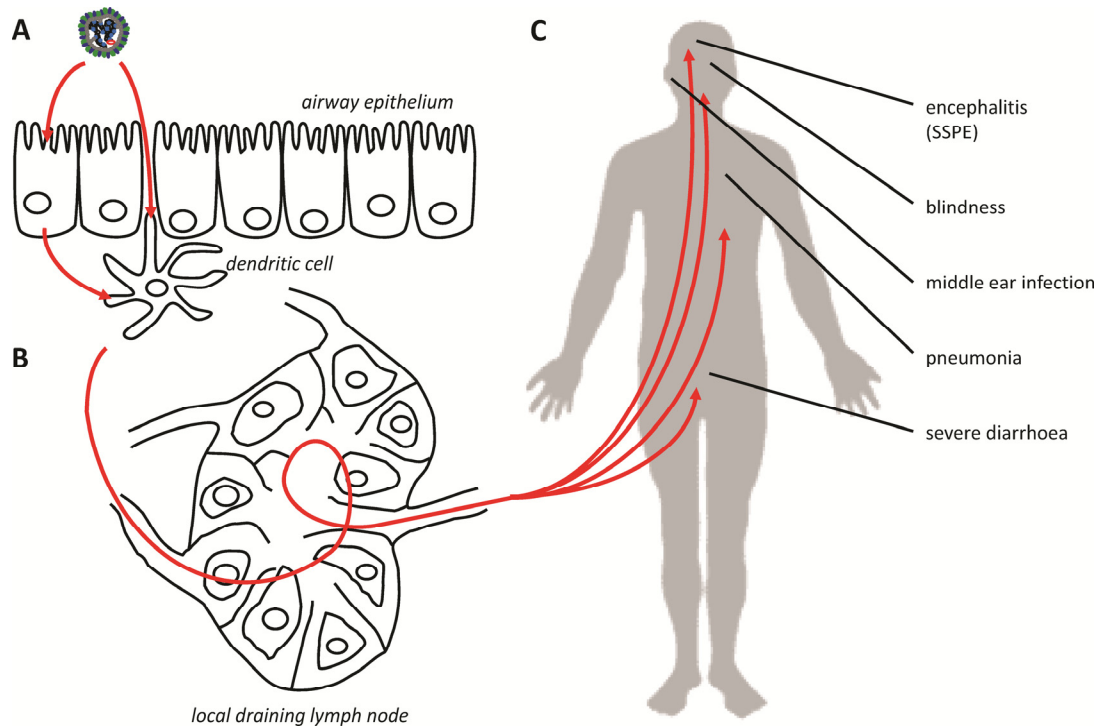


Figure 3: Model of MV infectious route.

(A) Primary infection of airway epithelial cells and/or dendritic cells either directly or via spread from epithelial cells. (B) Migration of infected DCs to local lymph nodes, the source of primary viremia. (C) Dissemination of MV to the whole organism upon onset of rash. Possible complications during infection due to MV include encephalitis, blindness, middle ear infection, pneumonia, and severe diarrhoea.

primary viremia. MV is further transmitted to other lymphoid tissue, and also spleen and liver, where it causes a second viremia. In the last step of infection, the virus disseminates to multiple organs and also to the epithelium of organs and the skin (Fig. 3C). MV infection results in a strong and life-long immunity (section 1.2.2). Apparently contradictory to this, MV causes a strong immunosuppression, which is characterized by lymphopenia, cytokine imbalance, shift of the Th-response towards Th2, and silencing of PBMC (for details see section 1.2.3). Due to this immunosuppressive phenotype, MV infection is closely associated with severe secondary infections, which are the major causes of mortality. Encephalitis, blindness, middle ear infection (*otitis media*), pneumonia, and severe diarrhea are the most prominent diseases (Fig. 3C). MV is also able to infect neurons and therefore can be the cause of diseases of the central nervous system (CNS) by itself. However, these cases are very rare (approx. 1 in 100,000 acute infections). If MV infection occurs in the early

childhood before the adaptive immune response has developed, some strains are able to persist in the host. Up to 15 years after initial infection, these viruses are able to reactivate and cause a slow, progressive disease with fatal outcome. This subacute sclerosing panencephalitis (SSPE) occurs in approx 1 in 10,000 – 300,000 acute infections (Takasu et al., 2003) and manifests in progressive cognitive and motor losses, seizures, and organ failure (reviewed in (Young and Rall, 2009)). Other neuronal diseases resulting from MV infection are postinfectious encephalomyelitis (PIE; (Johnson et al., 1984)), and Measles inclusion body encephalitis (MIBE; reviewed in (Johnson, 1998)).

All these complications emphasize the vaccination of the population against MV. So far, the World Health Organization (WHO) vaccination program resulted in a 74 % drop of MV mortality from the year 2000 (approx. 750,000 cases) to the year 2007 (approx. 197,000 cases) and the goal is to undercut 75,000 cases in 2010 (WHO/UNICEF Joint Statement, 2006; WHO, 2008). This goal is accomplishable especially due to the restriction of MV to human hosts and the lack of animal reservoirs. A comparable success was achieved in 1977, when the vaccination program led to the eradication of the smallpox virus (WHO, 2009). However, a lack of adherence to vaccine recommendations is an increasing problem in industrialized countries (Jansen et al., 2003), especially Germany. Here, in regular periods epidemics occur, like those in Hessen in 2005 (Uphoff and Hauri, 2005), in Baden-Württemberg and Nordrhein-Westfalen in 2006 (Siedler and Santibanez, 2006), in Nordrhein-Westfalen and Bavaria in 2007 (van Treeck, 2007), in Baden-Württemberg and Mecklenburg-Vorpommern in 2008 (Littmann, 2008) and in Nordrhein-Westfalen and Hamburg in 2009 (Jurke, 2009).

1.2 Immune response to measles virus infection

1.2.1 The Interferon system of the innate immune response

Interferons (IFNs) are the most important cytokines involved in the antiviral immune response. These are small proteins, which are grouped into three classes. Type-I IFNs consist of the families of IFN-alpha (IFN α), IFN-beta (IFN β), IFN-tau (IFN τ) and IFN-omega (IFN ω). The family of IFN α is the broadest

amongst type-I IFNs, with 13 different genes: $\alpha 1$, $\alpha 2$, $\alpha 4$, $\alpha 5$, $\alpha 6$, $\alpha 7$, $\alpha 8$, $\alpha 10$, $\alpha 13$, $\alpha 14$, $\alpha 16$, $\alpha 17$, and $\alpha 21$, whereas IFN β is encoded by a single gene only (reviewed in (Pestka et al., 2004)). IFN-gamma (IFN γ) makes up the class of type-II IFNs, whereas the latest family of IFN-lambda IFN λ (IFN $\lambda 1$, IFN $\lambda 2$, IFN $\lambda 3$) is known as type-III IFN (Ank et al., 2006). All types of IFN are produced and secreted by the cell following the activation of distinct signaling pathways upon recognition of non-self pathogen associated molecular patterns (PAMPs) and other danger signals to the cell.

Induction of interferon and proinflammatory cytokines by pattern recognition receptors

PAMP recognition is triggered by cellular pattern recognition receptors (PRRs; for review see (Brzózka et al., 2007; Pichlmair and Reis e Sousa, 2007; Kawai and Akira, 2008; Kumar et al., 2009)). These are grouped in two classes: the first class that has been identified consists of the Toll-like receptors (TLRs; Fig. 4A and B), membrane bound receptors containing leucine-rich repeats (LRRs) and intracellular Toll-interacting region (TIR) domains. Typical PAMPs are viral and bacterial nucleic acids (dsRNA: TLR3; ssRNA: TLR7/8; CpG-DNA: TLR9), or unusual proteins and protein modifications (peptidoglycans: TLR1/2/6; lipopolysaccharide (LPS): TLR4; flagellin: TLR5). Upon ligand binding, the TIR domain is activated and recruits a downstream signaling complex. Nucleic acid recognizing TLR3/7/8/9 are located in endosomal compartments, while all other TLRs are located at the cell surface. The second group of receptors, which also recognizes viral nucleic acids is located in the cytoplasm of cells and consists of a family of homologous helicases known as RIG-I-like receptors (RLRs; Fig. 4C). The first receptor identified is the retinoic acid inducible gene I (RIG-I), a RNA helicase which recognizes 5'-triphosphorylated (5'-ppp) ss/dsRNA (Hornung et al., 2006; Pichlmair et al., 2006; Cui et al., 2008). The melanoma differentiation-associated gene-5 (MDA-5) recognizing a so far unidentified RNA pattern which is contained in RNA of encephalomyocarditis virus (EMCV) and in synthetic poly(I:C), and laboratory of genetics and

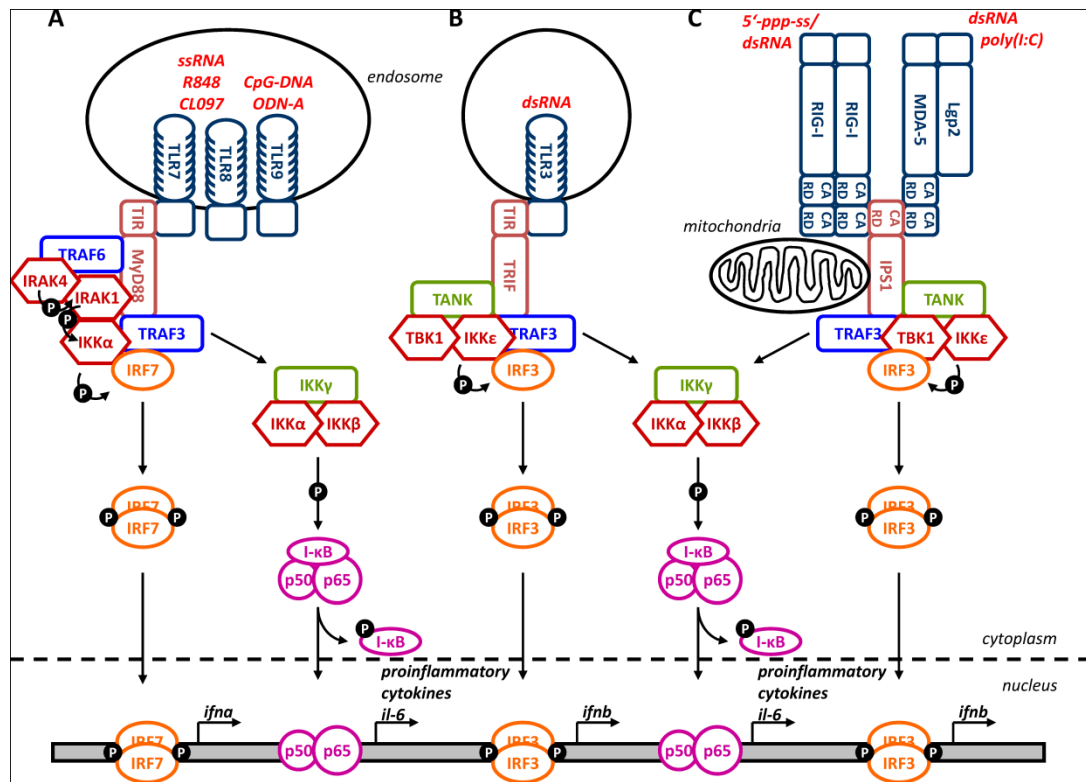


Figure 4: Pathways of IFN induction and NF- κ B activation by TLRs and RLRs.

(A) MyD88-dependent induction of IFN α and activation of NF- κ B by TLR7/8/9. (B) TRIF-dependent induction of IFN β and activation of NF- κ B by TLR3. (C) IPS1-dependent induction of IFN β and activation of NF- κ B by RLRs RIG-I, MDA-5, and Lgp2. *Color code:* dark blue: receptors; dark red: adapter proteins; light red: kinases; light blue: E3 ubiquitin ligases; light green: scaffold proteins/kinases; orange: IRFs; pink: NF- κ B and I- κ B- α ; P: phosphate residue.

physiology 2 (Lgp2) complete this family of RNA helicases (Zou et al., 2009). They share a common architecture with two N-terminal caspase recruitment domains (CARDs), a DExD/H box helicase domain, and a C-terminal regulatory domain (RD). However, Lgp-2 lacks the CARDs. Upon recognition of viral nucleic acids by the RD and activation of the helicase, the CARDs are exposed and fulfill downstream signaling.

The subfamily of TLR7/8/9 uses a common signaling complex (Fig. 4A), which is build up along the TIR-adapter protein myeloid differentiation primary response gene 88 (MyD88; (Honda et al., 2004)). This complex contains the E3 ubiquitin ligases tumor necrosis factor- α receptor associated factor 6 (TRAF6; (Kawai et al., 2004)) and TRAF3 (Oganesyan et al., 2006), the

Serine/Threonin kinases interleukin-1 receptor associated kinase (IRAK) 1 (Uematsu et al., 2005) and IRAK4 (Kim et al., 2007), as well as the inhibitor of kappa-B kinase alpha (IKK α ; (Hoshino et al., 2006)). The transcription factor interferon regulatory factor 7 (IRF7) is recruited to the signaling complex and activated in a concerted phosphorylation cascade (Honda et al., 2005). Upon activation, IRF7 builds homodimers, which translocate to the nucleus and bind to the promoter region of IFN α genes, thereby activating the transcription of multiple IFN α genes.

A second group of proinflammatory cytokines is activated by TLR7/8/9. They are dependent on the activation of the nuclear factor kappa-B (NF- κ B), which consists of two subunits p65 and p50. In the inactive form, NF- κ B is complexed by the inhibitor of kappa-B-alpha (I- κ B- α). Upon TLR activation, a heterotrimeric complex of the kinases IKK α , IKK β , and IKK γ (= NF-kappa-B essential modulator, NEMO) is activated in a MyD88-dependent manner and phosphorylates I- κ B- α . This leads to the degradation of I- κ B- α and the release of NF- κ B. This complex translocates to the nucleus and binds to the promoter regions of proinflammatory genes like interleukin-6 (IL-6).

TLR3, which recognizes dsRNA, uses a different signaling complex compared to TLR7/8/9 (Fig. 4B). The TIR-domain-containing adapter-inducing interferon-beta (TRIF) recruits TRAF3, and a kinase complex which is homologous to the IKK-complex and consists of IKK ϵ , TANK-binding kinase 1 (TBK1), and the TRAF-associated NF- κ B activator (TANK). The kinases are able to activate IRF3, and also IRF7, however, IRF3 is abundantly expressed in contrast to IRF7. Phospho-IRF3 dimers translocate to the nucleus as described for IRF7. IRF3-dimers bind mainly to the promoter of the IFN β gene. NF- κ B is also activated by TLR3.

The cytoplasmic RLRs use a different adapter protein, which is called interferon-beta promoter stimulator 1 (IPS1; Fig. 4C). This protein is also known as mitochondrial antiviral signaling protein (MAVS), virus-induced signaling adapter (VISA) or CARD-adapter inducing interferon-beta (CARDIF). It is located in the outer membrane of mitochondria (Kawai et al., 2005; Lin et al., 2006). RIG-I is thought to homodimerize upon ligand binding (Cui et al.,

2008), while MDA-5 and Lgp2 may act by the formation of heterodimers, which still has to be proven. Upon exposure of the CARDs, these are able to bind to the CARD of IPS1. The signaling complex associated with IPS1 is similar to the TLR3 complex and consists of TRAF3, TANK, TBK1, and IKK ϵ . Other factors were identified recently to be involved (TNFRSF1A-associated via death domain, TRADD; TBK1 binding protein, TBK1BP; (Ryzhakov and Randow, 2007; Michallet et al., 2008)), but their contribution to the activation of IRF3 needs to be clarified. NF- κ B activation is thought to be similar to TLR signaling.

RLRs and the components of their signaling complex, as well as TLR3 are expressed almost ubiquitously in many cell types and therefore are thought to represent a general first line of defense against viral infections. In contrast, TLR7/8/9, and IRF7 are expressed constitutively only in specialized immune cells, the plasmacytoid dendritic cells (pDCs; (Hornung et al., 2002)), or, in other cell types, only after stimulation with IFNs. This places signaling of TLR7/8/9 in a special position at the intersection between innate and adaptive immune response, which will be discussed in section 1.2.2.

While type-III IFN is upregulated by similar pathways as type-I IFN (Ank et al., 2006), type-II IFN induction is different and will not be further explained.

Type-I and type-II interferon signaling (JAK/STAT signaling)

Upon expression, IFNs are secreted by the cell. As most cytokines, they are ligands for specific receptors and can activate the downstream signaling pathways in an autocrine or paracrine manner (Fig. 5). Type-I IFN (IFN α/β) binds to the type-I interferon receptor (or interferon-alpha receptor, IFNAR), which exists on the surface of nearly all cell types (Fig. 5A). This receptor belongs to the group of phospho-tyrosine receptors. Upon ligation, two subunits of the IFNAR (1/2) dimerize and form an intracellular signaling complex. Recruited Janus kinase 1 (JAK1) and tyrosin kinase 2 (TYK2) are phosphorylated by the receptor and phosphorylate the IFNAR1/2 subunits in return. This leads to the recruitment of signal transducers and activators of transcription (STAT) 1 and 2, which in turn are activated by tyrosin

phosphorylation at specific residues. Activated STAT1 and STAT2 form a heterotrimeric complex together with IRF9, which is called interferon-stimulated gene factor 3 (ISGF3). This transcription factor translocates to the nucleus and binds to interferon stimulated response elements (ISRE), and promotes the expression of antiviral cytokines, so called Interferon stimulated genes (ISGs; reviewed in (Takaoka and Yanai, 2006; Brzózka et al., 2007)).

Type-II IFN signaling is closely related to type-I IFN signaling. IFN γ binds to the type-II interferon receptor (or interferon-gamma receptor, IFNGR), which activates STAT1 via JAK1 and JAK2 (Fig. 5B). STAT1 homodimers translocate to the nucleus and bind to gamma activated sequences (GAS), a second promoter element for ISGs (reviewed in (Takaoka and Yanai, 2006; Brzózka et al., 2007)).

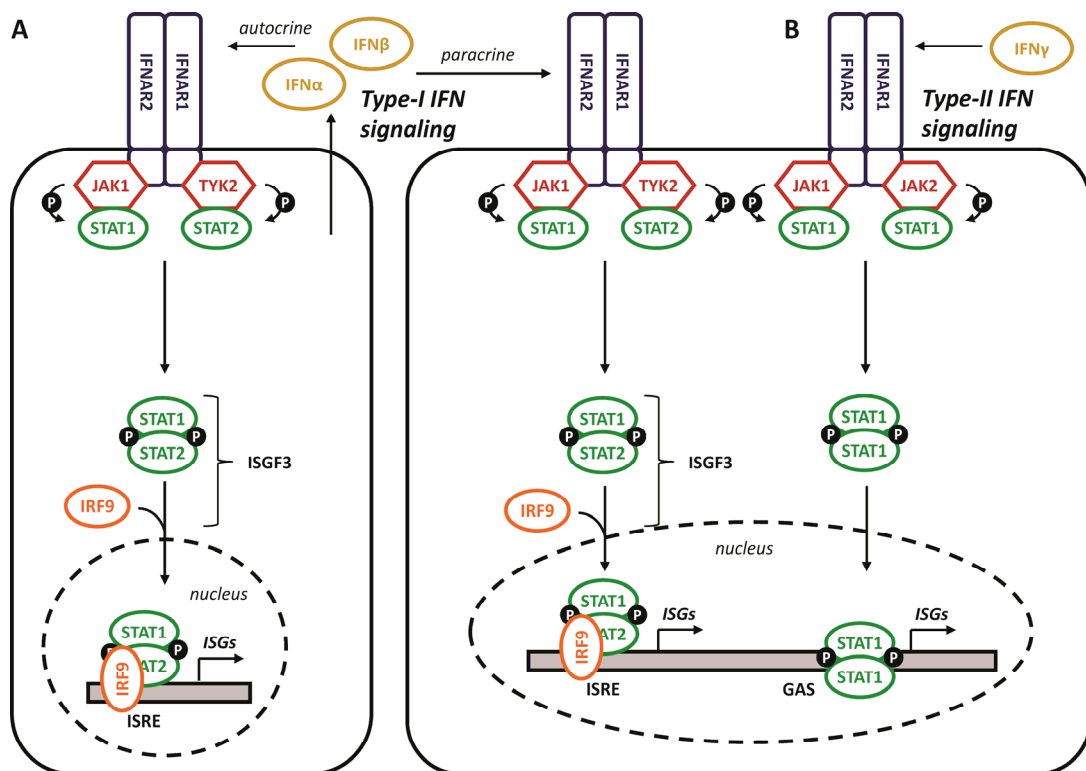


Figure 5: Type-I and Type-II IFN signaling pathways.

(A) Type-I IFN signaling by secreted IFN α and IFN β in an autocrine or paracrine manner. Activation of ISRE-driven ISGs. IRF9, STAT1, and STAT2 form the ISGF3. (B) Type-II IFN signaling by IFN γ activates transcription of GAS-promoter driven ISGs. *Color code:* gold: interferons; dark blue: receptors; red: kinases; green: STATs; orange: IRF9.

Among ISGs there are proteins with direct antiviral properties, like 2'-5'-oligoadenyl synthetase (2'-5'-OAS), or the Mx protein (Mx), but also signaling components of the IFN induction pathways are upregulated, like IRF7 and TLRs. This upregulation results in a positive feedback loop and further amplification of IFN production. To avoid overreaction of the system, also negative regulators of the signaling pathways are found among ISGs, like the suppressors of cytokine signaling (SOCS) 1 and 3, which inhibit further IFN signaling by interference with the JAK/STAT pathway (Song and Shuai, 1998).

In addition to the upregulation of ISG expression, IFNs fulfill functions in activation of the adaptive immune response upon viral infections.

1.2.2 MV specific adaptive immune response

After initial infection, macrophages (MΦs) and dendritic cells (DCs) build a first line of defense of the innate immune response (Fig. 6). MV is recognized by TLR2 via a not completely characterized mechanism (Bieback et al., 2002), maybe by interaction with the H protein. This leads to the production of proinflammatory cytokines IL-1, IL-6, and IL-12p40. In contrast, type-I IFN production is very low in MV infection, as MV actively suppresses the induction of type-I IFNs *in vivo* and *in vitro* (Naniche et al., 2000; Schlender et al., 2005). Following the activation of the innate immune response, cell-mediated immunity and humoral responses are mobilized.

An initial T-helper 1 (Th1)-response at the onset of the rash is characterized by the production of IFN γ and soluble Interleukin-2 receptor (IL-2R; (Griffin et al., 1990)). Soluble CD8 and β -2 microglobulin are present in the serum (Griffin et al., 1992) and MV specific CD8+ cytotoxic T-lymphocytes (CD8+CTL) are set up and activated (van Binnendijk et al., 1990). In the convalescent phase, a shift towards a Th2-biased immune response takes place ("polarization"), which is characterized by the production of IL-4, IL-5, and IL-10 (Griffin and Ward, 1993). This shift might contribute to the immunosuppressive phenotype of MV and the high susceptibility of MV infected persons to secondary infections (reviewed in (Schneider-Schaulies and Schneider-Schaulies, 2009); see also section 1.2.3). In the following, a short term effector memory leads to the

recovery from the infection and virus clearance. Long term central memory leads to the life-long protection from re-infection.

Activation of B cells by MV specific epitope presentation (mainly from N, H, and F proteins) leads to the production of neutralizing IgG1 and IgG3 antibodies. Further affinity maturation builds up a serologic memory (IgG2 and IgG4 antibodies), which is maintained by CD4⁺ T cells (TCD4⁺). This serologic memory results also in the life-long protection from re-infection and typically reaches titers of >200 mIU/mL of neutralizing antibodies (reviewed in (Naniche, 2009)).

DCs play a pivotal role at the intersection of innate and adaptive immune response (for review see (Reis e Sousa, 2004; Kadowaki, 2009)). They can be

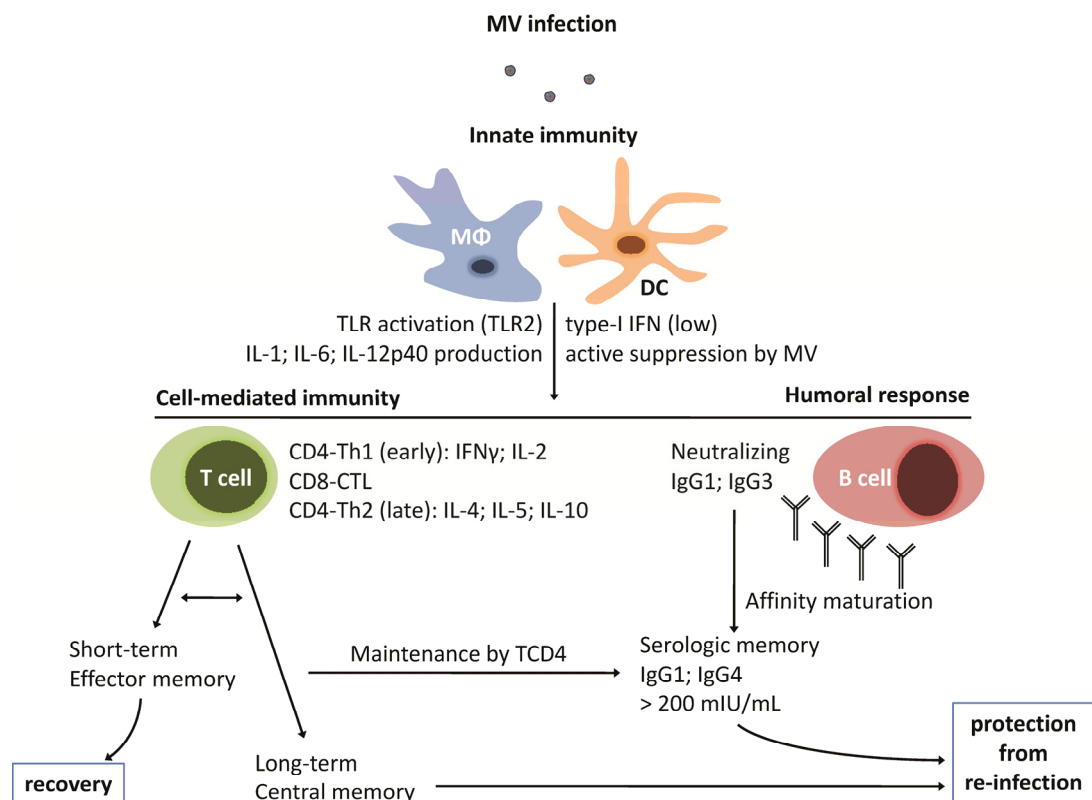


Figure 6: Immune response to MV infection in vivo.

Activation of the innate immune response in macrophages (M Φ) and dendritic cells (DC) leads to the upregulation of cytokines. This activates a T-cell mediated immune response, leading to the recovery through short-term effector memory, and a humoral response, leading to the production of neutralizing antibodies. Long-term central memory and serologic memory lead to the life-long protection from re-infection (Adapted from (Naniche, 2009)).

grouped in DCs of myeloid origin (mDCs) and those of plasmacytoid origin (pDCs). While mDCs are the major antigen presenting cell type (APC) and play a crucial role in activation of T and B cell responses, pDCs are the most important cytokine producers during infection, with IFN α as the most important cytokine. MV possesses several options to subvert the immune response of the host, and some are closely connected to DC functions. These mechanisms will be explained in the following.

1.2.3 Immunosuppression and immune antagonistic functions of MV

Viruses have evolved multiple mechanisms to subvert the host immune response. Here, cell tropism and the infectious route determine the implementation of these antagonistic mechanisms (reviewed in (Brzózka et al., 2007; Loo and Gale, Jr., 2007; Goodbourn and Randall, 2009)). In the case of MV, which predominantly infects immune cells, a very strong immunosuppression is induced upon infection. This includes at least three major mechanisms: (i) acute lymphopenia, (ii) silencing of peripheral blood lymphocytes (PBLs), and (iii) a strong cytokine imbalance (reviewed in (Schneider-Schaulies and Schneider-Schaulies, 2009)). Lymphopenia involves B cells, monocytes, neutrophils, as well as CD4⁺ and CD8⁺ T cells. Silencing of PBLs is mediated by the viral glycoproteins and does not require infection of the cells, but relies on the contact of the virus with the cell surface (Schlender et al., 1996). Cytokine imbalance leads to the polarization of the Th-response towards a Th2-biased immune response. This involves the modulation of DCs, which have been shown to be infected by MV *in vitro* (Minagawa et al., 2001). One mechanism is the interaction of MV with TLR2 (Bieback et al., 2002), which leads to the induction of the expression of the MV entry receptor CD150. MV in addition modulates antigen presentation as well as maturation of DCs. Type-I IFNs play a crucial role in this process of DC maturation (Klagge et al., 2000) and cytolytic activity (Vidalain et al., 2000). It has been shown that wt MV strains are only poor inducers of type-I IFNs (Naniche et al., 2000), whereas attenuated MVs induce higher amounts of IFN. Crucial for this is, for example, the accumulation of defective interfering RNAs (DI RNAs), which induce type-I IFNs in a RIG-I/MDA-5 dependent manner (Shingai et al., 2007). MV interferes

with signaling processes of the innate immune response on multiple steps, which have been characterized since a while on the molecular level. It has been shown that P and V are able to bind STAT1 and thereby inhibit its activation (Palosaari et al., 2003; Takeuchi et al., 2003; Caignard et al., 2007; Devaux et al., 2007). It has also been shown that V in addition is able to bind to STAT2 (Ohno et al., 2004; Ramachandran et al., 2008) via a distinct protein domain, and also to MDA-5 (Andrejeva et al., 2004; Childs et al., 2007). These features are common to almost all viruses of the *Paramyxoviridae* family. However, MV exhibits also unique mechanisms to subvert the innate immune response. The suppression of TLR7/9 mediated induction of IFN α in pDCs upon infection with the MV Schwarz vaccine strain has been reported previously (Schlender et al., 2005). Infected pDCs are unable to produce IFN α in response to the stimulation with external ligands for TLR7 (R848), or TLR9 (CpG-oligodeoxynucleotide (ODN) 2216). This mechanism might play a central role in the modulation of the host immune response by MV and is the major focus of this work.

1.3 Aims of this thesis

It was shown that MV is able to block the signal transduction of TLR7 and 9 upon infection of pDCs (Schlender et al., 2005). However, the mechanism behind this inhibition remained unclear. It was the aim of this study to identify the viral antagonist of the TLR7/9 mediated induction of IFN α and to describe the molecular basis underlying this antagonistic function. For this purpose, biochemical assays were established and the role of distinct viral proteins was tested in transient expression experiments. In particular, the role of the P gene products P, V, and C was addressed, as these proteins have been described previously to comprise different ways to subvert the innate immune response. From the data, a model was created and fit into the other known and described antagonistic functions of viruses of the *Paramyxoviridae* family and especially MV.

2 Materials and Methods

2.1 Materials

2.1.1 Chemicals

Fine chemicals were purchased from the following companies:

Acetic acid glacial, Rotipuran 100 % p.a.	Roth
Acetone, Rotipuran 99.8 % p.a.	Roth
Ammoniumchloride	Merck
Ammoniumpersulfate	Sigma-Aldrich
Ampicillin sodium salt (Amp)	Roth
Bacto yeast extract	BD
Bacto Tryptone	BD
β -Glycerophosphate disodium salt	Sigma-Aldrich
β -Mercaptoethanol	Sigma-Aldrich
Boric acid, ≥ 99.8 % p.a.	Roth
Brilliant blue	Biorad
Bromphenol blue	Sigma-Aldrich
BSA, fraction V	Sigma-Aldrich
Calciumchloride dihydrate	Sigma-Aldrich
Chloramphenicol succinate sodium salt (CAM)	Sigma-Aldrich
D-(+)-Glucose	Roth
Disodium-hydrogenphosphate-dihydrate	Merck
Dimethylsulfoxide (DMSO), p.a.	Roth
DL-Dithiothreitol, BioUltra, ≥ 99.5 % (DTT)	Sigma-Aldrich
Ethylene-diamin-tetraacetic acid-disodium salt (EDTA)VWR Prolabo	
Ethylene glycol tetraacetic acid (EGTA)	Sigma-Aldrich
Ethanol, p.a.	Merck

Ethidium bromide solution, 1 %	Roth
Ficoll 400	Pharm. Fine Chem.
Formic acid, p.a.	Merck
Geneticin (G418 sulfate)	Invitrogen Gibco
Glycerol, Rotipuran \geq 99.5 %	Roth
Glycine, > 99 % p.a.	Roth
HEPES Pufferan	Roth
Hydrochloric acid, Rotipuran 37% p.a.	Roth
Hygromycin B	Calbiochem
Imidazole	Merck
Isopropyl β -D-1-thiogalactopyranoside (IPTG)	Roth
Isopropanol, p.a.	Merck
Kanamycin monosulfate salt (Kan)	Sigma-Aldrich
Lithiumchloride, p.a.	Merck
Magnesiumchloride-hexahydrate	Fluka
Magnesiumsulfate-heptahydrate	Merck
Methanol, p.a.	Merck
Milk powder, blotting grade	Roth
NP-40 Substitute	Fluka
Orange G	Sigma-Aldrich
Paraformaldehyde	Merck
Polyethyleneimine (PEI), high MW, water-free	Sigma-Aldrich
Phenol red	Merck
Phenylmethylsulfonylfluoride (PMSF)	Serva
Potassiumacetate, extra pure	Merck
Potassiumchloride, p.a.	Merck
Potassium-dihydrogenphosphate, p.a.	Merck
Potassiumhydrogencarbonate	Merck
Rotiporese Gel 40 (29:1) Acrylamide/Bisacrylamide	Roth
Sodium-dodecylsulfate (SDS)	Serva
Sodiumacetate-trihydrate, p.a.	Merck
Sodiumchloride, p.a.	Merck
Sodiumhydrogencarbonate	Merck
Sodiumhydroxide	J.T.Baker

Sodiumorthovanadate	Sigma-Aldrich
Tetramethylethylenediamine (TEMED)	Roth
Tricine, Pufferan >99 %	Roth
Tris, Pufferan ≥ 99.9 %	Roth
Trisodiumcitrate-dihydrate >99 % p.a.	Roth
Triton X-100	Merck
Tween-20	Roth
Urea, ≥ 99.5 % p.a.	Roth
Xylenecyanol FF	Biorad

2.1.2 Kits

Plasmid purification:

Nucleobond PC 100 (Macherey&Nagel)

Cloning:

QIAquick PCR Purification Kit (QIAGEN)

QIAquick Nucleotide Removal Kit (QIAGEN)

QIAquick Gel Extraction Kit (QIAGEN)

RNA isolation:

RNeasy Mini Kit (QIAGEN)

Protein purification:

QIAexpress Kit (QIAGEN)

BCA Protein Assay Kit (Pierce)

Transfection:

Lipofectamine 2000 (Invitrogen)

Mammalian Transfection Kit (Stratagene)

Luciferase reporter gene assay:

Dual-Luciferase Reporter Assay System (Promega)

ELISA:

Mouse Interferon Alpha (Mu-IFN- α) ELISA Kit (PBL)

Northern blot:

Ready prime II Kit (GE Healthcare)

2.1.3 Enzymes

All enzymes and supplied buffers were used as recommended by the suppliers.

Restriction enzymes (New England Biolabs)

DNA polymerases:

BioPfu (biomaster)

Herculase (Stratagene)

RNase:

RNase A (Macherey&Nagel)

Phosphatase:

Calf Intestine Alkaline Phosphatase (CIAP; New England Biolabs)

Ligase:

T4 DNA Ligase (New England Biolabs)

Kinases:

IKK α (CHUK; Invitrogen)

IKK β (Invitrogen)

TBK1 (Invitrogen)

2.1.4 Recombinant proteins and peptides

Human Flt-3/Flk-2 Ligand (Flt3L; eBioscience)

I κ B- α (Santa Cruz)

IFN A/D (universal type-I IFN; PBC Biomedical Lab)

TNF α (mouse; Sigma-Aldrich)

V₂₄₀₋₂₆₄ WNGDRVFDIDRWCNPMCSKVTLGTIR (Metabion)

Vmut₂₄₀₋₂₆₄ WNGDRVFDIDRWCNPMCSKVAAAIR (Metabion)

V₂₅₇₋₂₆₆ KVTLGTIRAR (Metabion)

Vmut₂₅₇₋₂₆₆ KVAAAIRAR (Metabion)

2.1.5 Antibodies

Primary antibodies:

Anti-FLAG M2 (mouse monoclonal; Sigma-Aldrich)

Anti-FLAG M2 (rabbit polyclonal; Sigma-Aldrich)

Anti-His tag (mouse monoclonal; Cell Signaling)

Anti-MV-C 1240 Sompong (rabbit polyclonal; R. Cattaneo)
 Anti-MV-N (mouse monoclonal; Millipore)
 Anti-MV-N-FITC (mouse monoclonal; Millipore)
 Anti-MV-P #37069 (rabbit polyclonal; D. Gerlier; (Chen et al., 2003))
 Anti-MV-V Sompong (rabbit polyclonal; R. Cattaneo)
 Anti-p65(RelA) (rabbit polyclonal; Santa Cruz)
 Anti-RelB (rabbit polyclonal; Santa Cruz)
 Anti-RV-N-FITC (mouse monoclonal; FDI)
 Anti-RV-N/P (S50; rabbit polyclonal; J. Cox)
 Anti-RV-P (FCA05/1; rabbit polyclonal; Metabion)
 Anti-V5 mouse monoclonal; Invitrogen)

Secondary antibodies:

Anti-Mouse-Tetramethylrhodamin (Molecular Probes, Invitrogen)
 Anti-Mouse-IgG-HRP (Dianova)
 Anti-Rabbit-Alexa 488 (Molecular Probes, Invitrogen)
 Anti-Rabbit-IgG-HRP (Dianova)

2.1.6 Oligonucleotides

Oligonucleotides were purchased from *Metabion*.

Primer No.	Oligo Name	Sequence 5'-3'
4	Flag-IRAK1 Acc651 5'	TATGGTACCGCCACCATGGACTACAAAGACGATG ACGATAAAGCCGGGGGCGGGCCCG
5	IRAK1 NotI 3'	ATATGCGGCCGCTCAGCTCTGAAATTCATC
6	Flag-IRAK4 Acc651 5'	TATGGTACCGCCACCATGGACTACAAAGACGATG ACGATAAAAACAAACCCATAACACCATCA
7	IRAK4 NotI 3'	ATATGCGGCCGCTTAAGAAGCTGTCATCTC
8	MePVdeltaC forw	AGAGCAGGCACGCCACGTGAAAAACGGACTAGA ATGCATCC
9	MePVdeltaC rev	TGGCGTGCCTGCTCTTCTGCCATGG
10	Flag MV-PVdeltaC EcoRI 5'	ATAGAATTCGCCACCATGGACTACAAAGACGATG ACGATAAAGCAGAAGAGCAGGCACGC

Primer No.	Oligo Name	Sequence 5'-3'
11	Flag MV-C EcoRI 5'	ATAGAATTCGCCACCATGGACTACAAAGACGATG ACGATAAATCAAAAACGGACTGGAAT
37	MV-P XhoI 3'	ATACTCGAGCTACTTCATTATTATCTTCAT
38	MV-V XhoI 3'	ATACTCGAGTTATTCTGGGATCTCGGGGAG
39	MV-C XhoI 3'	ATACTCGAGTCAGGAGCTCGTGGATCTCCC
40	PV Nterm EcoRI 5'	ATAGAATTCGCCACCATGGCAGAAGAGCAGGCA
42	V Cterm EcoRI 5'	ATAGAATTCGCCACCATGCACAGACGCGAGATT
43	P Cterm XhoI 3'	ATACTCGAGCTACTTCATTATTATCTT
45	V Cterm XhoI 3'	ATACTCGAGTTATTCTGGGATCTCGGG
46	PV Nterm rev XhoI 3'	ATACTCGAGTTACCCCTTTTTAATGGG
47	P Cterm forw EcoRI 5'	ATAGAATTCGCCACCATGACAGACGCGAGATTA
48	MV-PV NheI 5'	ATAGCTAGCATGGCAGAAGAGCAGGCA
49	MV-P NotI 3'	ATATGCGGCCGCTACTTCATTATTAT
50	MV-V Not-I 3'	ATATGCGGCCGCTTATTCTGGGATCTC
59	MV-C NheI 5'	ATAGCTAGCATGTCAAAAACGGACTGGAAT
60	MV-C NotI 3'	TATAGCGGCCGCTCAGGAGCTCGTGGATCT
69	T7 Promoter Primer	TAATACGACTCACTATAGGG
70	T7 Terminator Primer	GCTAGTTATTGCTCAGCGG
93	IRF7 NheI fwd	ATAGCTAGCATGGCTGAAGTGAGGGGG
94	IRF7 NotI rev	ATATGCGGCCGCTCAAGGCCACTGACC
97	MV-V (165) NheI	ATAGCTAGCATCACTGACCGGGGA
98	MV-V (232) NheI	ATAGCTAGCCACAGACGCGAGATT
99	MV-V (164rev) NotI	ATATGCGGCCGCTTAAGCATATCCCTCGGT
100	MV-V (231rev) NotI	ATATGCGGCCGCTTACCCCTTTTTAATGGG
101	MV-P (232) NheI	ATAGCTAGCACAGACGCGAGATTA
104	IRF7-EcoRV-fwd	ATAGATATCATGGCCTTGCTCCTGAGAGG
105	IRF7-XhoI-rev	TATCTCGAGCTAGGCGGGCTGCTCCAGCTC
106	IRF3-EcoRV-fwd	ATAGATATCATGGGAACCCCAAAGCCACGG
107	IRF3-XhoI-rev	TATCTCGAGTCAGCTCTCCCCAGGGCCCTG
110	H232D fwd	CCCATTA AAAAGGGGGACAGACGCGAGATTAGCC TCATTTGGA
111	H232D,S237G fwd	CCCATTA AAAAGGGGGACAGACGCGAGATTGGCC TCATTTGGA
113	H232D,S237G rev	CCCCTTTTTAATGGGTGTCCCGGAA

Primer No.	Oligo Name	Sequence 5'-3'
114	T259A fwd	ACCCAATGTGCTCGAAAGTCGCCCTCGGAACCAT CAGGGCCAG
115	T259A rev	CTGGCCCTGATGGTCCGAGGGCGACTTTCGAGC ACATTGGGT
116	C272R fwd	CCAGGTGCACCTGCGGGGAACGTCCCCGAGTGTG TGAGCAATG
117	C272R rev	CATTGCTCACACACTCGGGGACGTTCCCCGCAGG TGCACCTGG
126	SV5-V EcoRI fwd	ATAGAATTCGCCACCATGGATCCCCTGAT
127	SV5-V XhoI rev	TATCTCGAGTTAAGTATCTCGTTC
128	SV5-V-MVV284-299 XhoI rev	TATCTCGAGTTATCTGGGATCTCGGGGAGATTG TGGTACCAGATTCCGGGTGTCCACTCCAGTATCTC GTTCCACATTCAGAGCA
129	MV-Vd284-299 XhoI rev	TATCTCGAGTTATGTATCAGTGCGGCA
130	SV5-V E183R fwd	CAATCGGATGGGTGGGAGATAGAGTCAAGGTCA CTGAGTGGTG
131	SV5-V E183R rev	CACCACTCAGTGACCTTGACTCTATCTCCCACCC ATCCGATTG
132	SV5-V F204A,E205R fwd	TCACCGCTGCAGCAAGGCGAGCTAGATGCACTTG TCACCAGTGTCC
133	SV5-V F204A,E205R rev	GGACACTGGTGACAAGTGCATCTAGCTCGCCTTG CTGCAGCGGTGA
134	MV-V R244E fwd	GCCTCATTGGAAACGGAGATGAGGTCTTTATTGA CAGGTGGTG
135	MV-V R244E rev	CACCACCTGTCAATAAAGACCTCATCTCCGTTCC AAATGAGGC
136	MV-V A265F,R266E fwd	TCACCCTCGGAACCATCAGGTTGAGTGCACCTG CGGGGAATGTCC
137	MV-V A265F,R266E rev	GGACATTCCTCCGAGGTGCACTCGAACCTGATGG TTCCGAGGGTGA
140	MV-V R244E,F246R,D248F fwd	GCC TCA TTT GGA ACG GAG ATG AGG TCC GTA TTT TCA GGT GGT GCA ACC CAA TGT G

Primer No.	Oligo Name	Sequence 5'-3'
141	MV-V R244E,F246R,D248F rev	CAC ATT GGG TTG CAC CAC CTG AAA ATA CGG ACC TCA TCT CCG TTC CAA ATG AGG C
142	MV-V 244E,F246K,D248T fwd	GCCTCATTTGGAACGGAGATGAGGTCAAAATTA CCAGGTGGTGCAACCCAATGTG
143	MV-V 244E,F246K,D248T rev	CACATTGGGTTGCACCACCTGGTAATTTTGACCT CATCTCCGTTCCAAATGAGGC
144	MV-V 259AAAA fwd	ACCCAATGTGCTCGAAAGTCGCCGCCGCAGCCAT CAGGGCCAGGTGCACCTG
145	MV-V 259AAAA rev	CAGGTGCACCTGGCCCTGATGGCTGCGGCGGCGA CTTTCGAGCACATTGGGT

ODN 2216 CpG oligonucleotide type A (InvivoGen):

GGG GGA CGA TCG TCG GGG GG

Poly(I:C) (Sigma-Aldrich)

2.1.7 Cell lines and media

BSR-T7/5

(BHK21-derived cells stably expressing T7 RNA polymerase) G-MEM+4

HEK-293T

(Human embryonic kidney cells) D-MEM+3

HEp-2

(Human epidermoid cancer cells) D-MEM+2

Huh7.5

(Human hepatoblastoma cells, clone 7.5) D-MEM+3

U3A3

(Human fibrosarcoma cells stably expressing GFP-LC3; L. Fragnet) D-MEM+3

Vero

(African Green Monkey kidney cells) D-MEM+3

Cell culture media and supplements:

• Dulbecco's Modified Eagle Medium (D-MEM)	Invitrogen
• Earles Balanced Salt Solution (EBSS)	Invitrogen
• Glasgow Minimum Essential Medium BHK-21 (G-MEM)	Invitrogen
• VLE-RPMI 1640	Biochrom
• Trypsin/EDTA	Invitrogen
• 100x Glutamine	Invitrogen
• Non-essential amino acids (NEAA)	Invitrogen
• Tryptose-phosphate broth	Invitrogen
• Penicillin/Streptomycin	Invitrogen
• Fetal bovine serum (FBS)	Invitrogen
• Newborn calf serum (NCS)	Invitrogen

D-MEM+3

= D-MEM + 10 % (v/v) FBS + 1 % (v/v) 100x L-Glutamine + Penicillin/Streptomycin

D-MEM+2

= D-MEM + 5 % (v/v) FBS + Penicillin/Streptomycin

G-MEM+4

= G-MEM + 10 % (v/v) NCS + 4 % (v/v) Tryptose-phosphate broth + 2 % (v/v) NEAA + Penicillin/Streptomycin

RPMI+5

= VLE-RPMI 1640 + 10 % (v/v) FBS + 1 % (v/v) L-Glutamine + 1 % Sodium-pyruvate (v/v) + 1 % NEAA (v/v) + Penicillin/Streptomycin

2.1.8 Viruses

All recombinant rabies viruses are derived from SAD-L16, a recombinant RV carrying the nucleotide sequence (completely sequenced) of the Street Alabama

Dufferin (SAD) B19 strain (NCBI accession no. EF206709; (Conzelmann et al., 1990)), which is an attenuated strain used for the oral immunization of foxes.

Measles virus was originated from a commercial batch of the Schwarz vaccine strain (MV(Schwarz); NCBI accession no. AF266291; (Schwarz, 1964)) and produced through 10 passages on HEp-2 cells and 2 passages on Vero cells (S. Moghim).

2.1.9 Plasmids and bacteria

Following bacteria strains were used for

plasmid DNA amplification: *XL-1 Blue* Supercompetent Cells (Stratagene)

recombinant protein expression: *Rosetta (DE3)* Competent Cells (Novagen)

Plasmids commercially available were purchased from following companies:

pCR3	Invitrogen	eukar. expr. vector (CMV promoter)
pDNR-LIB-IRAK4	RZPD	vector with IRAK4 cDNA
pISRE-Luc	Clontech	firefly luciferase (ISRE controlled)
pEGFP-N3	Clontech	eGFP vector (CMV promoter)
pET28a	Novagen	6xHis-tag bacterial expression vector
pNF- κ B-Luc	Stratagene	firefly luciferase (NF- κ B promoter)
pOTB7-IRAK1	RZPD	vector with IRAK1 cDNA
pOTB7-IRAK1c	RZPD	vector with IRAK1c cDNA
pRL-CMV	Promega	renilla luciferase (CMV promoter)

The following plasmids were kindly provided:

p55C1B-Luc	T. Fujita (Yoneyama et al., 1998)
pCDNA3.1-Flag-IRF3	J. Hiscott (Lin et al., 2000)
pCDNA3.1-TRAF6	A. Kieser (Schultheiss et al., 2001)
pCOOL-PIV5-V	N. Zheng (Li et al., 2006)
pFLAG-CMV2-hIRF7	J. Hiscott (Lin et al., 2000)
pFLAG-CMV2-mIRF7	S. Akira (Kawai et al., 2004)
pFLAG-IKK ϵ	K. Ruckdeschel (expression vector for Fl-IKK ϵ)
pGL3-IFN α 4-Luc	S. Akira (Kawai et al., 2004)
pGL3-IFN α 6-Luc	S. Akira (Kawai et al., 2004)
pIRF3-5D	J. Hiscott (Lin et al., 2000)

pIRF7-2D	J. Hiscott (Lin et al., 2000)
pRK5- IKK β -Fl tag!))	K. Ruckdeschel (expression vector for Fl-IKK β (C-term. tag!))
pRK7-Fl-IKK α	K. Ruckdeschel (expression vector for Fl-IKK α)
pRK7-myc-MyD88	K. Ruckdeschel (expression vector for myc-MyD88)

Plasmids generated in the lab:

pCR3-Ig	K. Brzózka (pCR3 with Ig-tag sequence upstream of MCS)
pCR3-MV-C	S. Moghim (pCR3 with MV C ORF)
pCR3-MV-P	S. Moghim (pCR3 with MV P mRNA)
pCR3-MV-V	S. Moghim (pCR3 with MV V mRNA)
pCR3-RV-P	K. Brzózka (pCR3 with RV P ORF)
pFLAG-TBK1	K. Brzózka, S. Marozin (expression vector for Fl-TBK1)
pSAD-G-DsRed	S. Finke (pSAD-L16 with add. DsRed gene behind G gene)
pSAD-L16	K. Conzelmann (Schnell et al., 1994)
pSAD-P Δ IND2	K. Brzózka (Brzózka et al., in preparation)
pTIT-RV-L	S. Finke (Finke and Conzelmann, 1999)
pTIT-RV-N	S. Finke (Finke and Conzelmann, 1999)
pTIT-RV-P	S. Finke (Finke and Conzelmann, 1999)

Plasmids generated during this thesis:

plasmid name	template	primer pair	restriction sites	vector backbone
pCR3-Fl-MV-P Δ C	pCR3-MV-P Δ C	10, 37	EcoRI, XhoI	pCR3
pCR3-Fl-MV-V Δ C	pCR3-MV-V Δ C	10, 38	EcoRI, XhoI	pCR3
pCR3-Fl-MV-C	pCR3-MV-C	11, 39	EcoRI, XhoI	pCR3
pCR3-Ig-MV-P	pCR3-MV-P Δ C	---	EcoRI, NotI	pCR3-Ig-RV-P
pCR3-Ig-MV-V	pCR3-MV-V Δ C	---	EcoRI, NotI	pCR3-Ig-RV-P
pCR3-Ig-MV-C	pCR3-MV-C	---	EcoRI, NotI	pCR3-Ig-RV-P
pCR3-Ig-MV-PV _N	pCR3-MV-V Δ C	40, 46	EcoRI, XhoI	pCR3-Ig
pCR3-Ig-MV-P _C	pCR3-MV-P Δ C	47, 43	EcoRI, XhoI	pCR3-Ig
pCR3-Ig-MV-V _C	pCR3-MV-V Δ C	42, 45	EcoRI, XhoI	pCR3-Ig
pCR3-MV-V Δ 284- 299	pCR3-MV-V Δ C	40, 129	EcoRI, XhoI	pCR3

plasmid name	template	primer pair	restriction sites	vector backbone
pET28a-MV-PΔC	pCR3-MV-PΔC	48, 49	NheI, NotI	pET28a
pET28a-MV-VΔC	pCR3-MV-VΔC	48, 50	NheI, NotI	pET28a
pET28a-MV-V(165-299)	pCR3-MV-VΔC	97, 50	NheI, NotI	pET28a
pET28a-MV-V(232-299)	pCR3-MV-VΔC	98, 50	NheI, NotI	pET28a
pET28a-MV-PV _N	pCR3-MV-VΔC	48, 100	NheI, NotI	pET28a
pET28a-MV-PV(1-164)	pCR3-MV-VΔC	48, 99	NheI, NotI	pET28a
pET28a-MV-P _c (232-507)	pCR3-MV-PΔC	101, 49	NheI, NotI	pET28a
pCR3-PIV5-V	pCOOL-PIV5-V	126, 127	EcoRI, XhoI	pCR3
pCR3-PIV5-V:MV-V284-299	pCOOL-PIV5-V	126, 128	EcoRI, XhoI	pCR3
pSAD-G-MVP	pCR3-MV-PΔC	48, 49	NheI, NotI	pSAD-G-DsRed
pSAD-G-MVV	pCR3-MV-VΔC	48, 50	NheI, NotI	pSAD-G-DsRed
pSAD-G-MVC	pCR3-MV-C	59, 60	NheI, NotI	pSAD-G-DsRed
pSAD-PΔIND2-G-MVP	pSAD-G-MVP	---	SnaBI, MluI	pSAD-PΔIND2(49.1)
pSAD-PΔIND2-G-MVV	pSAD-G-MVV	---	SnaBI, MluI	pSAD-PΔIND2(49.1)
pSAD-PΔIND2-G-MVC	pSAD-G-MVC	---	SnaBI, MluI	pSAD-PΔIND2(49.1)
pCR3-FI-IRAK1	pOTB7-IRAK1	4, 5	Acc65I, NotI	pCR3
pCR3-FI-IRAK1c	pOTB7-IRAK1c	4, 5	Acc65I, NotI	pCR3
pCR3-FI-IRAK4	pDNR-LIB-IRAK4	6, 7	Acc65I, NotI	pCR3
pCDNA3.1-FL-IRF3-5D	pIRF3-5D	106, 107	EcoRV, XhoI	pCDNA3.1-Flag-IRF3
pCDNA3.1-FL-IRF7-2D	pIRF7-2D	104, 105	EcoRV, XhoI	pCDNA3.1-Flag-IRF3
pET28a-IRF7	pFLAG-CMV2-mIRF7	93, 94	NheI, NotI	pET28a

plasmid name	strategy	template	primer pair
pCR3-MV-PΔC	mutagenesis	pCR3-MV-P	8, 9
pCR3-MV-VΔC	mutagenesis	pCR3-MV-V	8, 9
pCR3-MV-V(H232D)	mutagenesis	pCR3-MV-VΔC	110, 113
pCR3-MV-V(H232D,S237G)	mutagenesis	pCR3-MV-VΔC	111, 113
pCR3-MV-V(T259A)	mutagenesis	pCR3-MV-VΔC	114, 115
pCR3-MV-V(C272R)	mutagenesis	pCR3-MV-VΔC	116, 117
pCR3-MV-V(H232D,C272R)	mutagenesis	pCR3-MV-V(H232D)	116, 117
pCR3-MV-V(R244E)	mutagenesis	pCR3-MV-VΔC	134, 135
pCR3-MV-V(A265F,R266E)	mutagenesis	pCR3-MV-VΔC	136, 137
pCR3-MV-V(R244E,F246R,D248F)	mutagenesis	pCR3-MV-VΔC	140, 141
pCR3-MV-V(R244E,F246K,D248T)	mutagenesis	pCR3-MV-VΔC	142, 143
pCR3-MV-V(T259A,L260A,G261A,T262A)	mutagenesis	pCR3-MV-VΔC	144, 145
pCR3-PIV5-V(E183R)	mutagenesis	pCR3-PIV5-V	130, 131
pCR3-PIV5-V(F204A,E205R)	mutagenesis	pCR3-PIV5-V	132, 133

2.1.10 Buffers and solutions

Mini Preparation

Flexi I	100 mM 10 mM 200 µg/mL	Tris-HCl, pH 7.5 EDTA Rnase
Flexi II	200 mM 1 % (w/v)	NaOH SDS
Flexi III	3 M 2 M	K-acetate Acetic acid, pH 5.75

Immunoprecipitation

Co-IP buffer	50 mM 150 mM 2 mM 1 mM 0.5 % (v/v) 1 tablet	Tris-HCl, pH 7.5 NaCl EDTA Na ₃ VO ₄ NP-40 substitute Complete protease inhibitor cocktail / 50 mL
--------------	--	---

Protein gels

10 % APS	10 % (w/v)	Ammoniumpersulfate
----------	------------	--------------------

Jagow gel buffer	3 M 0.3 % (w/v)	Tris-HCl, pH 8.45 SDS
Jagow anode buffer	2 M	Tris-HCl, pH 8.9
Jagow kathode buffer	1 M 1 M 1 % (w/v)	Tris-HCl, pH 8.25 Tricine SDS
Protein lysis buffer	62.5 mM 2 % (v/v) 10 % (v/v) 6 M 5 % (v/v) 0.01 % (w/v) 0.01 % (w/v)	Tris-HCl, pH 6.8 SDS Glycerine Urea β -Mercapto ethanol Bromphenol blue Phenol red
Coomassie staining		
Staining solution	50 % (v/v) 10 % (v/v) 0.1 % (w/v)	Methanol Acetic acid Brilliant blue
Wash solution	50 % (v/v) 10 % (v/v)	Methanol Acetic acid
Western blotting		
10x Semi dry buffer	480 mM 390 mM 0.05 % (w/v)	Tris-HCl, pH 8.6 Glycine SDS
1x Semi dry buffer	100 mL 180 mL 720 mL	10x Semi dry buffer Methanol abs. H ₂ O
1x PBS	1.37 M 27 mM 12 mM 65 mM	NaCl KCl KH ₂ PO ₄ Na ₂ HPO ₄ ·2H ₂ O (pH 7.4)
PBS-Tween	1 X 0.05 % (v/v)	PBS Tween-20
Agarose gels		
10x TAE	2 M 0.25 M 0.25 M	Tris-HCl, pH 7.8 Na-acetate trihydrate EDTA
1x TAE +EtBr	300 mL 2700 mL 150 μ L	10x TAE H ₂ O Ethidium bromide solution 1 %

OG loading buffer	50 % (v/v) 15 % (w/v) 0.125 % (w/v)	10x TAE Ficoll 400 Orange G
10x TE	100 mM 10 mM	Tris-HCl, pH 7.5 EDTA
Blue juice	0.125 % (w/v) 0.125 % (w/v) 0.125 % (w/v) 15 % (w/v) 50 % (v/v)	Bromphenol blue Xylenecyanol Orange G Ficoll 400 10x TAE
1 kb marker buffer	380 µL 100 µL 20 µL	1x TE Blue juice 1 kb DNA ladder

Northern blot

RNA agarose gel	2 g 4 mL 26.7 mL 167.3 mL	Agarose (RNA grade) 50x Phosphate buffer Formaldehyde, 37 % H ₂ O ultra pure
50x Phosphate buffer	250 mM 250 mM	Na ₂ HPO ₄ x2H ₂ O (pH 6.8-7.0) NaH ₂ PO ₄ xH ₂ O
Glyoxal solution	8.8 M	Glyoxal
10x SSC	1.5 M 150 mM	NaCl Na-citrate x2H ₂ O (pH 7.0)
Zeta Hybridising buffer	250 mM 250 mM 1 mM 7 % (w/v)	Na ₂ HPO ₄ x2H ₂ O (pH 7.2) NaH ₂ PO ₄ xH ₂ O EDTA SDS
Zeta Wash buffer 5 %	8 % (v/v) 1 mM 5 % (w/v)	50x Phosphate buffer EDTA SDS
Zeta Wash buffer 1 %	8 % (v/v) 1 mM 1 % (w/v)	50x Phosphate buffer EDTA SDS

Bacteria growth media

LB	85 mM 0.5 % (w/v) 1 % (w/v) 1 mM	NaCl Bacto yeast extract Bactotryptone MgSO ₄
LB++	1 X 20 mM 10 mM	LB MgSO ₄ KCl

Ni-NTA purification

5x Lysis/wash buffer	250 mM	KH ₂ PO ₄ , pH 7.5
	1 M	NaCl
	75 mM	Imidazole
5x Elution buffer	250 mM	KH ₂ PO ₄ , pH 7.5
	1 M	NaCl
	1.5 M	Imidazole
1x Lysis/wash buffer / 1x Elution buffer	20 % (v/v) 0.07 % (v/v)	5x buffer β-Mercaptoethanol

***In vitro* assay buffers**

5x Kinase assay buffer	125 mM	HEPES, pH 7.5
	0.05 % (v/v)	Triton X-100
	50 mM	MgCl ₂
	5 mM	EGTA
	2.5 mM	Na ₃ VO ₄
	25 mM	β-Glycerophosphate
Kinase dilution buffer	10 mM	DTT
	20 mM	Tris-HCl, pH 7.5
	10 % (v/v)	Glycerol
	0.02 % (v/v)	Triton X-100
	0.1 mg/mL	BSA
	0.5 mM	Na ₃ VO ₄
2 mM	DTT	

Immunofluorescence

3 % PFA/PBS	1 X	PBS
	3 % (w/v)	Paraformaldehyde
80 % Acetone	800 mL	Acetone p.a.
	200 mL	H ₂ O _{dd}
50 mM NH ₄ Cl/PBS	1 X	PBS
	50 mM	NH ₄ Cl
0.5 % Triton X-100/ PBS	1 X	PBS
	0.5 % (v/v)	Triton X-100
0.1 % Triton X-100/ PBS	80 % (v/v)	1x PBS
	20 % (v/v)	0.5 % Triton X-100/PBS

Cell preparation

Erythrocyte lysis buffer (ACK)	1 mM	KHCO ₃ , pH 7.4
	150 mM	NH ₄ Cl
	0.1 mM	EDTA

Cell culture

5 mM EDTA/PBS	1 X	PBS
	5 mM	EDTA

Phosphate-free Krebs-	20 mM	HEPES, pH 7.5
Ringer-Bicarbonate	118 mM	NaCl
Medium (PKRB)	4.75 mM	KCl
	1.2 mM	MgCl ₂
	0.2 mM	CaCl ₂
	25 mM	NaHCO ₃
	10 mM	D-Glucose

2.1.11 Equipment

Berthold Centro LB960 luminometer
 Biometra® Standard Power Pack P25
 Biometra® Thermocycler T3
 Biometra® Vacu-Blot System
 BioRAD Gel Doc System
 Branson Digital Sonifier W-250 D
 Daewoo C.R.S. microwave oven
 Eppendorf Centrifuge 5417C (rotor F45-30-11)
 Eppendorf Centrifuge 5804R (rotor F-45-30-11)
 Eppendorf Mixer 5432
 Eppendorf Pipettes (2.5 / 10 / 20 / 100 / 200 / 1000 µL)
 Eppendorf Thermomixer 5436
 Gilson Pipettes (2 / 10 / 20 / 200 / 1000 µL)
 Heraeus Variofuge 3.0R (rotor #8074)
 Hermle Centrifuge Z160M
 IBS Pipetboy acu
 IBS Vacusafe comfort vacuum pump system
 IKA® Minishaker MS1
 Integra Biosciences Fireboy plus
 Kern GJ Balance
 Kühner bacteria shaker ISF-1-W
 Labotect Forma Scientific Water-Jacketed Incubator 3250
 Liebherr Freezer GU1202
 Liebherr Fridge KU1710
 Marienfeld Neubauer improved counting chamber
 Molecular Devices Versamax microplate reader
 Molecular Dynamics PhosphoScreen

Molecular Dynamics Storm Scanner
MS Laborgeräte Optimax Typ TR developing machine
Nikon TMS light microscope
Nunc™ ilShin® Deep freezer
Olympus IX71 UV-light microscope
Peqlab Horizontal Gel System S/M/L/XL
Peqlab Nanodrop ND-1000 Spectrophotometer
Peqlab Semi Dry Blotting System
Peqlab Vertical Gel Electrophoresis System (Size S/M/L)
Pharmacia Biotech Electrophoresis Power Supply EPS 200
Sorvall Centrifuge Evolution RC (SLC6000 and SS34 rotors)
Stuart roller mixer SRT2
The Baker Company Sterilguard Class II Type A/B3 sterile workbench
Thermo Scientific Nanodrop ND-1000
Vacuubrand Vacuum Pump Unit ME 2S
VELP Scientifica Magnetic Stirrer/heater Unit
Zeiss LSM-510 Laser Scanning Microscope (Ar- / HeNe 633nm- / HeNe 543nm-
laser)

2.1.12 Miscellaneous

0.25 mL polypropylene reaction tubes (Eppendorf)
0.5 / 1.5 / 2 mL polypropylene reaction tubes (Eppendorf)
0.5 – 10 kb RNA ladder (Invitrogen)
1 kb DNA ladder (Invitrogen)
15 / 50 mL reaction tubes (BD Falcon®)
18 x 18 mm Coverslips (Roth)
2 / 10 / 20 / 200 / 1000 µL SafeSeal® Tips (Biozym®)
2 mL serological pipettes (costar)
3.5 / 6 / 10 cm cell culture dishes (BD Falcon®)
5 / 10 / 25 mL serological pipettes (Sarstedt)
6 / 12 / 24 / 48 / 96-well multiwell™ plates (BD Falcon®)
Agarose Electrophoresis grade (Invitrogen)
Amicon Ultra-15 Centrifugal Filter Devices MWCO 10,000 (Millipore)

Anti-FLAG® M2 Affinity Gel (Sigma-Aldrich)
ATP (Sigma-Aldrich)
ATP, gamma[³²P]- (Hartmann Analytic)
CTP, alpha[³²P]- (Hartmann Analytic)
dNTP Set (BIOLINE)
Duralon-UV™ membranes (Stratagene®)
Hyperfilm-ECL (GE Healthcare Amersham)
Immobilon-P (PVDF) membrane (Millipore)
Low molecular weight DNA marker (New England Biolabs)
Microscope slides, 76 x 26 mm (Roth)
Nitrocellulose membrane (Schleicher&Schuell)
Nunclon 60-well plates (Nunc™)
Precision Plus Protein Standard All Blue (Biorad)
Protein A-HRP (Zymed)
Protein A-Sepharose (GE Healthcare)
SnakeSkin Pleated Dialysis Tubing 3,500 MWCO (Pierce)
T25 / T75 / T125 cell culture flasks (BD Falcon®)
Western lightning chemiluminescence reagent plus (Perkin-Elmer)
Whatman paper (3MM)

2.2 Methods

2.2.1 Molecular biological methods

2.2.1.1 Cloning and mutagenesis

Polymerase-chain-reaction (PCR)

Standard reaction batches for the amplification of DNA fragments contained:

100 – 500 ng	template DNA
0.25 μ M	primer A (fwd)
0.25 μ M	primer B (rev)
10 % (v/v)	DMSO
1 X	reaction buffer
0.25 μ M	dNTPs (each)
2.5 U	DNA Polymerase
@ 100 μ L	H ₂ O _{dd}

In case of fragments below 5,000 bp bioPfu DNA polymerase (biomaster) was used for amplification. Herculase (Stratagene) was used for the amplification of bigger fragments.

A typical PCR program consisted of the following elements:

#	temperature	time	function	slope
1	95 °C/ 98 °C	60 s/ 30 s	enzyme activation	30 – 35 cycles
2	95 °C/ 98 °C	30 s/ 10 s	melting	
3	42 – 50 °C	30 s	primer annealing	
4	72 °C	1 min/ 500 bp (bioPfu) or 15 s/ 1000 bp (Herculase)	elongation	
5	72 °C	10 – 20 min	final elongation	
6	4 °C	∞	cooling	

PCR fragments were purified using the *QIAquick PCR Purification Kit* (QIAGEN).

Mutagenesis PCR

These reactions were carried out to introduce nucleotide mutations into plasmids:

100 – 500 ng	template DNA
0.25 μ M	primer A (fwd)
0.25 μ M	primer B (rev)
1 X	reaction buffer
0.25 μ M	dNTPs (each)
2.5 U	DNA Polymerase
@ 100 μ L	H ₂ O _{dd}

#	temperature	time	function	slope
1	95 °C/ 98 °C	60 s/ 30 s	enzyme activation	 18 - 20 cycles
2	95 °C/ 98 °C	30 s/ 10 s	melting	
3	42 – 50 °C	30 s	Primer annealing	
4	72 °C	1 min/ 500 bp (bioPfu)	elongation	
		or 15 s/ 1000 bp (Herculase)		
5	72 °C	10 min	final elongation	
6	4 °C	∞	cooling	

Upon completion of PCR, template DNA was digested using 2.5 U of the restriction enzyme DpnI, which was added directly to the PCR reaction batch (37 °C, 1 – 4 h). Mutagenesis PCR batches were transformed directly into *XL-1 Blue* chemically-competent cells without additional purification of the DNA.

Agarose gel electrophoresis

Gels containing 1x TAE and 1 % agarose were used to analyze the length of PCR products and restrictions. For the analysis of fragments > 10,000 bp, gels containing 0.7 % agarose were used and for fragments < 500 bp, gels containing 2 % agarose were used.

Probes were mixed with 20 % (v/v) Orange G, loaded onto the gels and subjected to electrophoresis at 120 – 140 V for 30 – 150 min, depending on the length of the fragments and agarose concentration. Electrophoresis buffer contained 1 x TAE and 50 µL/L of a 1 % Ethidiumbromide solution.

Gels were analyzed on a Biorad GelDoc System using UV light.

Restriction assays

1 µg of plasmid was digested with restriction enzymes to verify them by their restriction pattern. Reactions were performed in 10 µL total volume as recommended by the supplier.

To create sticky ends in PCR fragments or for quantitative plasmid restriction, 5 – 10 µg of DNA was digested in a total volume of 50 µL.

Gel extraction

DNA fragments were subjected to agarose gel electrophoresis and bands of required length were cut out of the gel. DNA was purified from the gel slice using the *QIAquick Gel Extraction Kit* (QIAGEN).

Ligation

DNA fragments and vector backbones were ligated using T4 DNA Ligase (New England Biolabs). Reaction batches contained:

0.5 µL	Purified vector backbone
7 µL	Purified DNA fragment
1 X	T4 DNA Ligase reaction buffer
200 U	T4 DNA Ligase
@ 20 µL	H ₂ O _{dd}

Reactions were incubated either at R.T. for 2 h or at 16 °C o/n. 10 µL of the reaction were transformed directly into *XL-1 Blue* chemically-competent cells without further purification.

2.2.1.2 Working with bacteria

Transformation

50 μL of the chemical-competent strain *XL-1 Blue* were thawed on ice and 0.5 – 1 μg of plasmid DNA was added. The mixture was incubated for 20 min on ice, followed by a heat shock (42 $^{\circ}\text{C}$, 2 min) and repeated incubation on ice for 2 min. Afterwards, 200 μL of LB++ medium were added and the bacteria were shaken at 37 $^{\circ}\text{C}$ for at least 30 min (~800 rpm).

In case of transformation of bacteria for expression of recombinant protein, 20 μL of the chemical-competent strain *Rosetta (DE3)* were used instead of *XL-1 Blue*.

Plating

Transformed bacteria were plated on LB-agar plates supplied with 25 mg/mL of antibiotics (ampicillin, kanamycin, chloramphenicol) according to the resistance genes on the transformed plasmids. The plates were incubated at 37 $^{\circ}\text{C}$ o/n until single bacteria colonies were visible.

Liquid culture

For Mini preparation, single colonies were inoculated into 1 mL of LB-medium supplied with 25 mg/mL of antibiotics and shaken at 37 $^{\circ}\text{C}$ o/n.

For Midi preparation, 75 μL of the suspension of transformed bacteria were directly inoculated to 50 mL of LB-medium supplied with 25 mg/mL of antibiotics and shaken at 37 $^{\circ}\text{C}$ o/n.

For expression of recombinant proteins, single colonies were inoculated into 1 mL of LB-medium supplied with 25 mg/mL of kanamycin and 25 mg/mL of chloramphenicol and shaken at 37 $^{\circ}\text{C}$ o/n.

Glycerol stocks

For expression of recombinant proteins, o/n liquid cultures were mixed with an equal amount of pure glycerol and stored at -86 °C. These stocks were used to inoculate 50 mL liquid cultures (see 2.2.3.9).

2.2.1.3 Plasmid preparation

Mini Preparation

1 mL of an o/n culture of transformed bacteria was pelleted (14,000 rpm, 1 min, R.T.) and the supernatant was discarded. The pellet was resuspended in 200 µL of Flexi I solution. 200 µL of Flexi II solution were added, mixed gently and incubated at R.T. for 5 min. After complete lysis of the bacteria, 200 µL of Flexi III solution were added, mixed gently and incubated on ice for another 5 min. The resulting debris was pelleted by centrifugation (14,000 rpm, 7 min, R.T.) and the cleared lysate was mixed with 400 µL of pure Isopropanol. Plasmid DNA was pelleted by centrifugation (14,000 rpm, 7 min, R.T.), the supernatant was discarded, the pellets were dried at R.T. and resolved in 50 µL H₂O_{dd} by shaking for several minutes.

Midi Preparation

Plasmid DNA for transfection experiments was extracted from 50 mL of an o/n culture of transformed bacteria using the *Nucleobond AX-100 Kit* (Macherey&Nagel) according to the manufacturer's proceedings.

DNA concentration was determined using the *Nanodrop 1000* (Pqlab) and DNAs were stored at -20 °C.

2.2.1.4 Sequencing

Sequencing reactions were performed by *MWG Eurofins* (Martinsried, Germany) using the *Value Read Tube protocol*. 1 – 2 µg of template DNA were mixed with 15 pmol of a sequencing oligo and the total volume was adjusted with H₂O_{dd} to 15 µL.

The results were analyzed electronically using the *DNAMAN* (Version 5.0 or higher) and *Chromas* (Version 1.45) software.

2.2.1.5 RNA isolation

Total cellular RNA was isolated using the *RNeasy Mini Kit* (QIAGEN). 1x10⁶ cells were lysed in 200 – 400 µL buffer RLT containing 0.1 % β-mercapto ethanol. The lysates were mixed with 1 equivalent of DEPC treated 70 % ethanol and mixed thoroughly. The lysates then were loaded onto columns and centrifuged (10,000 rpm, 30 s, R.T.). The flow through was discarded and the columns were washed once with 700 µL of buffer RW1 and two times with 500 µL of buffer RPE again by centrifugation (10,000 rpm, 30 s, R.T.). Afterwards, the columns were centrifuged two times (14,000 rpm, 2 min, R.T.) to remove residual buffer. The RNA was eluted by two times centrifugation of 30 µL of DEPC treated H₂O_{dd} (10,000 rpm, 1 min, R.T.). RNA concentration was determined using the *Nanodrop 1000* (Peachlab) and RNAs were stored at -20 °C.

2.2.2 Cell biological and virological methods

2.2.2.1 Cell culture

Passaging of cell lines

Cell lines were kept in specific growth media (see 2.1.7) and cell culture flasks (T25 or T75) in incubators at 37 °C and 5 % CO₂.

Adherent growing cells were trypsinated using Trypsin/EDTA and split every 3-4 days at various ratios from 1:4 to 1:10 depending on the growth rate of each cell line.

Cell lines growing in suspension were split directly.

BSR-T7/5 cells were supplemented with 2 mg/mL G418 (Geneticin) every other passage. U3A3 cells were supplemented with 2 mg/mL G418 (Geneticin) and 0.5 mg/mL Hygromycin every other passage.

Seeding of cells

Adherent growing cell lines were trypsinated and resuspended in growth medium. Cell numbers/mL were calculated based on estimated cell numbers/flask (T25: 3×10^6 ; T75: 9.4×10^6) or determined using a *Neubauer counting chamber*.

Cells were seeded in various culture dishes as follows:

dish	number of cells	total volume of growth media
10 cm ² dish	1.5×10^6	10 mL
6 cm ² dish	6×10^5	2-5 mL
3.5 cm ² dish	3×10^5	2 mL
6-well	3×10^5	2 mL
12-well	2×10^5	0.5-1 mL
24-well	1×10^5	300-500 μ L
48-well	5×10^4	200-400 μ L
96-well	$1-2 \times 10^4$	100-200 μ L

2.2.2.2 Isolation and cultivation of bone marrow derived cells (BMDCs)

Femur and tibia were isolated from hindlimbs of C57/BL6 mice and bone marrow was extracted by extensively flushing with 1x PBS. Bone marrow was passed through a 40 μ m cell strainer using 1x PBS and the cell suspension was centrifuged (400 g; 4°C; 7 min).

The supernatant was discarded and the cell pellet was resuspended in 2 mL of 1x ACK and incubated at R.T. for 2 min (erythrocyte lysis). 28 mL of 1x PBS

were added to stop the lysis process and the cells were pelleted again by centrifugation (400 g; 4 °C; 7 min).

The pellet was resuspended in 10 mL of 1x PBS and the cell number was determined using a *Neubauer counting chamber*. $2\text{-}3 \times 10^6$ cells/mL were cultivated in T25 cell culture flasks.

To stimulate differentiation of BMDCs into pDCs, 20 ng/mL of human recombinant Flt3-L as well as 50 μM of β -mercaptoethanol were added to the cell culture and cells were incubated at 37 °C and 5 % CO₂ for 7 days.

2.2.2.3 Transfection

Cells were transfected with DNA, RNA or peptides using *Lipofectamine 2000* (Invitrogen) or calciumphosphate method (*Mammalian Transfection Kit*; Stratagene) according to the manuals.

For co-immunoprecipitation assays, a solution containing 1 $\mu\text{g}/\mu\text{L}$ PEI instead of *Lipofectamine 2000* solution was used following the *Lipofectamine 2000* protocol.

2.2.2.4 Infection assays

According cell numbers were seeded in multiwell plates and directly infected in suspension with calculated MOIs of rapidly thawed virus stocks.

2.2.2.5 Generation of MV stocks

Two confluent T75 flasks of Vero cells were harvested and pelleted by centrifugation (1,600 rpm, 4 °C, 10 min). The supernatant was discarded, cells were resuspended in 500 μL of growth medium and infected with MV to an MOI = 0.25. The total volume was adjusted to 2.5 mL and the suspension was incubated at 37 °C for 1 h with shaking gently every 10 min. Afterwards, the

infected cells were seeded equally in 6 T75 cell culture flasks with a total of 16 mL growth medium/flask and incubated at 37 °C for 40-48 h.

As soon as most cells had formed numerous small syncytia, the cells were frozen at -20 °C. Cells were thawed on ice and lysates were cleared from cell debris by centrifugation (1,600 rpm, 4 °C, 10 min). Cleared lysates were aliquoted and stored at -86 °C.

2.2.2.6 Generation of RV stocks

One confluent T25 flask of BSR-T7/5 cells was split 1:4, the cells were infected with RV at an MOI = 0.1 and incubated at 37 °C.

The supernatant was collected 72 h p.i. (1st harvest), cleared from cell debris by centrifugation (1,600 rpm, 4 °C, 10 min), aliquoted and stored at -86 °C. Cells were supplied with fresh growth medium and incubated at 37 °C.

A 2nd harvest was performed analogous to the first harvest 144 h p.i.

2.2.2.7 Generation of recombinant RV (helper virus free)

BSR-T7/5 cells were seeded in 6-well plates 16 h prior to transfection. Growth medium was replaced with D-MEM 1 h prior to transfection.

10 µg of pSAD (RV genome encoding plasmid) and 5 µg pTIT-RV-N, 2.5 µg pTIT-RV-P and 2.5 µg pTIT-RV-L helper plasmids were transfected using the calciumphosphate method. The cells were washed twice with growth medium, supplied with 2 mL of growth medium 3.5 h p.tr. and incubated at 37 °C for 72 h.

The supernatant was collected 72 h p.tr., cell debris was removed by centrifugation (1,600 rpm, 4 °C, 10 min) and put on freshly seeded BSR-T7/5 cells in 6-wells. These were incubated at 37 °C for 72 h (Supernatant passage 1A). The transfected cells were supplied with 2 mL of fresh growth medium and incubated at 37 °C for another 72 h.

The supernatants of the transfected cells were collected again 144 h p.tr. and treated as before (Supernatant passage 1B). The transfected cells were trypsinized and 25 % of the cells were seeded in new 6-wells (Split), whereas 75 % of the cells were seeded in T25 cell culture flasks and incubated at 37 °C for further 72 h.

All 6-wells (Supernatant passage 1A, 1B; Split) were analyzed by IF using acetone fixation and FITC-labelled anti-N antibody (see 2.2.3.7) for the formation of viral foci.

The supernatants of virus containing T25 cell culture flasks were harvested, cell debris was removed by centrifugation (1,600 rpm, 4 °C, 10 min), supernatants were aliquoted and stored at -86 °C. Viral titers were determined as described in 2.2.2.8.

2.2.2.8 Titration of virus stocks

In case of MV, Vero cells were used for titration of virus stocks, in case of RV, BSR-T7/5 cells were used.

2×10^4 cells were seeded into 96-wells to a total volume of 100 μ L/well and incubated at 37 °C for 2 h.

500 μ L of virus stocks were thawed on ice and serially diluted 1:10, resulting in dilution series from (10^0 [=undiluted] to 10^{-8}).

100 μ L of each dilution was added to one well in duplicates and cells were incubated at 37 °C for 48 h.

Cells were fixed using the PFA/ NH_4Cl (for MV) or acetone (for RV) protocol (see 2.2.3.7). Cells were stained with diluted FITC-labelled anti-N antibodies (MV: Millipore; RV: FDI) and incubated either at 4 °C (MV) or 37 °C (RV) for 2 h.

Foci were counted from each well using a UV microscope (Olympus) and foci forming units per mL (ffu/mL) were calculated from these results.

2.2.3 Biochemical and immunological methods

2.2.3.1 Luciferase reporter gene assays

The *Dual luciferase reporter gene system* (Promega) was used according to the manual with a few modifications.

1×10^5 cells/well of HEK-293T, Huh7.5, or BSR-T7/5 cells were seeded approx. 16 h prior to transfection in 24-well plates in a total volume of 300 μ L.

Cells were transfected using *Lipofectamine 2000* with 100 ng of firefly-reporter plasmid, 10 ng of renilla-reporter plasmid and various expression plasmids with a total DNA amount of 0.5 – 2 μ g/well.

In case of stimulation with RLR-ligands, TLR-ligands, or interferon, stimulating agents were added to the medium 6 h p. tr.

Cells were lysed 24 h p. tr. using 200 μ L of 1x Passive Lysis Buffer (Promega) and 20 μ L of each lysate was transferred to a 96-well plate for luminescence. Measurement of luciferase activity was performed in a *LB 960 Luminometer* (Berthold) using 40 μ L of each substrate solution and a measuring time of 5 s/well for each luciferase. Results were analyzed using the *MikroWin 2000* (Mikrotek) and *Microsoft Excel* (Microsoft) software. Assays were performed in at least triplicates and mean values and standard deviation were calculated.

2.2.3.2 Co-Immunoprecipitation

6×10^5 cells of HEK-293T cells were seeded in 6 cm² dishes approx. 16 h prior to transfection in a total volume of 2 mL.

Cells were transfected using *Lipofectamine 2000* or the PEI-method with various combinations of tagged and untagged cellular and viral protein expression vectors.

Cells were harvested 24 h p. tr. using 1 mL/well of PBS/EDTA and divided in a 900 μ L and a 100 μ L fraction. Both fractions were pelleted by centrifugation (2,500 rpm, 4 °C, 5 min). Supernatants were discarded and the 100 μ L pellets were taken up in 250 μ L of Protein lysis buffer (= 10 % input). The 900 μ L

pellets were lysed in 300-500 μ L of Co-IP buffer for 30-120 min at 4 °C on a rolling incubator. The cell debris was pelleted by centrifugation (14,000 rpm, 4 °C, 15 min) and the cleared supernatants were transferred on either Protein A-conjugated Sepharose beads for pull-down of Ig-tagged proteins or on FLAG M2-agarose beads for pull-down of FLAG-tagged proteins. Cell lysates and beads were incubated for 2-4 h at 4 °C on a rolling incubator. Beads were pelleted by centrifugation (14,000 rpm, 4 °C, 2 min) and the supernatant was discarded. The beads were resuspended in 500 μ L Co-IP buffer and incubated for 10 min at 4 °C on a rolling incubator. This wash step was repeated 3 times. Afterwards pellets were resuspended in 250 μ L of Protein lysis buffer (= 90 % Co-IP) and the probes were subjected to denaturing PAA-gel electrophoresis and Western blotting.

2.2.3.3 Denaturing Polyacrylamid (PAA)-gel electrophoresis

component	separating gels				stacking gel 4 %
	8 %	10 %	12 %	16 %	
Acrylamid	7.2 mL	9.0 mL	10.8 mL	14.4 mL	1.4 mL
Jagow gel buffer	12.0 mL	12.0 mL	12.0 mL	12.0 mL	3.5 mL
H ₂ O _{dd}	14.6 mL	12.9 mL	11.1 mL	7.4 mL	9.0 mL
Glycerol	2.0 mL	2.0 mL	2.0 mL	2.0 mL	--
TEMED	17.0 μ L	17.0 μ L	17.0 μ L	17.0 μ L	18.0 μ L
10 % APS	175.0 μ L	175.0 μ L	175.0 μ L	175.0 μ L	116.0 μ L

Jagow PAA-separating gels were casted with a content of PAA varying from 8 to 16 % (standard: 10 %) and a standard size of approx. 15 x 10 cm² with the substances listed below. Following polymerization of the separating gels, 4 % Jagow stacking-gels were casted and 15-pocket or 24-pocket combs were used to create pockets.

Protein lysates were incubated at 95 °C for 5 min and centrifuged shortly to pellet residual cell debris or Co-IP beads. Up to 50 μ L of protein lysates were casted in each pocket. As molecular weight standard, 8 μ L of *Precision Plus Protein Standard* (Biorad) was loaded directly into one pocket.

Gel electrophoresis was carried out o/n at 30 – 75 V in an electrophoresis chamber filled with Jagow Kathode and Anode buffers.

2.2.3.4 Western blot (Semi dry method)

After gel electrophoresis, stacking gels were removed and separating gels were washed in 20 mL of 1x Semi dry buffer for 5 min.

Whatman paper and nitrocellulose membranes were soaked with 1x Semi dry buffer. In case of the usage of PVDF membranes instead of nitrocellulose membranes, these were activated by washing with methanol p.a. first, followed by washing with 1x Semi dry buffer.

Layers of Whatman paper, membrane, PAA gel and finally Whatman paper again were put on top of each other according to the manual of the blotting chamber (Peqlab). Blotting was performed at 400 mA/gel for 2 h.

Afterwards, membranes were incubated for at least 1 h in blocking solution (2.5 % milk powder or BSA in PBS/Tween (nitrocellulose) or 2.5 % milk powder or BSA in PBS (PVDF)).

2.2.3.5 Immunodetection

After blocking, membranes were washed extensively in PBS/Tween (e.g. 20 mL, 3x 10 min) followed by incubation with primary antibodies either at R.T. on a shaking device for 2 h or at 4 °C on a rolling incubator o/n.

Primary antibodies were diluted as recommended by the supplier in PBS/Tween supplemented with 0.04 % (w/v) sodium azide and 150 µg/mL BSA.

Following repeated washing steps with PBS/Tween (e.g. 20 mL, 3x 10 min), the membranes were incubated with HRP-conjugated secondary antibodies, which were diluted 1:10,000 in PBS/Tween at R.T. for 2 h. In some cases, HRP-conjugated Protein A (diluted 1:10,000) was used instead of antibodies.

Afterwards, excessive antibody was removed by extensive washing (e.g. 20 mL, 3x 10 min).

ECL solution (500 µL/blot) was prepared according to the supplier's manual, blots were incubated with the solution and chemiluminescence was detected immediately using *Hyperfilm-ECL* (GE Healthcare Amersham) for various periods of time.

2.2.3.6 Immunofluorescence (IF)

Cells were seeded on glass cover slips for confocal IF microscopy.

For fixation, cells were washed once with 1x PBS and incubated either with 80 % (v/v) acetone at 4 °C for 20 min, or with 3 % (w/v) PFA/PBS at R.T. for 20 min followed by incubation with 50 mM NH₄Cl/PBS at R.T. for 10 min.

In case of PFA/NH₄Cl fixation, cells were permeabilized by incubation with 0.5 % (v/v) Triton X-100/PBS at R.T. for 5 min.

Afterwards cells were incubated with 2.5 % (w/v) milk powder or BSA dissolved in 0.1 % (v/v) Triton X-100/PBS at R.T. or 4 °C for 15 – 30 min to block unspecific antibody binding sites.

After extended washing steps (e.g. 3x PBS), cells were incubated with primary antibody solution prepared in 0.1 % (v/v) Triton X-100/PBS according to the suppliers' recommendations (standard: 1:200 – 1:2,000) at R.T. for 45-120 min. The volume of the antibody solutions was kept as low as possible.

Afterwards cells were washed again 3x with PBS and incubated with fluorescence dye-labelled secondary antibody solution (standard: 1:200 in 0.1 % (v/v) Triton X-100/PBS) at R.T. or 4 °C for 120 min. In case of the usage of directly labelled primary antibodies, this step was skipped.

Cover slips were washed again 3x with PBS and 1x with H₂O_{dd} and fixed on microscope slides using *Vectashield mounting medium* (Vector Labs). Slides were dried o/n at 4 °C.

Confocal analysis was performed on a *Laser Scanning Microscope* (Zeiss) using *LSM Meta* software (Zeiss).

Non-confocal UV-microscopy was performed on a *UV-microscope* (Olympus) using *analySIS* software (Olympus).

2.2.3.7 Enzyme-linked immunosorbent assay (ELISA)

ELISA for murine IFN α was performed with supernatants of treated pDC cultures using the *Mouse Interferon Alpha (Mu-IFN- α) ELISA Kit* (PBL) according to the supplier's protocol. The readout was performed with a *Versamax Microplate reader* (Molecular Devices) using the software *Softmax Pro* (Molecular Devices) and *Microsoft Excel* (Microsoft).

2.2.3.8 Expression and Ni-NTA purification of recombinant proteins from bacteria

100 mL LB medium supplemented with 25 mg/mL of Kanamycin and 25 mg/mL of Chloramphenicol were inoculated with few μ L of transformed *Rosetta (DE3)* from glycerol stocks and grown at 37 °C o/n.

20 mL of this bacteria culture were inoculated to 1 L of LB-medium (+Kan/Cam) and grown at 37 °C to an OD = 0.5. As soon as this OD was reached, IPTG was added to the culture at a final concentration of 0.5 mM to induce protein expression from the pET28a-vector. The bacteria culture was shaken at 18-20 °C o/n.

After pelleting of the bacteria by centrifugation (6,000 rpm, 4°C, 40 min), the bacteria were resuspended in 5 mL/g wet weight of cold 1x Lysis/wash buffer and lysed by sonication at 4 °C for 10-30 min.

The suspension was cleared from cell debris by centrifugation (17,000 rpm, 4 °C, 45 min) and the supernatant was incubated with Ni-NTA agarose beads (1 mL/ 10 mL lysate) on a rolling incubator at 4 °C for 2 h.

The lysate-beads-suspension was loaded on a chromatography column at 4 °C and the flow through was collected. The beads were washed with 10 mL of cold

1x Lysis/wash buffer three times and the wash fractions were collected. Afterwards, resin bound protein was eluted by 5x 3 mL of 1x Elution buffer. All fractions were collected separately.

25 μ L of each collected fraction were mixed with an equal amount of Protein lysis buffer and subjected to PAA gel-electrophoresis. The gels were stained with Coomassie blue to visualize protein content.

Elution fractions containing protein of the predicted size were combined and dialyzed against 1x ATPase buffer.

In case of low protein content, the yielding solution was concentrated using *Amicon Ultra-15 Centrifugal Filter Devices* by centrifugation (3,500 rpm; 4°C; 10-60 min).

Protein content was determined using the *BCA Protein Assay Kit* (Pierce).

Protein lysates were shock frosted in liquid nitrogen and stored at -86 °C.

2.2.3.9 *In vitro* kinase assays

Recombinant proteins were combined using 100 ng of recombinant kinases (His-IKK α / -IKK β / -TBK1) per reaction volume, 100 – 500 ng of substrate (GST-I- κ B- α / His-IRF7) and increasing amounts of recombinant viral proteins (His-MV-V / -MV-P / fragments), varying from 0 – 1,600 pmol / reaction volume.

In a second vial, 5x Kinase assay buffer and ATP (final conc. 200 μ M) were mixed and tracing amounts of γ -³²P-labelled ATP were added. The ATP reaction mix was added to start the reaction. Aliquots were taken from the reaction volume at defined time points and mixed with Protein lysis buffer to stop the reaction.

The lysates were separated using PAA gel electrophoresis (10 % PAA-Gel; 40 V; o/n) and blotted on nitrocellulose or PVDF membranes (400 mA; 2 h). The membranes were exposed to a *PhosphoScreen* (Molecular Dynamics) for 2 – 72 h and screens were scanned using a *STORM Scanner* (Molecular Dynamics).

Images were analyzed using the *ImageQuant* (Molecular Dynamics) and *Microsoft Excel* (Microsoft) software.

2.2.3.10 *In vivo* ³²P-labelling

6x10⁵ Huh7.5 cells were seeded in 6 cm culture dishes and transfected with plasmids encoding Fl-tagged IKK α , IRF7, and MV V (2 μ g/plasmid) using *Lipofectamine 2000*. Cells were washed three times with PKRB and pulsed with 1 mCi/well of H₃³²PO₄ (in PKRB) 3 h p. tr. for further 3 h. Afterwards, PKRB was removed, cells were washed once with growth medium and incubated for 18 h at 37 °C and 5 % CO₂.

Fl-tagged proteins were pulled down using the *anti-FLAG® M2 affinity gel* (Sigma-Aldrich) as described in section 2.2.3.2. After SDS-PAGE (1 % PAA; 60 V; o/n) and Western blotting (nitrocellulose membrane; 400 mA; 2 h), the blots were exposed to a *PhosphoScreen* for 72 h and autoradiography was detected as described above.

2.2.3.11 Northern blot

Total RNA extracts of infected BSR-T7/5 cells were prepared 48 h p. i. as described above (see section 2.2.1.5). 2 μ g total RNA were adjusted to 7.2 μ L total volume. 3 μ L of 5x Phosphate buffer and 1.8 μ L of glyoxal solution were added. The mixture was heated to 56 °C for 30 – 45 min and spinned down. Finally, 3 μ L of Blue juice were added to the solution.

2 g of agarose (RNA grade) were dissolved in 167.3 mL of H₂O_{dd} (ultrapure) and 4 mL of 50x Phosphate buffer by heating and stirring. 26.7 mL of 37 % formaldehyde were added to the solution after cooling down to approx. 30 °C and the final volume was adjusted to 200 mL with H₂O_{dd} (ultrapure). A 24 cm x 20 cm gel was casted from the solution.

RNA probes were loaded to the gel and electrophoresis was performed using 1x Phosphate buffer at 25 V o/n. RNA was stained using acridine orange solution and 1x Phosphate buffer as washing solution to visualize rRNAs.

The RNA was transferred to a nylon membrane (Stratagene®; 2 h, -100 mbar) using the *Vacu-Blot system* (Biometra®). After drying, the RNA was cross-linked with the membrane (0.125 J).

Probes were generated by radioactive labelling of specific PCR products (25 ng) with α -³²P-CTP using the *Ready prime II Kit* (GE Healthcare) according to the manual.

Membranes were pre-incubated with Zeta hybridising buffer (68 °C) for 10 min, then incubated with probes in 8 mL Zeta hybridising buffer at 68 °C o/n. Afterwards, the membranes were washed once with Zeta wash buffer 5 % and twice with Zeta wash buffer 1 % (68 °C; 20 min each). Membranes were dried and exposed to a *PhosphoScreen* o/n. Autoradiography was detected as described above.

3 Results

3.1 Reconstitution of MyD88-dependent induction of IFN α in cell lines and establishment of luciferase reporter gene assays

The MyD88-dependent induction of IFN α via TLR7/8/9 is naturally available only in pDCs. However, this highly specialized hematopoietic cell type is neither suitable for cultivation like an immortalized cell line and therefore has to be extracted freshly each time from blood probes or bone marrow, nor is it applicable for transfection of DNA or purified proteins.

For this reason, I decided to study the MyD88-dependent induction of IFN α in cultured cell lines, in which this signaling pathway naturally is not active, since main components, namely TLRs and the transcription factor IRF7, are not expressed constitutively. Therefore, as a first point, the signaling complex had to be reconstituted in those cell lines. It is a well established procedure to activate signaling processes simply by overexpressing components of the signaling complex. In this case, expression of IRF7 is essential, as this factor is not expressed in cell lines, but crucial for functional induction of IFN α . Overexpression of IRF7 of either human (h) or murine (m) origin by transfection of an expression vector resulted in a dose-dependent and strong activation of different IFN α promoters (α 1, α 4, and α 6), as could be shown in luciferase reporter gene assays (Fig. 7A). However, as I did not yet know how this signaling cascade is inhibited by MV, I also wanted to study the influence of other components of the signaling complex. Therefore, I decided to reduce the amount of transfected IRF7 expression vector to only intermediate induction activity and to increase the IFN α promoter activity by co-expression of MyD88 as scaffold protein for the signaling complex, and the crucial

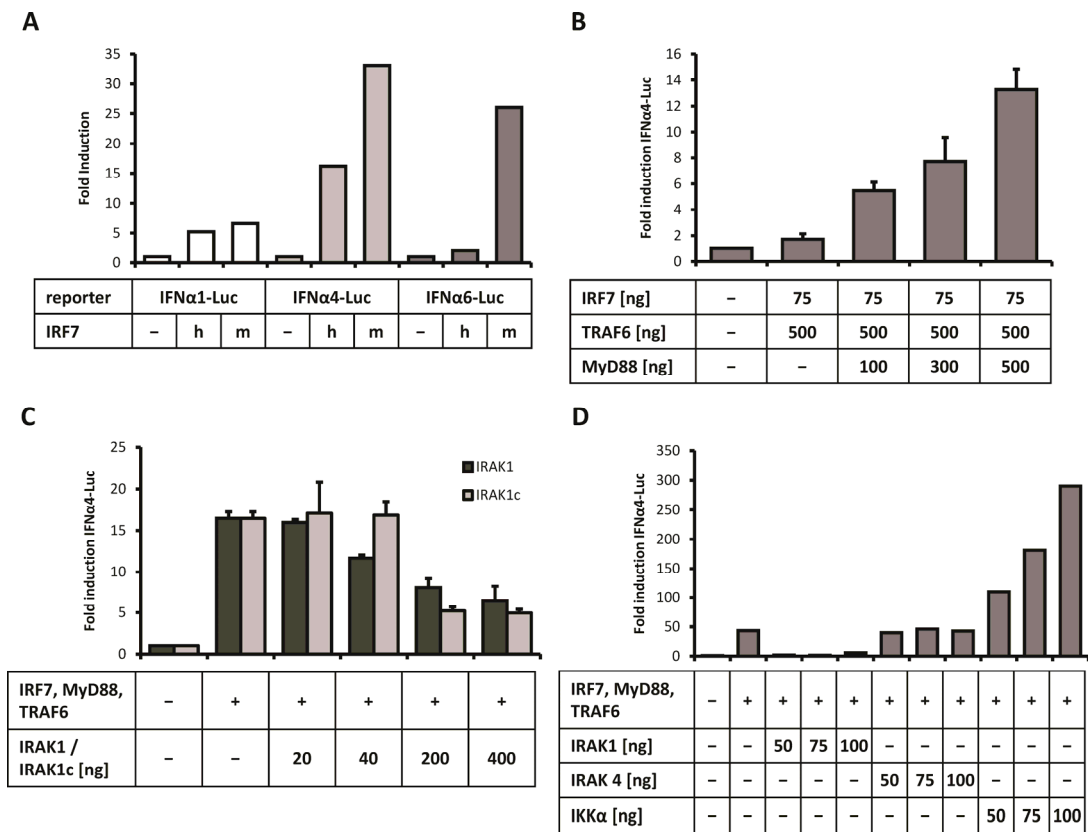


Figure 7: Reconstitution of the MyD88-dependent signaling complex leading to the induction of IFN α in cell lines.

(A) Luciferase reporter-gene assay with IRF7 constructs of human (h) and murine (m) origin using reporter genes under the control of murine IFN α 1, α 4, and α 6 promoters. Murine IRF7 works best with IFN α 4- and IFN α 6-promoters. (B) Luciferase reporter-gene assay with IRF7, TRAF6, and increasing amounts of MyD88 using the IFN α 4-promoter driven reporter gene. Increasing amounts of MyD88 have a cumulative effect on the reporter activity. (C) Luciferase reporter gene assay with IRF7, MyD88, TRAF6, and increasing amounts of IRAK1 or IRAK1c constructs. Both splicing variants of IRAK1 have a negative impact on the induction of IFN α 4-promoter driven luciferase. (D) Luciferase reporter-gene assay with IRF7, MyD88, TRAF6, and increasing amounts of IRAK1, IRAK4, or IKK α . Only IKK α strongly enhances the IFN α 4-promoter driven expression of luciferase. All assays are normalized using co-transfection of CMV-promoter driven renilla luciferase. Mock transfection is set to 1.

E3-ubiquitin ligase TRAF6 (Fig. 7B). This resulted in a moderate increase of the promoter activity, which was dependent on the dose of transfected expression vectors, which was kept constant at 500 ng/well in case of TRAF6, but varied in case of MyD88 from 0 – 500 ng/well. Already co-transfection of only 100 ng of the MyD88 expression vector led to a 3-fold increase of the promoter activity.

Co-transfection of 500 ng of the expression vector increased the promoter activity by 7-fold, whereas co-transfection of the same amount of the TRAF6 expression vector resulted in less than 2-fold increase. However, the promoter activation was only moderate, so it was likely that still a crucial component was missing to completely reconstitute the signaling complex. Several kinases had been described to play a crucial role in the MyD88-dependent TLR-signaling, among them IRAK1, IRAK4, and IKK α . Overexpression of these kinases resulted in diverse phenotypes. Overexpression of IRAK1 and IRAK1c, a splicing variant of IRAK1, from 20 – 400 ng of expression vector resulted in a strong and dose-dependent inhibition of the IFN α promoter activity (Fig. 7C and D). Overexpression of IRAK4 by co-transfection of 50 – 100 ng of expression vector did not show a significant influence on the activation of the promoters (Fig. 7D). Only overexpression of IKK α showed a strong and dose-dependent increase of the signal, when comparable levels of the expression vector were co-transfected (50 – 100 ng/well). This indicated that IKK α is crucial for the activation of IRF7 (Fig. 7D).

Optimization of the protocol resulted an optimal ratio of 1:5:5:5 of expression plasmids for IRF7:MyD88:TRAF6:IKK α . This transfection mix was further used to stimulate IFN α promoter activity in different cell lines like human HEK-293 or HEK-293T cells, Huh7.5 cells, or hamster BHK21-derived BSR-T7/5 cells. However, the total amount of transfected DNA varied in different cell lines and was optimized individually (data not shown). For Huh7.5 and HEK-293T cells, the amount of plasmid mix transfected was 300 ng/well.

Having established this tool, I now was able to analyze the influence of viral proteins on this signal transduction complex.

3.2 Identification of V as inhibitor of MyD88-dependent induction of IFN α

Several functions of paramyxoviral P gene products P, V, and C as antagonists of the innate immune system have already been described. I therefore

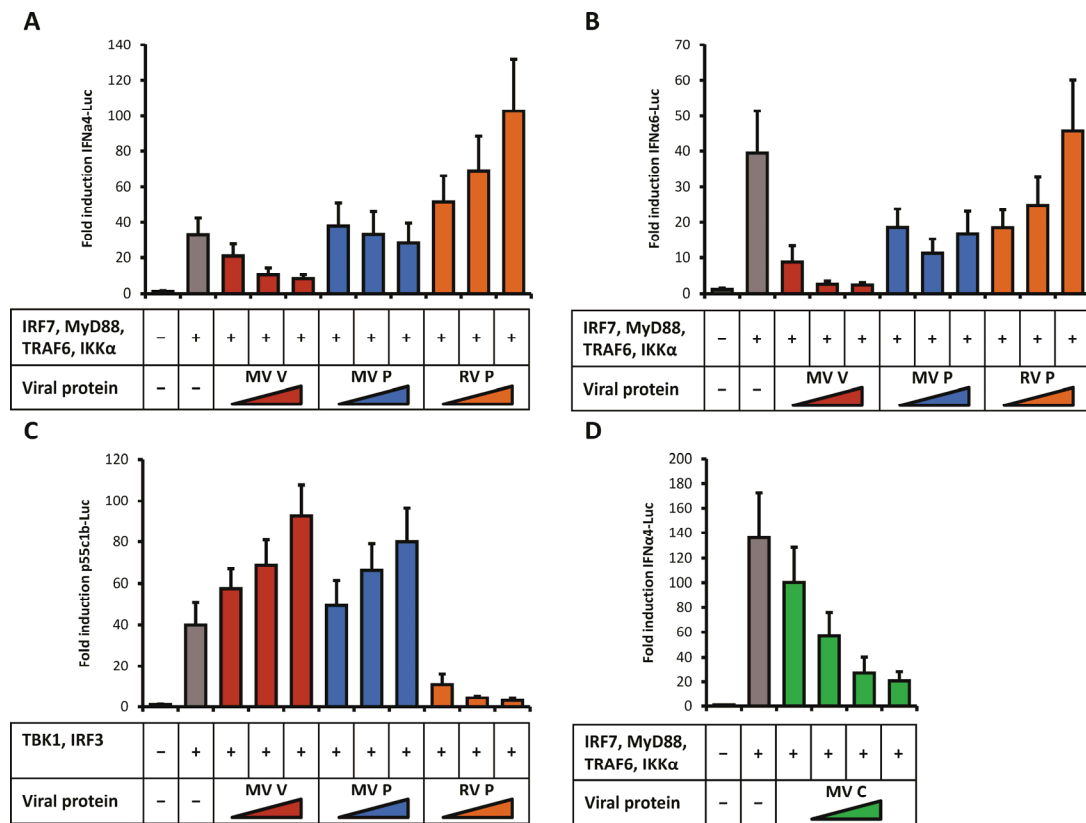


Figure 8: Identification of the viral antagonist of IFN α induction.

Luciferase reporter-gene assays with IRF7, MyD88, TRAF6 and IKK α , as well as luciferase under the control of various IFN-promoters. Co-transfection of increasing amounts of viral expression plasmids (250; 500; 750 ng/well). (A) IFN α 4-promoter driven luciferase expression is inhibited by MV V co-expression in a dose-dependent manner. MV P and RV P have no inhibitory activity. (B) IFN α 6-promoter driven luciferase expression is inhibited by MV V in a similar way like IFN α 4-Luc. (C) Luciferase reporter-gene assay with TBK1 and IRF3, inducing 55c1b (IRF3-binding site of IFN β -promoter) driven luciferase expression. MV P and V do not inhibit IFN β induction, but RV P strongly prevents IFN β induction. (D) MV C co-expression also negatively influences IFN α 4-promoter driven luciferase expression. All assays are normalized using co-transfection of CMV-promoter driven renilla luciferase. Mock transfection is set to 1.

investigated the role of these proteins in the inhibition of the MyD88-dependent IFN α inducing pathway. Huh7.5 cells were used in luciferase reporter gene assays as these cells express non-functional RIG-I, which is unable to induce IFN β production upon recognition of viral (triphosphate or double-stranded) RNA due to a point mutation.

Cells were co-transfected with the IFN α -inducing plasmid mix containing IRF7, MyD88, TRAF6, and IKK α expression vectors (300 ng/well), and increasing amounts of expression vectors (250 – 750 ng/well) for MV P, MV V (both

unable to express MV C due to silent mutations), or RV P, which was chosen as a control protein with well characterized functions in inhibition of TBK1/IRF3-mediated induction of IFN β . Cells were harvested 24 h p. tr. and cell lysates were analyzed for luciferase expression. Indeed, overexpression of MV V showed an inhibitory effect on the expression of firefly luciferase either under control of the IFN α 4 (Fig. 8A), or IFN α 6 promoter (Fig. 8B), indicating that MV V is able to counteract the activation of IFN α promoters by IRF7/MyD88/TRAF6/IKK α . In contrast, neither MV P nor RV P showed an inhibitory effect on this signaling complex.

Similar experiments were performed simulating the induction of IFN β by TLR3, or RIG-I, respectively. In this case, TBK1 and IRF3 expression vectors were transfected instead of the plasmid mix for IFN α induction. Expression of firefly luciferase was controlled by the p55-C1B promoter element, which consists of repeats of the IRF3-binding site of the natural IFN β promoter (Fig. 8C). Co-expression of RV P showed a dose-dependent inhibitory effect on this pathway, as it has been described earlier (Brzózka et al., 2005). In contrast, neither MV P, nor MV V showed a negative effect on this signal transduction complex.

I also examined whether MV C could play a role in inhibition of the MyD88-dependent IFN α inducing pathway. Therefore, MV C expression vector was co-transfected (500 – 1250 ng/well) with the IFN α -inducing plasmid mix and luciferase reporter gene assays were performed analyzing the IFN α 4 promoter activity (Fig. 8D). The result clearly shows that MV C also has a negative impact on the functionality and efficiency of the MyD88-dependent signaling complex.

In summary, MV V and C could be identified as antagonists of MV inhibiting the MyD88-dependent IFN α induction. In contrast, MV P does not share this function. Also, this inhibitory function of MV V is specific for the MyD88-dependent signaling complex consisting of IRF7/MyD88/TRAF6/IKK α , but the TRIF- or IPS1-dependent signaling complex (IRF3/TBK1) is not inhibited by MV V.

In the next step, I tried to identify the targets of MV V and C, assuming direct protein-protein interactions being responsible for the inhibitory effect.

3.3 Identification of interaction partners of V

I performed co-immunoprecipitation experiments in order to identify potential interaction partners of MV V. For this reason, expression vectors for MV P, V, and C proteins were generated in which an Ig-tag was fused N-terminally to the viral proteins (Ig-MV-P/V/C). These fusion proteins were co-expressed with FLAG®-tagged signaling components in HEK-293T cells. The cells were lysed 24 h p. tr. and Ig- tagged proteins were precipitated under native conditions using protein A conjugated sepharose beads. The precipitates were analyzed for interaction partners by Western blotting, using specific antibodies against signaling proteins or FLAG®-epitope tag antibody in case of FLAG®-tagged

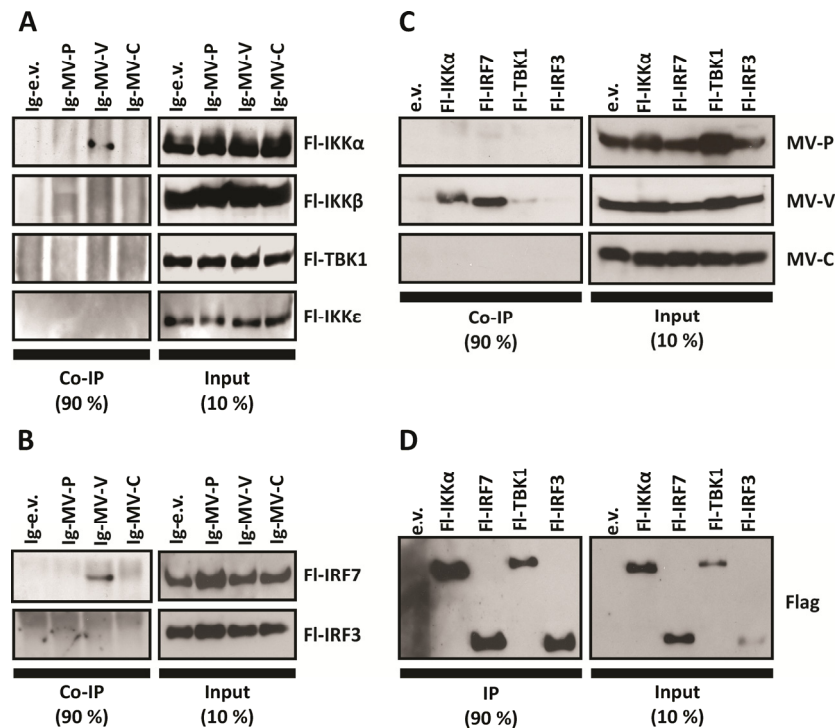


Figure 9: Identification of interaction partners of MV V.

Co-immunoprecipitation experiments reveal specific interaction of MV V with IKKα and IRF7. (A and B) Pull-down of Ig-tagged MV P, V, or C (or Ig-empty vector) with sepharose A beads. (A) Co-expression of the kinases FI-IKKα, -IKKβ, -TBK1, or -IKKε. Only FI-IKKα co-precipitates specifically with Ig-MV-V. (B) Co-expression of the transcription factors FI-IRF7 or FI-IRF3. FI-IRF7 co-precipitates with Ig-MV-V, while FI-IRF3 does not. (C and D) Pull-down of FI-tagged IKKα, IRF7, TBK1, or IRF3 (or empty vector) with Anti-FLAG® agarose beads. Co-expression of MV P, V, or C. (C) Only MV V co-precipitates with FI-IKKα, and -IRF7, while MV P and C do not. (D) IP of FI-tagged IKKα, IRF7, TBK1, and IRF3.

signaling proteins. Two components of the signaling complex were co-precipitated: both Fl-IKK α and Fl-IRF7 bound specifically to Ig-MV-V, but not to Ig-MV-P, or -C, or Ig-tag only (Fig. 9A and B). In contrast, neither the IKK α -homologs IKK β , IKK ϵ , or TBK1, nor the IRF7-homolog IRF3 bound specifically to Ig-MV-V, emphasizing the specificity of MV V for IKK α and IRF7 as interaction targets.

To confirm these results, extracts of cells co-expressing Fl-tagged signaling components and untagged MV P, V, or C were subjected to co-immunoprecipitation experiments using *anti-FLAG® agarose beads* to pull down Fl-tagged proteins and analyzed for binding of viral proteins by Western blot. Again, MV V was co-precipitated specifically with Fl-IKK α , as well as with Fl-IRF7, but not with Fl-TBK1, or Fl-IRF3 (Fig. 9C and D). Moreover, only MV V, but not MV P, or C bound to Fl-IKK α and Fl-IRF7.

Taken together, I could show that MV V specifically interacts with two components of the MyD88-dependent signaling complex. These are the transcription factor IRF7 and IKK α , the kinase responsible for the activation of IRF7. The interaction could be confirmed by co-immunoprecipitation experiments when pulling down either viral or signaling protein. Furthermore, MV V specifically interacted only with IKK α , and IRF7, but not with their homologous proteins, which are involved either in induction of IFN β (TBK1, IKK ϵ , IRF3), or in the activation of NF- κ B (IKK β). On the other hand, no interaction partners of MV C could be identified. This leads to the assumption that MV C may control gene expression on a different stage. I further concentrated on the function of MV V.

3.4 Identification of the V interaction domain

The next goal was to narrow down the domains of MV V interacting with IKK α and IRF7. As V and P share a common N-terminal domain of 231 amino acids, and only V, but not P showed binding to IKK α , and IRF7, the interaction with both signaling components must be mediated by the V-specific C-terminus of the protein, and not to the N-terminus. In order to confirm this theory, we

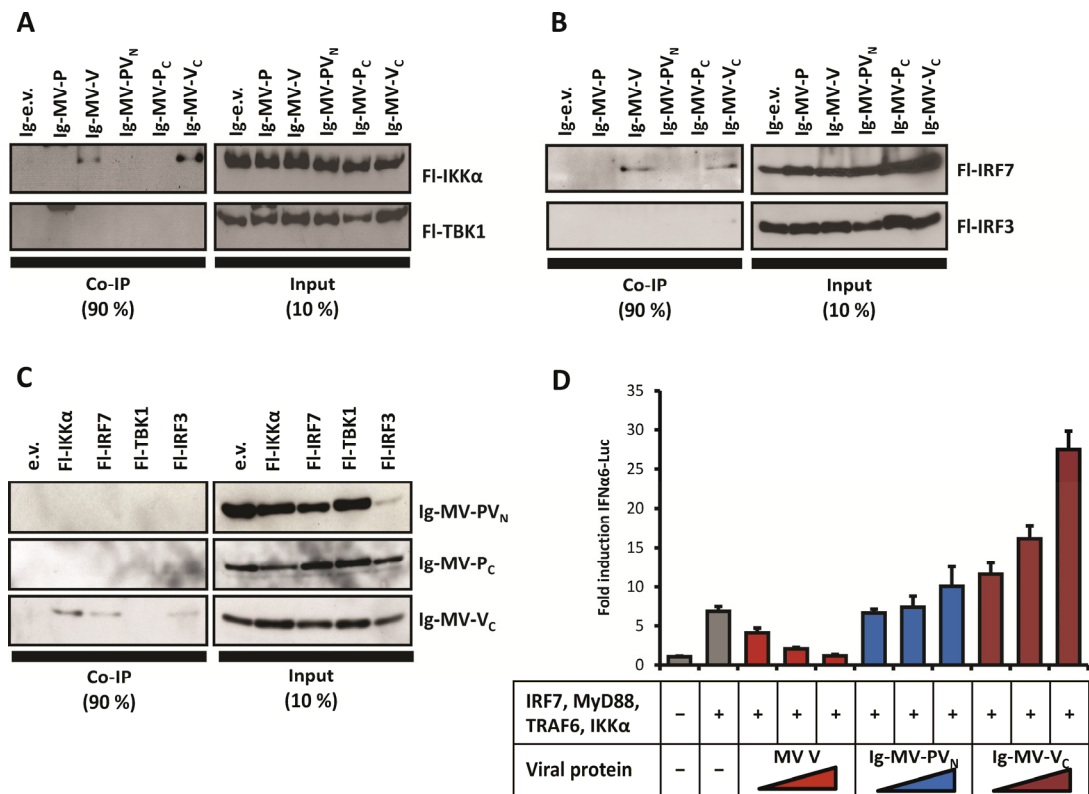


Figure 10: Identification of the MV V interaction domain.

(A – C) Co-immunoprecipitation experiments with truncated MV P and V narrow interaction domain of V down to the V C-terminus. (A) Pull-down of Ig-tagged P, V, or truncated PV_N, P_C, or V_C (or empty vector) with sepharose A beads. Co-expression of FI-IRKα, or -TBK1 reveals specific interaction of IKKα with the V_C domain of V. (B) Co-expression of FI-IRF7 or -IRF3 shows interaction of IRF7 with V_C. (C) Pull-down of FI-tagged IKKα, IRF7, TBK1, or IRF3 with anti-FLAG® agarose beads and co-expression of truncated Ig-tagged PV_N, P_C, or V_C. IKKα and IRF7 are bound specifically to the V_C domain. (D) Luciferase reporter gene assay with IRF7, MyD88, TRAF6, and IKKα, as well as luciferase under the control of the IFNα6-promoter. Co-expression of increasing amounts of (untagged) MV V, or Ig-tagged PV_N, or V_C (250; 500; 750 ng expression vector). While full-length MV V acts as inhibitor, truncated Ig-fusion proteins are unable to do so. The assay is normalized using co-transfection of CMV-promoter driven renilla luciferase. Mock transfection is set to 1.

generated expression vectors for N-terminally Ig-tagged PV_N (Ig-MV-PV_N; common N-terminal domain of P, and V), P_C (Ig-MV-P_C; P-specific C-terminus), and V_C (Ig-MV-V_C; V-specific C-terminus) proteins. Co-immunoprecipitation experiments were performed with signaling proteins using these protein domains. As expected, Ig-MV-V_C specifically pulled down both FI-IRKα and FI-IRF7, but not FI-TBK1 or FI-IRF3 (Fig. 10A and B). Neither Ig-MV-PV_N nor Ig-

MV-P_C was able to bind any of the tested proteins. Also, when pulling down Fl-IKK α , and Fl-IRF7, only Ig-MV-V_C could be co-precipitated, but not Ig-MV-PV_N or -P_C (Fig. 10C).

I also was interested in the question, whether the V_C domain alone would be sufficient for the inhibition of IFN α -promoter activity. I therefore performed a luciferase reporter gene assay, comparing the effect of full length MV V with the PV_N, and V_C fragments. Unfortunately, untagged V_C could not be expressed or was not detectable by Western blot due to its small MW. I therefore decided to test Ig-MV-V_C (and -PV_N) in the reporter gene system. In contrast to full length MV V, neither Ig-MV-PV_N nor Ig-MV-V_C was able to inhibit IFN α 6-promoter activity (Fig. 10D). Indeed, Ig-MV-V_C strongly increased the promoter activity, which might be due to unspecific effects of the Ig-tag. Therefore, the question, whether V_C alone is sufficient to inhibit IFN α induction could not be answered so far.

Taken together, these data support the assumption that the interaction of MV V with IKK α , and IRF7 requires the V-specific C-terminus. Both functions of MV V seem to be strongly connected to each other, as they are both performed by the same protein domain, which comprises a 68 aa Zinc-finger motif.

In the next step, the consequences of binding of MV V to IKK α and IRF7 on the signaling proteins had to be elucidated.

3.5 Influence of V on activation of IRF7 by IKK α

There are multiple possibilities, how binding of MV V to IKK α and IRF7 could block downstream signaling. On the one hand, MV V binding to IRF7 could capture the transcription factor and hinder its recruitment to the signaling complex – or, in case of binding post activation, the release of active IRF7, or its transport to the nucleus. On the other hand, binding to IKK α could inhibit its kinase activity, or the recruitment and activation of IRF7.

In order to address these questions, prokaryotic expression vectors for N-terminally 6xHis-tagged V (His-MV-V), and IRF7 (His-IRF7) were generated.

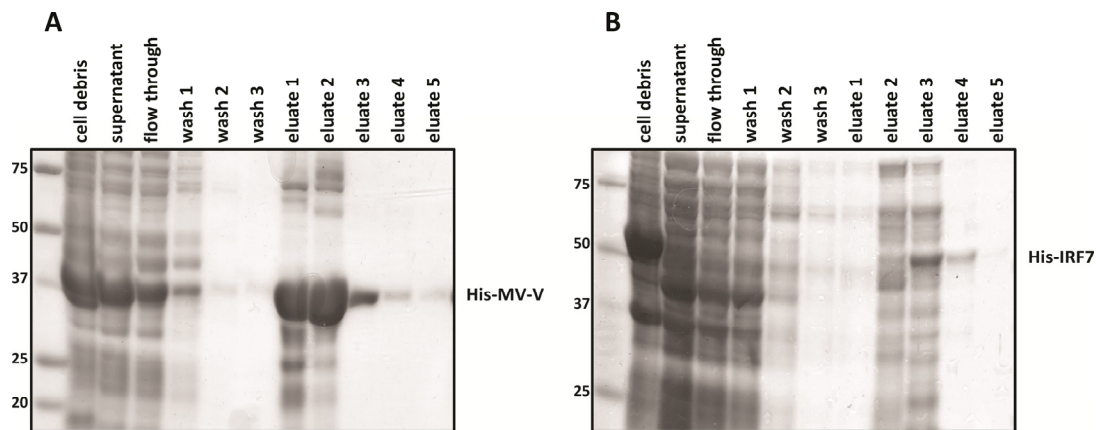


Figure 11: Purification of recombinant proteins from *E. coli*.

His-tagged MV V and IRF7 were expressed in *E. coli* and purified via Ni-NTA affinity chromatography. Different steps of the purification procedure were analyzed by SDS-PAGE and stained with Coomassie. (A) Purification of His-MV-V reveals high amounts of recombinant protein in the eluate. (B) His-IRF7 is expressed to lower levels than His-MV-V and only a minor fraction is found in the eluate.

The recombinant proteins were expressed in *E. coli* and purified via a Ni-NTA affinity-matrix (Fig. 11A and B). I performed *in vitro* kinase assays using 100 ng of commercially available recombinant His-IKK α and equal amounts of the purified His-IRF7 as substrate. Increasing amounts of His-MV-V (200 – 1600 pmol/reaction) were added and kinase activity within 16 min of reaction time was determined by ^{32}P -labeling of the recombinant proteins and Western blot analysis (Fig. 12A). Increasing amounts of MV V indeed had an inhibitory effect on kinase activity of IKK α in terms of generation of ^{32}P -labeled IRF7. However, total protein amounts of His-IKK α and His-IRF7 were equal in all reaction batches as confirmed by detection of total proteins using an anti-His antibody. Strikingly, His-MV-V itself acted as an excellent substrate for IKK α and was phosphorylated to a high extent. Quantification of the intensity of the ^{32}P -IRF7 bands gave a closer insight into the inhibitory mechanism (Fig. 12B). Low doses of His-MV-V (200, 400 pmol/reaction) could not prevent IRF7-phosphorylation over the reaction time. In contrast, high doses of His-MV-V (800, 1600 pmol/reaction) almost completely inhibited the phosphorylation of IRF7 even during 16 min of reaction time. This indicates a competitive mechanism by which MV V inhibits phosphorylation of IRF7. Accordingly, V binds to IKK α instead of IRF7, gets phosphorylated and is released again afterwards. As long

as unphosphorylated V is available, IRF7 phosphorylation is inhibited, but as soon as all available V has been phosphorylated, IRF7 can be recruited to IKK α and will be activated via phosphorylation.

To proof *in vivo* the data obtained *in vitro*, Fl-tagged versions of IKK α , IRF7, and MV V were transfected into HEK-293T cells and the cells were harvested 24 h p. tr. Native cell lysates were prepared and Fl-tagged components were precipitated using the *anti-FLAG® affinity gel*, which had been used also for co-immunoprecipitation experiments before. The precipitates were analyzed by

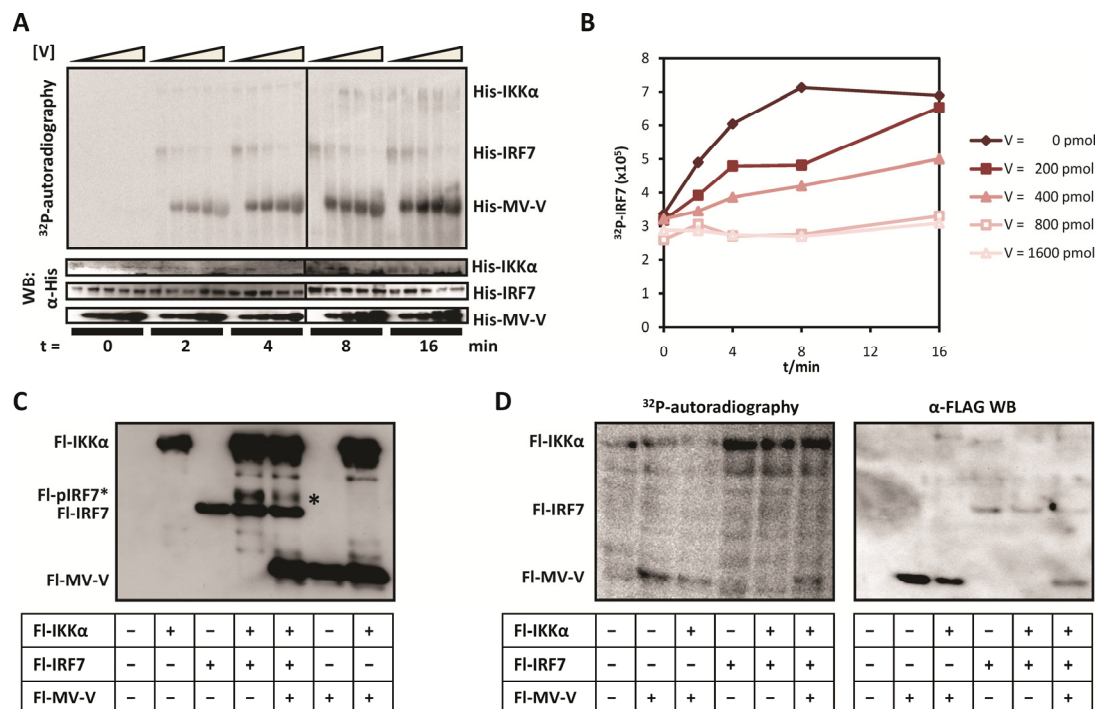


Figure 12: Inhibition of phosphorylation of IRF7 by IKK α in the presence of V.

(A and B) Time resolved *in vitro* kinase assay using recombinant His-IKK α , -IRF7, and MV-V. (A) Autoradiography of 32 P-labelled probes and Western blot control using an anti-His-tag antibody. While V acts as a substrate for IKK α , phosphorylation of IRF7 is inhibited in a dose-dependent manner. (B) Quantification of phospho-IRF7 bands. Increasing amounts of V lead to a stronger inhibition of IRF7-phosphorylation. (C) Pull-down of Fl-tagged IKK α , IRF7, and MV V with anti-FLAG® agarose beads. An additional shifted band of IRF7 (corresponding to pIRF7) appears in the presence of IKK α . Co-expression of V leads to a decrease of the amount of pIRF7. (D) *In vivo* 32 P-labeling and pull-down of Fl-IKK α , -IRF7, and -V. Autoradiography of pull-down extracts and Western blot control using an anti-FLAG® antibody. Phosphorylation of V can be detected in the presence or absence of Fl-IKK α . IRF7 phosphorylation cannot be detected although expression of Fl-IRF7 can.

Western blotting with anti-FLAG® antibody (Fig. 12C). Specific bands were obtained with MWs of approx. 86 kDa representing Fl-IKK α , 53 kDa representing Fl-IRF7, and 37 kDa representing Fl-MV-V. An additional specific band (marked by *) with a higher MW than Fl-IRF7 was observed in cells co-transfected with Fl-IKK α and Fl-IRF7, which most likely represents the phosphorylated (activated) form of Fl-IRF7. A clear reduction of the intensity of this band was observed, when Fl-MV-V was expressed in addition to Fl-IKK α and Fl-IRF7. These data confirm the inhibition of IRF7-phosphorylation by MV V in transfected cells. However, although large amounts of MV V were indicatedly apparent, phosphorylation of MV V could not be demonstrated by this experiment. For this reason, ³²P-labeling experiments in cell culture were performed. Huh7.5 cells were transfected with Fl-IKK α , Fl-IRF7, and Fl-MV-V and labeled with ³²P-phosphoric acid. Fl-tagged proteins were pulled down and analyzed by SDS-PAGE for incorporation of ³²P by autoradiography and for protein expression by Western blotting (Fig. 12D). In the Western blot control, Fl-IRF7 as well as Fl-MV-V could be detected, whereas the band for Fl-IKK α appeared to be very faint. However, on the autoradiogram, phosphorylation could be detected only for Fl-MV-V, but not for Fl-IRF7. As the levels of pulled down Fl-IRF7 in contrast to Fl-MV-V were not very high, this could be the reason for the undetectable levels of ³²P-IRF7. Furthermore, phosphorylation of Fl-MV-V seemed to be independent of the expression of Fl-IKK α , leading to the assumption, that Fl-MV-V is a potential substrate for endogenous IKK α and possibly other kinases.

To further characterize the phosphorylation sites of MV V, I expressed and purified different N- or C-terminally deleted mutants of His-MV-V, as well as His-MV-P and tested *in vitro* the ability of the proteins to serve as substrate for His-IKK α (Fig. 13A and B). Unexpectedly, all tested N-terminally deleted constructs showed similar phosphorylation levels (Fig. 13A). Only His-MV-V₂₃₂₋₂₉₉, which comprises the MV VC-terminus (V_C), did not appear as a clear band on the autoradiogram. Also full length His-MV-P, as well as the N-terminal domain of P/V (His-MV-PV₁₋₂₃₁), a shorter C-terminally deleted fragment, His-PV₁₋₁₆₄, and also the MV P C-terminus (His-MV-P₂₃₂₋₅₀₇) served as a substrate

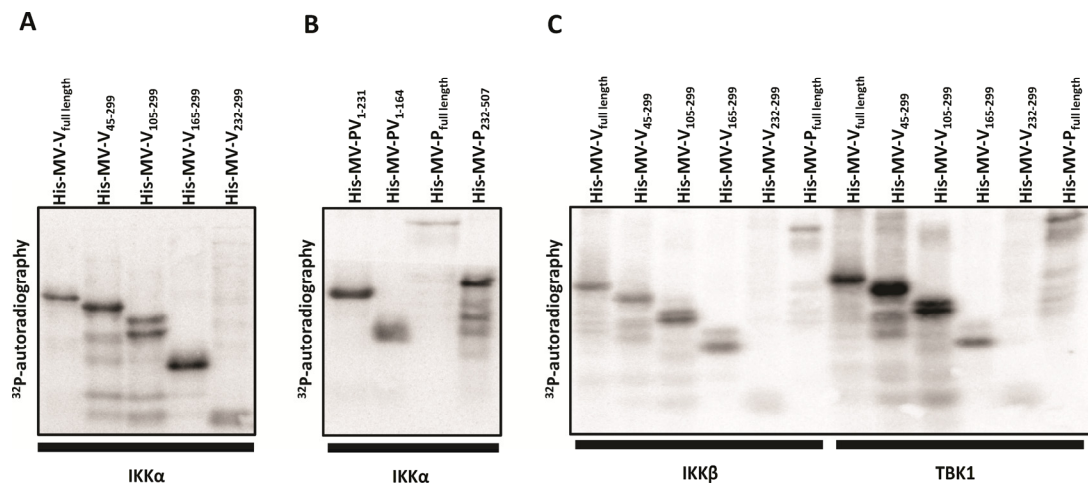


Figure 13: *In vitro* kinase assay with truncated MV V and P and kinases IKK α , IKK β , and TBK1.

N- and C-terminally truncated His-tagged MV V and P were expressed in bacteria, purified via Ni-NTA affinity chromatography and subjected to *in vitro kinase* assays to detect phosphorylation sites of V. Probes were analyzed by Western blot and ^{32}P -autoradiography. (A) All N-terminally deleted V constructs (V_{45-299} , $V_{105-299}$; $V_{165-299}$, $V_{232-299}$) are phosphorylated by IKK α comparable to full length V. (B) C-terminally deleted constructs (PV_{1-164} , PV_{1-231}) as well as full length P and P_C ($P_{232-507}$) serve as substrates for IKK α . (C) V, P, and N-terminally deleted V proteins serve as substrates for His-IKK β , and His-TBK1.

for His-IKK α (Fig. 13B). These data suggest that more than one phosphorylation site can be found in different domains of MV V, and also of MV P. Interestingly, His-MV-P may act as a substrate for IKK α *in vitro*, although an interaction of these proteins in co-immunoprecipitation experiments could not be detected.

Furthermore, His-IKK β , and His-TBK1 were tested for their ability to phosphorylate His-MV-V constructs *in vitro* (Fig. 13C). Like His-IKK α , both kinases were able to phosphorylate all tested constructs of His-MV-V except for His-MV- $V_{232-299}$.

As His-MV-P also served as a substrate for His-IKK α , I had to prove the specificity of His-MV-V to inhibit the phosphorylation of IRF7. Therefore, I performed in parallel *in vitro* kinase assays comparing the effects of His-MV-V and His-MV-P on IRF7- phosphorylation (Fig. 14A and B). In the autoradiogram,

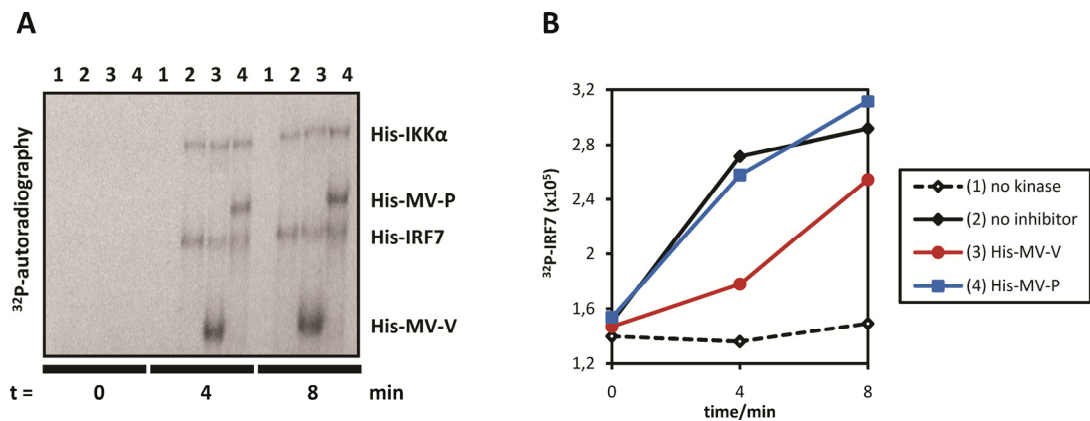


Figure 14: MV V, but not P is able to inhibit IRF7-phosphorylation *in vitro*.

Time resolved *in vitro* kinase assay comparing the effects of His-V and His-P on the phosphorylation of IRF7 by IKKα. Probes were analyzed by Western blot and ³²P-autoradiography. (A) The ³²P-autoradiogramm shows decreased levels of pIRF7 in presence of V, but not P. (B) Quantification of phospho-IRF7 bands confirm the inhibitory effect of V, but not of P.

phosphorylated His-MV-V as well as His-MV-P could be detected (Fig. 14A). However, although both recombinant proteins served as a substrate for His-IKKα, only His-MV-V showed a clear inhibitory effect on the phosphorylation of IRF7, as the amount of ³²P-IRF7 was clearly reduced in the presence of His-MV-V, but not of His-MV-P (Fig. 14B).

Taken together, we were able to show *in vitro* and in cell culture that MV V acts as a decoy substrate for IKKα, thereby preventing the phosphorylation and activation of IRF7. Phosphorylation sites of MV V could not be identified by *in vitro* kinase assays due to the high reactivity of recombinant kinases, which also may lead to the phosphorylation of non-physiological substrates. However, serving as a decoy substrate for IKKα does not seem to be sufficient for effective inhibition. Binding of MV V to IRF7 should also be an important factor of the inhibitory mechanism. For this reason, in the next step we focused on the interaction of V and IRF7.

3.6 Inhibition of both inactive and active IRF7 by V

Binding of MV V to IRF7 could inhibit the induction of IFN α both prior to and after phosphorylation of IRF7. Binding to inactive IRF7 would lead to the obstruction of recruitment of IRF7 to the signaling complex. On the other hand, I had to test the option, whether IRF7 could also be bound by MV V and thereby

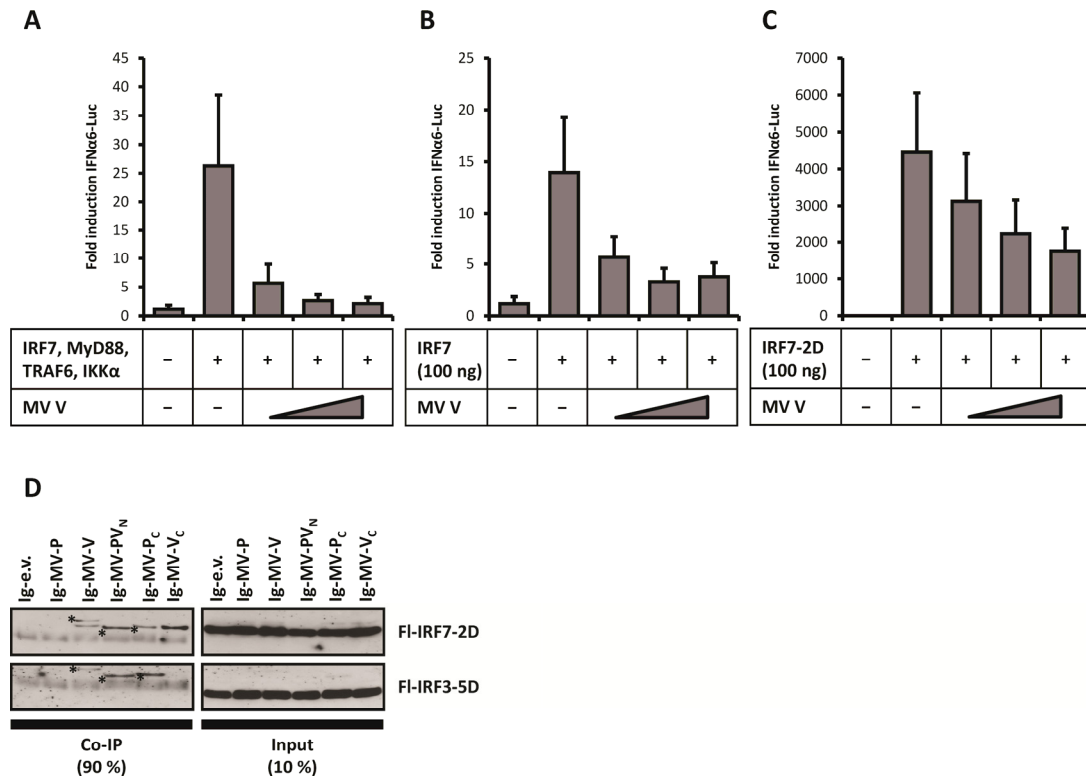


Figure 15: Inhibition of active IRF7 by MV V.

(A - C) Luciferase reporter gene assay using luciferase under the control of the IFN α 6-promoter. (A) IRF7, MyD88, TRAF6, and IKK α were expressed to stimulate luciferase expression. Increasing amounts of V (250; 500; 750 ng of expression vector) inhibit luciferase expression dose-dependently. (B) Only IRF7 (100 ng expression vector) was used to stimulate luciferase expression. Co-expression of V inhibits luciferase expression. (C) Constitutive active IRF7-2D (100 ng of expression vector) induce high amounts of IFN α 6-promoter driven luciferase. V is able to inhibit also activated IRF7. All assays are normalized using co-transfection of CMV-promoter driven renilla luciferase. Mock transfection is set to 1. (D) Pull-down of Ig-tagged MV P, V, PV_N, P_C, or V_C (or empty vector) with sepharose A beads. Co-expression of FI-tagged IRF7-2D or IRF3-5D. Only FI-IRF7-2D co-precipitates with Ig-MV-V and -V_C comparably to FI-IRF7. As the Ig-tag is recognized by the secondary antibody used, bands of Ig-MV-V, Ig-MV-PV_N, and Ig-MV-P_C are visible on both blots (marked by *) for FI-IRF7-2D and FI-IRF3-5D.

inhibited in its activated (phosphorylated) form. A mutant IRF7 construct has been shown to act as a constitutive active form of IRF7 (Lin et al., 2000). Two serine mutations to aspartate (S477D, S479D) generate a phosphomimetic form of IRF7 (IRF7-2D).

First, I compared the inhibitory effect of MV V on wild type and constitutive active IRF7 in our reporter gene system (Fig. 15A-C). The induction of IFN α 6-promoter activity either by expression of IRF7, MyD88, TRAF6, and IKK α as described above (including 20 ng of IRF7 expression vector), or by high level overexpression of IRF7 only (100 ng of plasmid), was inhibited efficiently by increasing amounts of MV V (Fig. 15A and B). Overexpression of IRF7-2D by transfection of 100 ng of the expression vector caused an approx. 200-fold higher activation of the IFN α 6-promoter, compared to the other methods, in which IRF7 needs to be phosphorylated first to reach an activated level (Fig. 15C). Also in this case, MV V showed a clear inhibitory effect in a dose-dependent manner, however, this effect was much less prominent (\approx 60 % reduction of promoter activity) compared to the transfection mix (\approx 92 %), or IRF7 only (\approx 73 % reduction).

Next, I performed co-immunoprecipitation experiments with Fl-IRF7-2D to prove that MV V is able to bind IRF7 independently of its phosphorylation status (Fig. 15D). Indeed, when pulling down Ig-MV-V, or Ig-MV-V_C, I was able to co-precipitate Fl-IRF7-2D, but not with Ig-MV-P, Ig-MV-PV_N, or Ig-MV-P_C. In contrast, Fl-IRF3-5D, a constitutive active form of IRF3 (Lin et al., 2000), did not bind to Ig-MV-V or any other tested construct. Obviously, bands of the Ig-tagged V, PV_N, and P_C (marked by *) reacted with the secondary antibody and, unfortunately, appeared in the blot at a position similar to Fl-IRF7-2D, as these constructs have similar MWs. The bands can also be observed in the blot against Fl-IRF3-5D, but this construct migrates to a lower MW.

In summary, these data support the hypothesis that MV V is able to bind both the inactive and the active form of IRF7, thereby preventing recruitment of IRF7 to the signaling complex, but also further downstream signaling of activated IRF7.

3.7 Infection studies of primary BMDC with recombinant rabies viruses expressing MV P, V, or C

So far, all experiments were done in transfectable cell lines using cDNA to overexpress the viral and cellular proteins, thereby creating an artificial system, in which the signaling complex of TLR7/9 was reconstituted and the effect of V was studied. Now, the data obtained should be confirmed in primary pDCs differentiated from murine bone marrow derived cells (BMDCs). As MV is almost

exclusively restricted to humans and some primates, and, as a second reason, a reverse genetics system for MV is not available in the lab, I generated recombinant rabies viruses (RV) derived from the laboratory strain SAD-L16 (in the following entitled as wt RV) expressing MV proteins P, V, or C from a newly introduced additional gene (Fig. 16A). The generation of these recombinant viruses was performed as previously described (Schnell et al., 1994). Furthermore, recombinant RVs with a deletion in the RV-P gene (Δ aa 181-186 = Δ IND2), which leads to a defect in inhibition of IFN β induction by the TBK1/IRF3-dependent RLR signaling (SAD-P Δ IND2; (Brzózka et al., 2005) and unpublished data), were engineered to express MV P, V or C.

The recombinant viruses were characterized on BSR-T7/5 cells by growth curves (Fig. 16B and C), on RNA level by Northern blot (Fig. 16E and F), and on protein expression level by Western blot (Fig. 16G). The different viruses showed similar growth kinetics in comparison with wt SAD-L16 (Fig. 16B) or SAD-P Δ IND2, respectively (Fig. 16C). Even the mutation in the essential RV P gene does not influence the growth of the recombinant viruses on IFN incompetent BSR-T7/5 cells. All viruses show comparable levels of mRNA for the RV nucleoprotein (RV N), as well as comparable amounts of genomic / antigenomic RNA (Fig. 16E). The different lengths of the genomic RNAs arise from the insertion of the ORFs of MV P, V, or C, which are approx. 1.6 kb, 1.0 kb, or 0.5 kb in length, respectively. Using a specific probe for the MV C coding sequence, we were able to visualize the mRNAs for MV P, V, and C, which are expressed from the particular viruses (Fig. 16F). The amounts of the different mRNAs are on equal levels. Western blot analysis of cell lysates revealed that all

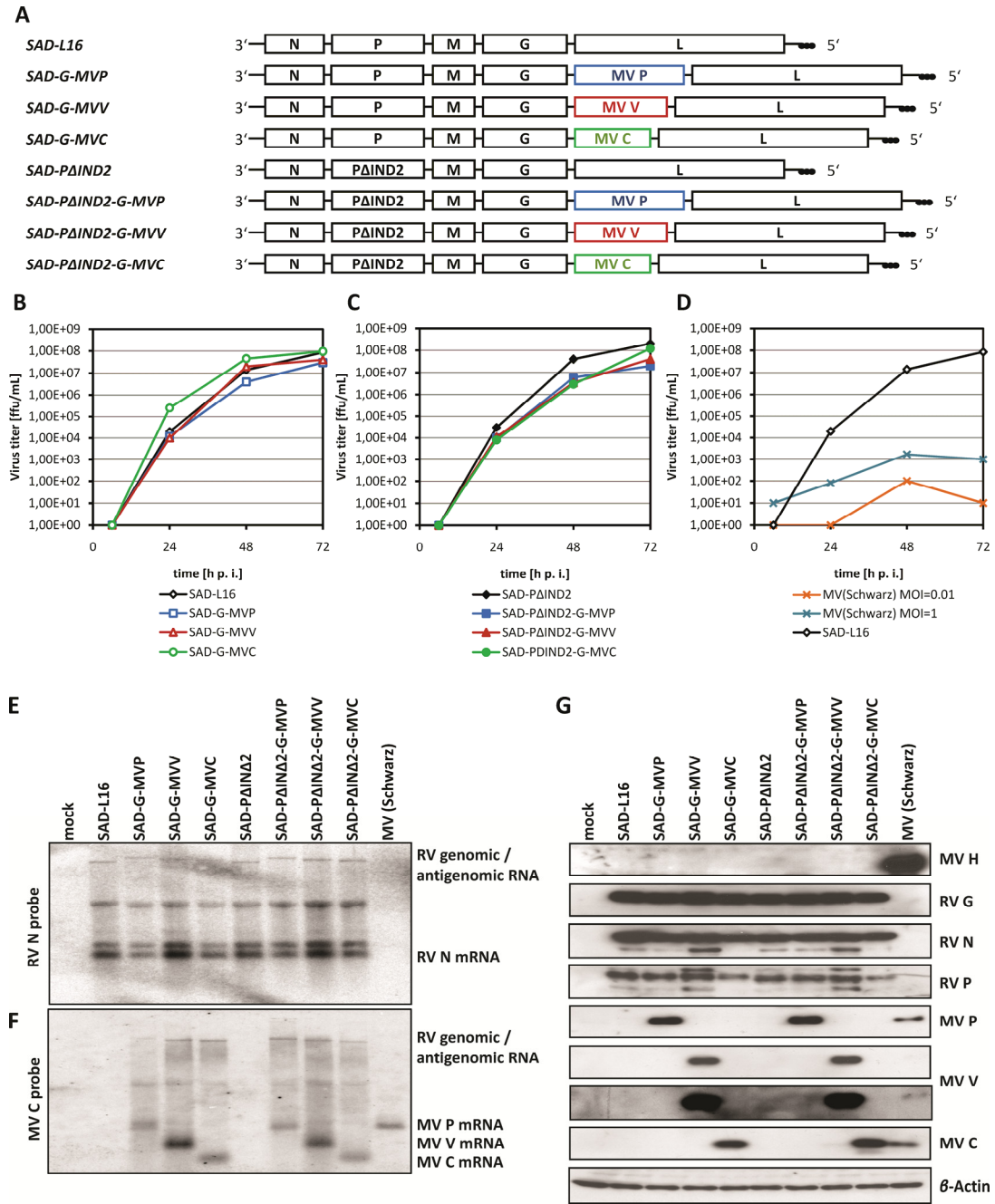


Figure 16: Generation and characterization of recombinant rabies viruses expressing MV P, V, or C.

(A) Schematic representation of the genomic organization of recombinant wt RV (SAD-L16) and recombinant RVs expressing MV P (SAD-G-MVP), V (SAD-G-MVV), or C (SAD-G-MVC) from an additional gene inserted between RV G and L genes. Corresponding recombinant RVs were generated using a recombinant RV with a deletion in the RV P gene (Δ IND2). (B – C) Characterization of recombinant RVs by growth curves on BSR-T7/5 cells. (B) Wt derived recombinant RVs grow to similar titers as SAD-L16. SAD-G-MVC grows with slightly increased kinetics. (C) SAD- Δ IND2 derived recombinant RVs grow to similar titers as parental virus. In addition, the growth kinetics are comparable to SAD-L16. (D) Comparison of growth kinetics of wt RV and MV (Schwarz strain) on BSR-T7/5 cells. Although the cells are of non-human origin,

the MV(Schwarz) produces detectable titers in the supernatant of infected cells. (E – F) Northern blot analysis of infected BSR-T7/5 cells. Total RNA was extracted 48 h p. i. (MOI = 1) and subjected to Northern blot analysis. (E) Detection of RV N mRNA and genomic/antigenomic RNA using a N specific ³²P-labeled probe. Different lengths of RV genomes due to the inserted genes are visible. The amount of N mRNA differs slightly among the viruses. (F) Detection of MV specific mRNAs and genomic/antigenomic RNA using a C specific ³²P-labeled probe. Genomes of rec. RVs expressing MV genes, as well as mRNAs for MV P, V, and C are detectable using the C specific probe. The genomes are of different length reflecting the length of the inserted ORFs (P: +1.6 kb; V: +1.0 kb; C: +0.5 kb). P/C and V/C mRNAs are detectable in MV infected cells. They appear as one band, as they differ only in 1 nt in length. MV genomic RNA is not detectable. (G) Western blot analysis of BSR-T7/5 cells infected (MOI = 1) with recombinant RVs or MV(Schwarz). Cell lysates were prepared 48 h p. i. Levels of RV specific proteins (G, N, P) are comparable in all recombinant viruses. The mutated PΔIND2 protein migrates to a slightly lower MW. MV P, V, and C are expressed by the respective viruses to comparable levels. In MV(Schwarz) infected cells, H, P, as well as C proteins are detectable, while V is expressed very weakly.

viruses show equal expression levels of RV essential proteins N, P, and G (Fig. 16G). In addition, MV P, V, or C are expressed to a high extent from respective recombinant viruses.

In these experiments, we infected BSR-T7/5 cells also with MV (Schwarz strain). Although the cells are hamster derived, we clearly saw productive infection with MV, though at low level. On mRNA level, the MV P+C and V+C mRNAs, which differ only in one nucleotide in length, can be detected as a single band with the MV C probe (Fig. 16F). On protein level, high levels of MV H could be detected, as well as low levels of MV P, and the non-structural MV C, which should be detectable only after successful infection and viral transcription (Fig. 16G). MV V levels were very low in these experiments, but detectable after long exposure of the hyperfilm. Virus progeny could also be shown by growth curves (Fig. 16D). Notably, only virus titers from supernatants of infected cells were determined, although in the case of MV most of the virus is cell associated. MV infectivity was also determined on other non-human cell lines, like murine NA cells (data not shown and (Abdullah et al., 2009)).

The recombinant RVs and MV were used in the next step to analyze their ability to infect BMDC-derived murine pDCs and thereby inhibit the production of IFN α by these cells *in vitro*. BMDCs were extracted from femur and tibia of C57/BL6 mice and differentiated with Flt3-L into a cell population, which contained approx. 14 % of pDCs, as confirmed by FACS staining specific for CD11c and B220 (Fig. 17A). These cells were infected with recombinant RVs, or MV (Schwarz strain) at an MOI of 3. The cells were stimulated 24 h p. i. either with the TLR9 ligand CpG ODN2216 (3 μ g/mL), or with the TLR7 ligand R848 (2 μ g/mL), or left untreated. Supernatants and cells were harvested 48 h p. i. and murine IFN α specific ELISA was performed with the supernatants (Fig. 17B). PDCs produced low amounts of IFN α upon infection with recombinant RVs, or MV. No significant differences between different RVs, or between RV and MV infection were detectable. Uninfected pDCs responded with the

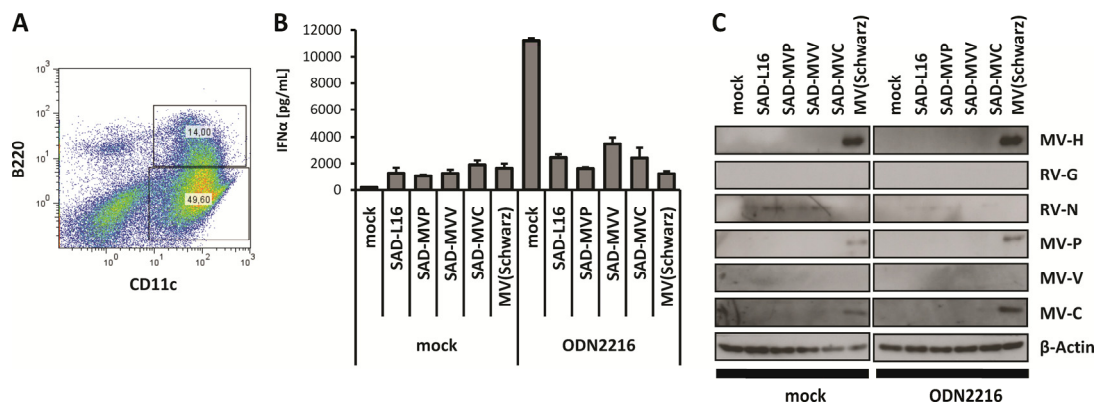


Figure 17: IFN α production in murine bone marrow-derived pDCs.

BMDCs were isolated from C57/BL6 mice and cultivated in the presence of Flt-3L. Cells were infected with recombinant RVs or MV(Schwarz) at a MOI of 3 and treated with 3 μ g/mL CpG ODN2216 24 h p. i., or left untreated. 24 h later, cells were harvested and lysed, and supernatants were harvested and IFN α production was measured by ELISA. (A) FACS analysis of cultivated BMDCs 7 d p. treatment with Flt-3L. Cells were stained against pDC markers B220 and CD11c. 14 % of the cells were B220⁺ CD11c⁺ and therefore claimed to represent pDCs. 49.6 % were B220⁻ CD11c⁺ mDCs. (B) IFN α ELISA of supernatants. All infected cells produce low amounts of IFN α in comparison to uninfected cells. Uninfected cells produce high amounts of IFN α upon stimulation with CpG ODN2216. In infected cells, IFN α production upon ODN2216 treatment is abolished. (C) Western blot analysis of cell lysates. Infection was determined by viral antigens (RV G, N; MV H, P, V, C) and compared to β -actin. While MV infection was successful, RV infection was poorly detectable.

production of high amounts of IFN α to treatment with ODN2216. Infection with MV, but also with wt RV, minimized the levels of IFN α in the supernatants almost to the levels of infected, but untreated cells. Additional expression of MV P, V, or C from the recombinant RVs did not significantly alter the levels of IFN α production. Only in case of infection with SAD-G-MVP a decrease of IFN α compared to wt RV was detectable. Infection was confirmed by Western blot analysis of the cell lysates (Fig. 17C). The murine pDCs were productively infected by MV, as MV H, P, and the non-structural C were expressed at detectable levels. In contrast, RV infection produced almost undetectable levels of RV N and G. As a consequence, MV P, V, and C expression was not detectable in the respective recombinant RV infected cells. Taken together, these results imply that infection of murine pDCs with MV leads to a block in TLR9 signaling. In contrast, RV infection might affect the cells in an early step of infection so that virus replication is hindered, as the Western blot control suggests. In addition it appears that the functionality of the pDCs is also drastically disturbed, as RV infected cells do not respond any more to ODN2216. One explanation might be that RV infection kills the cells at a very early stage of infection. Therefore, the recombinant RVs are not suitable to study the effect of MV V in primary dendritic cells.

3.8 Analysis of V of different strains – search for IFN α -ineffective V mutants

In the literature, many examples can be found, in which wt MV was attenuated by passaging on IFN-incompetent cell lines. As a result of this attenuation the viruses generally show an increased immunogenicity. Comparison of the V protein sequences of wt and attenuated MVs reveal specific mutations in the gene products (Fig. 18). As one example, attenuation of the MV strain G954 (G954-PBL) by passaging 13 times on Vero cells leads to a critical mutation in the V gene (H232D), which might have a negative effect on the functionality of the V C-terminus (Druelle et al., 2008). This attenuated virus (G954-V13) shows higher responsiveness to treatment with type-I IFN than the parental strain, implying a crucial role of V_C in the inhibition of JAK/STAT signaling, which has also been investigated *in vitro* (Ramachandran et al., 2008).

In addition to the G954 strain, the Davis87 strain was described to show a comparable phenotype in a rhesus macaque model (Bankamp et al., 2008). Interestingly, the attenuated Davis87 (D-CEF), which has been propagated on chicken embryonic fibroblasts (CEFs) for several passages, showed the same mutation H232D that was observed in G954-V13. Furthermore, the mutation Y110H appeared in Davis87 (D-CEF). This tyrosine residue has been shown to be critical for binding of STAT1, as the Y110H mutants of MV P, and V have been described to be defective in STAT1 binding (Ohno et al., 2004; Caignard et al., 2007; Devaux et al., 2007).

In the CAM-70 strain, which is a highly attenuated Japanese vaccine strain (Borges et al., 2008), Y110 is mutated to cysteine, which could result in the same STAT1-binding deficient phenotype as the Y110H mutation.

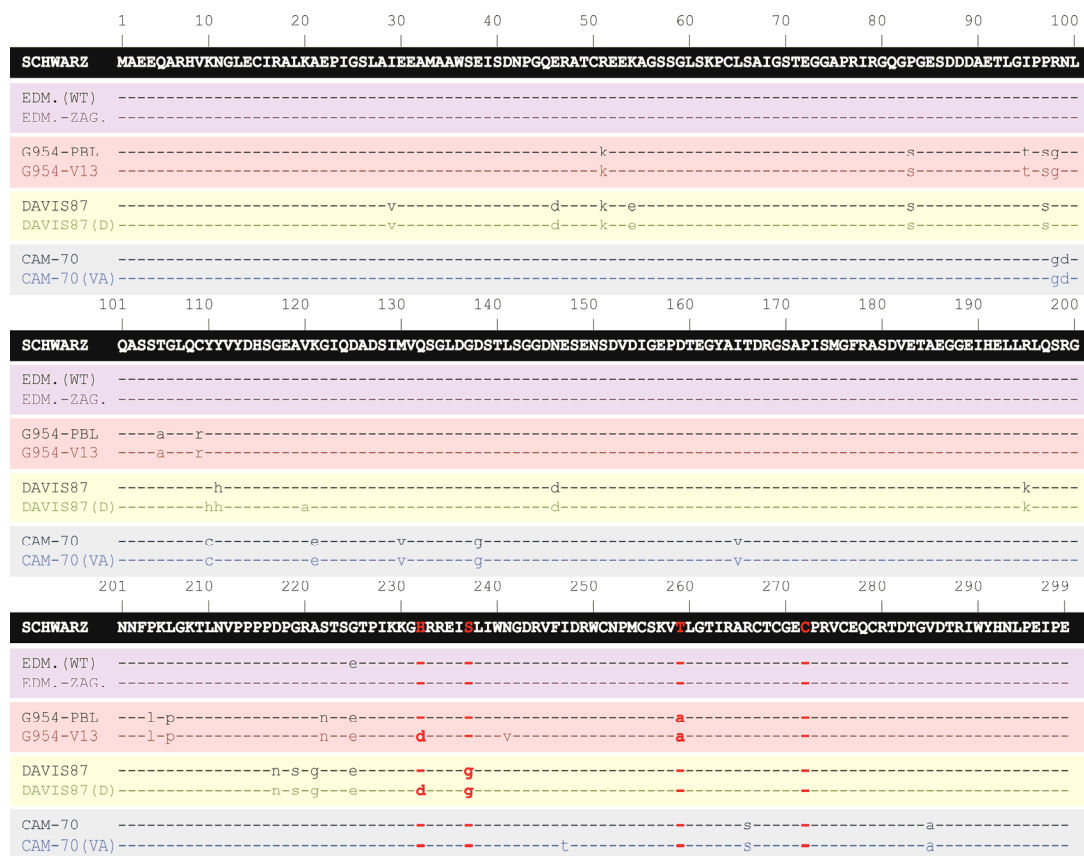


Figure 18: V protein amino acid sequence comparison of different MV strains.

MV (Schwarz strain) V sequence is compared to V sequences of wt and attenuated strains Edmonston wt (EDM. (WT)), Edmonston-Zagreb (EDM.-ZAG); G954-PBL, G954-V13; Davis87, Davis87 (D-CEF) (Davis87 (D)); CAM-70 and CAM-70 vaccine strain (CAM-70 (VA)). Amino acid mutations are indicated by single letter code. Mutations introduced into MV (Schwarz strain) V are highlighted in red.

In contrast, the V protein of the Edmonston wild-type strain, which is the parental strain of the Schwarz vaccine strain (as well as of other vaccine strains like Edmonston-Zagreb, Rubeovax, Moraten, and AIK-C), shows almost complete sequence identity to Schwarz strain V, except G225, which originally is a glutamic acid residue in Edmonston wt (Parks et al., 2001). This suggests that Schwarz strain V should have wt MV function.

The Davis87 and G954 strains bore two further mutations, which were interesting for our studies. S237G appeared both in the wt and attenuated Davis87 strain, T259A was present in the wt and attenuated G954 strain. Both mutations affected potential phosphorylation sites in the V_c domain, which could be of importance for the inhibition of IKK α .

In the following, H232D, H232D-S237G, and T259A mutations were introduced into the Schwarz strain V protein (Table 1). Additionally, the C272R mutant was generated, although this mutation has not been described to occur during attenuation. However, this residue has been described to be crucial for STAT2-binding activity of V (Ohno et al., 2004) and therefore was thought to exhibit a positive control for deficiency in IFN signaling.

Mutations were introduced into the V ORF by PCR mutagenesis as described in section 2.2.1.1.

Table 1: Nucleotide mutations introduced into MV(Schwarz) V to generate specific aa mutants.

mutant	wt amino acid	mutation	wt codon	mutation
MV V H232D	H232	D	C694	G
MV V H232D-S237G	H232	D	C694	G
	S237	G	A709	G
MV V T259A	T259	A	A775	G
MV V C272R	C272	R	T814	C
MV V H232D-C272R	H232	D	C694	G
	C272	R	T814	C

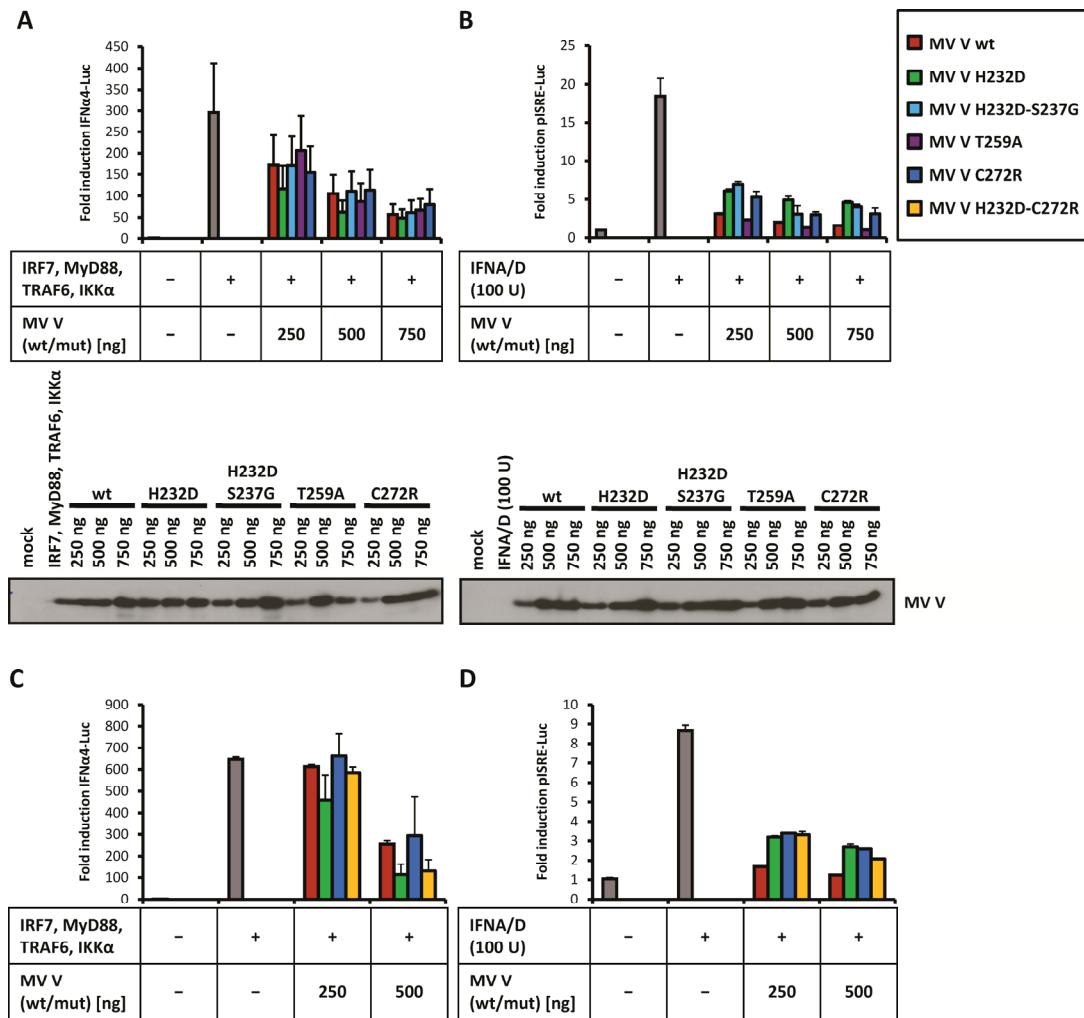


Figure 19: Analysis of V mutants for their capacity to inhibit IFN α induction and type-I IFN signaling.

Luciferase reporter-gene assays for IFN α induction or type-I IFN signaling. (A and C) IFN α 4-promoter driven luciferase expression by IRF7, MyD88, TRAF6, and IKK α . Increasing amounts of mutant V proteins (250; 500; 750 ng expression vector) show no or only little (H232D) differences from inhibition by V wt. (B and D) ISRE-promoter driven luciferase expression stimulated with 100 U/ well of recombinant type-I IFN A/D. Mutations of Zn-binding amino acids H232, and C272 show loss of inhibition capacity compared to V wt. All assays are normalized using co-transfection of CMV-promoter driven renilla luciferase. Mock transfection is set to 1.

(A and B) Western blot analysis of the luciferase assay lysates. The different V mutants are expressed like wt V dependent on the amount of transfected plasmid (250 / 500 / 750 ng).

The mutant V proteins were tested in the luciferase reporter gene system for their ability to inhibit the activation of the IFN α 4 promoter by the overexpression of IRF7/MyD88/TRAF6/IKK α and compared with wt V (Fig. 19A). All mutants showed similar inhibition capacities like wt V and were

expressed to similar levels as confirmed by Western blot analysis of the luciferase assay lysates. In contrast, when I investigated the functionality of the mutant V proteins in inhibition of type-I IFN signaling, I was able to observe significant effects of some mutants (Fig. 19B). Cells were transfected with different amounts of wt or mutant V, as well as a luciferase reporter controlled by the ISRE-promoter. Cells were stimulated with 100 U of recombinant type-I IFN (IFN α /D) 6 h p. tr. V constructs with mutations in the Zn-binding C-terminus showed significant defects in their ability to inhibit JAK/STAT signaling: H232D, H232D-S237G, and C272R all showed a decrease of the inhibitory function of approx. 50 %, which might be due to a destabilization of the Zn-finger domain (model see Fig. 20A). However, the remaining capacity to inhibit ISRE-Luc promoter activity was still very strong. Again, expression of all V constructs was analyzed by Western blot (Fig. 19B). All constructs were expressed to equal levels dependent on the amount of transfected expression vector. Therefore, I was interested, whether we could further destabilize the C-terminus by simultaneous mutation of two Zn-binding residues. I generated the H232D-C272R mutant and tested, whether this construct had lost its inhibitory function in both IFN α induction and type-I IFN signaling. In comparison with wt V or the single amino acid mutants H232D and C272R, the double mutant H232D-C272R did not show an altered phenotype in the inhibition of IFN α induction (Fig. 19C). In addition, also the inhibitory capacity in IFN signaling could not be further decreased by combining H232D and C272R mutations (Fig. 19D).

In summary, the approach of comparison of V sequences of different MV strains did not lead to the identification of crucial amino acids responsible for the inhibition of IFN α induction by MV V. However, I was able to show that the destabilization of the C-terminal domain of V leads to a decrease in the ability to block type-I IFN signaling, which might be due to weaker binding of STAT2. In the next step, I went further to analyze the sequences of V proteins of different paramyxoviruses.

3.9 Sequential and mutational analysis of paramyxoviral V proteins

V protein sequences of the following viruses from the subfamily of *Paramyxovirinae* were collected and aligned using the *ClustalX2* software (Larkin et al., 2007): Newcastle disease virus (Genus: *Avulavirus*), Hendra virus (HENV), Nipah virus (NiV; both *Henipavirus*), canine distemper virus (CDV), dolphin morbillivirus (DMV), measles virus, peste-des-petits-ruminants virus (PPRV), rinderpest virus (RPV; all *Morbillivirus*), Sendai virus (SenV;

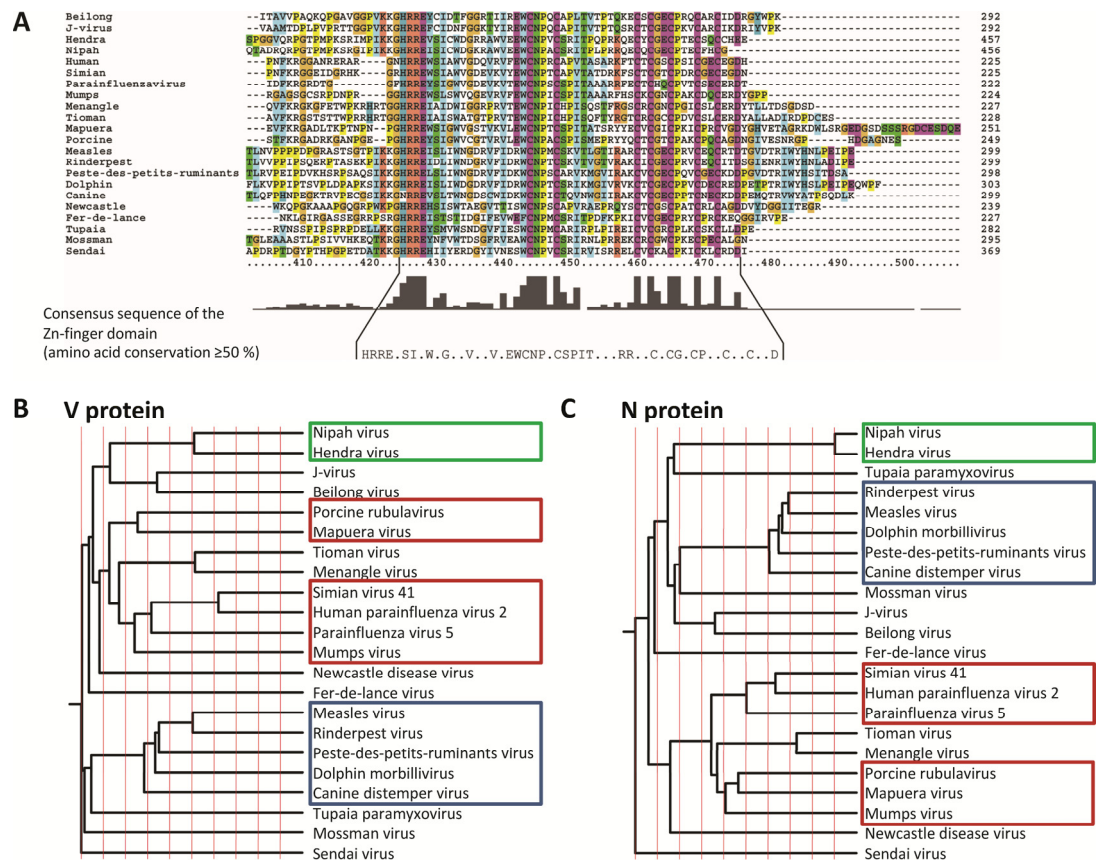


Figure 20: Amino acid sequence comparison of V from different *Paramyxovirinae*.

(A) Sequence alignment of the V_C domain of V using *ClustalX2*. The Zn-binding domain is highly conserved among almost all viral V proteins. A consensus sequence was generated by choosing amino acids with conservation of $\geq 50\%$. (B and C) Phylogenetic trees based on the complete V protein sequence (B) or N protein sequence (C) using *TraceSuite II*. The V protein based tree reveals grouping of V proteins according to the different genera. Similar results are obtained comparing N sequences. Colored frames indicate different genera. Red: *Rubulaviruses*; blue: *Morbilliviruses*; green: *Henipaviruses*. Unframed: other genera and unclassified *Paramyxovirinae*.

Respirovirus), human parainfluenza virus2 (hPIV2), Mapuera virus, mumps virus (MuV), parainfluenza virus 5 (PIV5; formerly known as simian virus 5 – SV5), porcine rubulavirus, simian virus 41 (all *Rubulavirus*), Beilong virus, fer-de-lance virus, J-virus, Menangle virus, Mossman virus, Tioman virus, and Tupaia virus (all unclassified *Paramyxovirinae*). The N-terminus of the V protein shows high variability over all *Paramyxovirinae*, but sequences within the different genera show high homology (see Appendix B). Notably, the C-terminal Zn-finger domain is conserved among all viruses (Fig. 20A). This

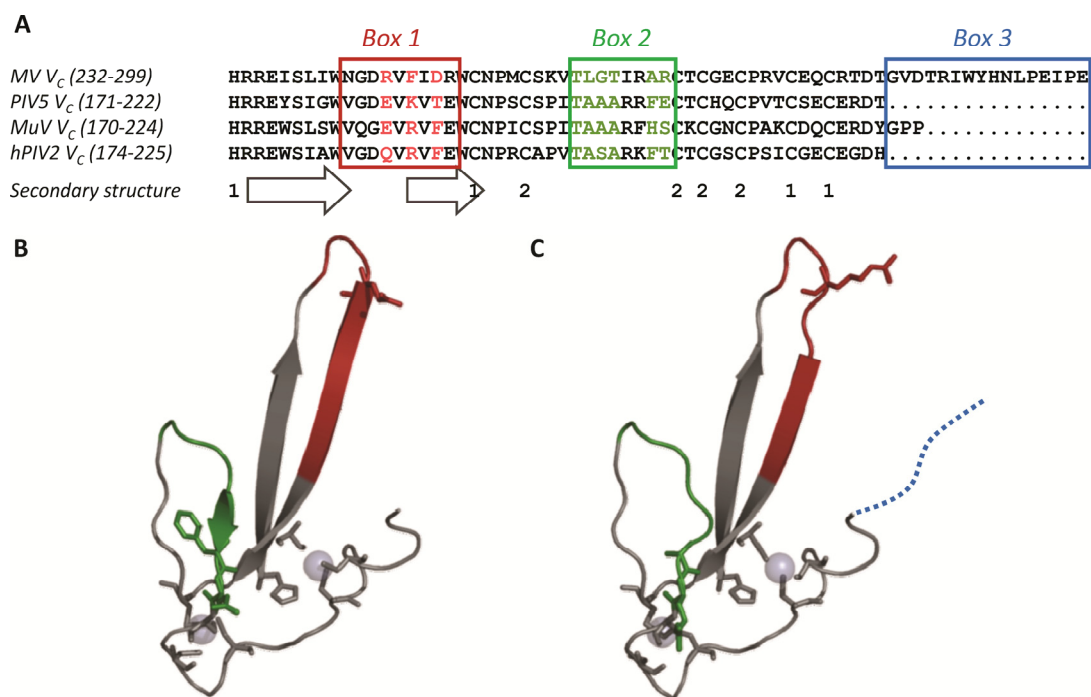


Figure 21: Sequence comparison of MV V_C and rubulaviral V_C and homology modelling of MV V_C based on the PIV5 V_C structure.

(A) Sequence alignment of V_C domains of MV, PIV5, MuV, and hPIV2. Secondary structure elements are indicated by arrows (β -strands) and numbers (1, 2: Zn-binding residues). Amino acids of Box1, Box2, and Box3 are highlighted by red, green, or blue frames, respectively. Amino acids mutated in MV V are highlighted in red and green. (B) PIV5 V_C structure model. Box1 and Box2 elements are highlighted in red or green respectively. Zn-binding residues and mutated residues are highlighted as stick-models. (C) Homology model of MV V_C based on the PIV5 V_C structure information. Highlights as in (B). The Box3 region could not be modeled and is therefore displayed as a dotted line. Both MV model and PIV5 structure are closely related to each other. However, the detailed conformation of selected residues strongly differs in both models.

indicates the important role of the domain. With the help of the *Evolutionary Trace Server (TraceSuite II*; (Innis et al., 2000)), I generated a phylogenetic tree based on the sequence alignment of the V protein (Fig. 20B) and compared this phylogenetic tree with the N protein-based tree (Fig. 20C; alignment see Appendix A). Viruses of the genera *Morbillivirus* (blue box) or *Rubulavirus* (red box) grouped nicely into branches of both trees. The unclassified Tioman virus and Menangle virus shared highest homology to Rubulaviruses. The V proteins of *Morbilliviruses* have are separated very early from *Rubulavirus* or *Henipavirus* (green box) V proteins. This might explain the unique function of MV V concerning binding to IKK α and IRF7, which is not shared by V proteins of other genera. In contrast, N protein sequences are not separated as conspicuously as V protein sequences and show higher homology to *Henipavirus* N proteins. The unclassified *Paramyxoviruses* Beilong virus and J-virus V proteins cluster together with *Henipaviruses*, whereas N proteins share similarity with *Morbillivirus* sequences. Vice versa behave the sequences of Tupaia paramyxovirus. SenV is the most distant *Paramyxovirus* regarding both V and N sequences.

Next, I had a closer look on the sequences of MV V and *Rubulavirus* V proteins, namely of MuV, hPIV2, and PIV5. These V proteins have recently been described to inhibit TBK1/IKK ϵ /IRF3 dependent induction of IFN β by a very similar mechanism as MV V inhibits IKK α /IRF7 (Lu et al., 2008). Sequence alignment of the V C-terminal domains of these viruses revealed few amino acid mutations within the highly conserved domain (Fig. 21A). These mutations could determine the specificity of V in inhibition of either the one or the other signaling complex. Also the binding of STAT2 has recently been mapped for MV V to two subdomains within the C-terminus, further referred to as Box1 (aa 241-249), and Box2 (aa 260-266), which both cooperate in STAT2 binding (Ramachandran et al., 2008).

A homology model of the MV V C-terminus was created (Fig. 21C; Johannes Söding, Gene Center), using the crystal structure of PIV5 V as template (Fig. 21B; (Li et al., 2006)). Due to the high homology of both sequences, the resulting model of the MV V C-terminus was extremely similar to the PIV5 V crystal structure. However, although the architecture of the domains is equal,

they contain striking differences on single amino acid level, which might explain the functional differences of PIV5 V and MV V. These mutations could have impact on the protein surface charge or polarity and thereby could determine substrate binding specificity. I selected amino acids, which differed between MV and the *rubulaviral* V proteins and generated amino acid exchange mutants of MV V and MuV V or PIV5 V, respectively (Table 2).

The mutation R244E and the triple mutations R244E-F246R-D248F (based on the MuV V sequence), and R244E-F246K-D248T (based on the PIV5 V sequence) all lie within the Box1 region, whereas the mutants T259AAAA and A265F-R266E affect the Box2 region. We also generated PIV5 V mutants containing the respective MV V amino acid residues: E183R and F204E-E205R. A third class of mutants was generated in which we deleted the Box3 region from MV V (MV V Δ 284-299) and fused these amino acids to PIV5 V (PIV5 V:MV-V284-299).

The MV and PIV5 V mutants were tested for their ability to inhibit IFN α 4 promoter activation in luciferase reporter gene assays and compared to wt MV and PIV5 V (Fig. 22A). MV V R244E and A265F-R266E did not show an altered phenotype compared to wt MV V, neither did PIV5 V E183R. The mutant PIV5 A204F-E205R was more competent in inhibiting IFN α induction than wt PIV5 V, but the effect was less intense than inhibition by wt MV V. Deletion of Box3 in MV V (MV V Δ 284-299) led to an increased inhibitory function compared to wt MV V (Fig. 22B). On the other hand, fusion of MV V284-299 to the C-terminus of PIV5 V (PIV5 V:MV-V284-299) had no effect on PIV5 V. This leads to the assumption that the Box3 region of MV V does not mediate the inhibitory function of MV V, but rather could suppress this function.

As the mutation of one amino acid in Box1, or of two amino acids in the Box2 region was not sufficient to completely abolish MV V functionality, I generated mutants with three amino acid exchanges in Box1 (R244E-F246R-D248F and R244E-F246K-D248T), or four amino acid exchanges in the Box2 region (T259AAAA). These mutants were also tested in their ability to suppress IFN α 4 promoter activity (Fig. 23A), or type-I IFN-dependent ISRE activation (Fig. 23B) in luciferase reporter gene assays. MV V R244E-F246R-D248F and R244E-

Table 2: Nucleotide mutations introduced into MV(Schwarz) V to generate specific *rubulavirus* analog mutants.

mutant	wt amino acid	mutation	wt nucleotide	mutation
MV V R244E	R244	E	C730 G731 C732	G A G
MV V R244E-F246R- D248F ("MuV-like")	R244	E	C730 G731 C732	G A G
	F246	R	T736 T737 T738	C G T
	D248	F	G742 A743	T T
MV V R244E-F246K- D248T ("PIV5-like")	R244	E	C730 G731 C732	G A G
	F246	K	T736 T737 T738	A A A
	D248	T	G742 A743	A C
MV V A265F-R266E ("PIV5-like")	A265	F	G793 C794	T T
	R266	E	A796 G797	G A
MV V T259A-L260A- G261A-T262A (= T259AAAA)	T259	A	A775	G
	L260	A	C778 T779	G C
	G261	A	G782	C
	T262	A	A784	G
MV VΔ284-299	Deletion of amino acids 284-299 (Box3)			
PIV5 V E183R ("MV-like")	E183	R	G547 A548	A G
PIV5 V F204A-E205R ("MV-like")	F204	A	T610 T611	G C
	E205	R	G613 A614	A G
PIV5 V:MV-V284-299	C-terminal fusion of MV V Box3 (aa 284-299)			

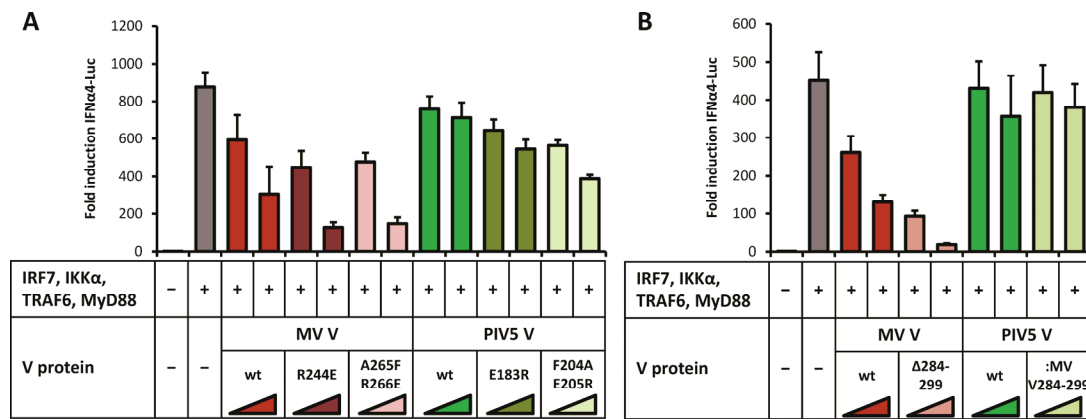


Figure 22: Inhibition of IFN α induction by MV and PIV5 V mutant proteins.

Luciferase reporter-gene assays with IRF7, MyD88, TRAF6 and IKK α , as well as luciferase under the control of the IFN α 4-promoter. (A) Single or double amino acid exchanges from MV V to PIV5 V and vice versa do not alter the phenotypes of wt MV V or PIV5 V. MV V inhibits IFN α induction, while PIV5 V does not. (B) Deletion of Box3 (aa 284 – 299) from MV V and insertion of these amino acids to the PIV5 V C-terminus has no negative influence on MV V or PIV5 V activity. MV V Δ 284-299 rather inhibits IFN α induction better than wt MV V. All assays are normalized using co-transfection of CMV-promoter driven renilla luciferase. Mock transfection is set to 1.

F246K-D248T only showed minor differences in inhibition of IFN α induction compared to wt MV V. In contrast, MV V T259AAAA was unable to accomplish its inhibitory function. In comparison, all mutants still were able to inhibit type-I IFN signaling (Fig. 23B), however, this function was slightly declined compared to wt MV V. This might be due to the fact, that the mutations introduced only affect binding of STAT2, whereas STAT1 binding and degradation is still functional (Ramachandran et al., 2008).

Next, I tested whether the mutants MV V R244E-F246R-D248F, R244E-F246K-D248T, and T259AAAA still were able to bind IKK α and IRF7, or whether the binding capacity was lost in the mutants (Fig. 23C). In accordance with the results of the reporter gene assay, I found both mutants MV V R244E-F246R-D248F and R244E-F246K-D248T still being able to bind to both IKK α and IRF7, whereas the mutant MV V T259AAAA was no longer able to fulfill the binding.

I further was interested whether these amino acids are exposed to the surface of the protein. I therefore generated a surface model of the full length PIV5 V from the crystal structure of the protein (Fig. 24A). As expected, the respective

amino acids A199-A200-A201 (shown in green) are located at the surface of PIV5 V and form a pocket, which could be responsible for protein-protein interactions. Assuming that the tertiary structure of MV V is similar to PIV5 V, one may conclude that the amino acids L260-G261-T262 are also exposed to the surface of MV V and form a characteristic binding pocket.

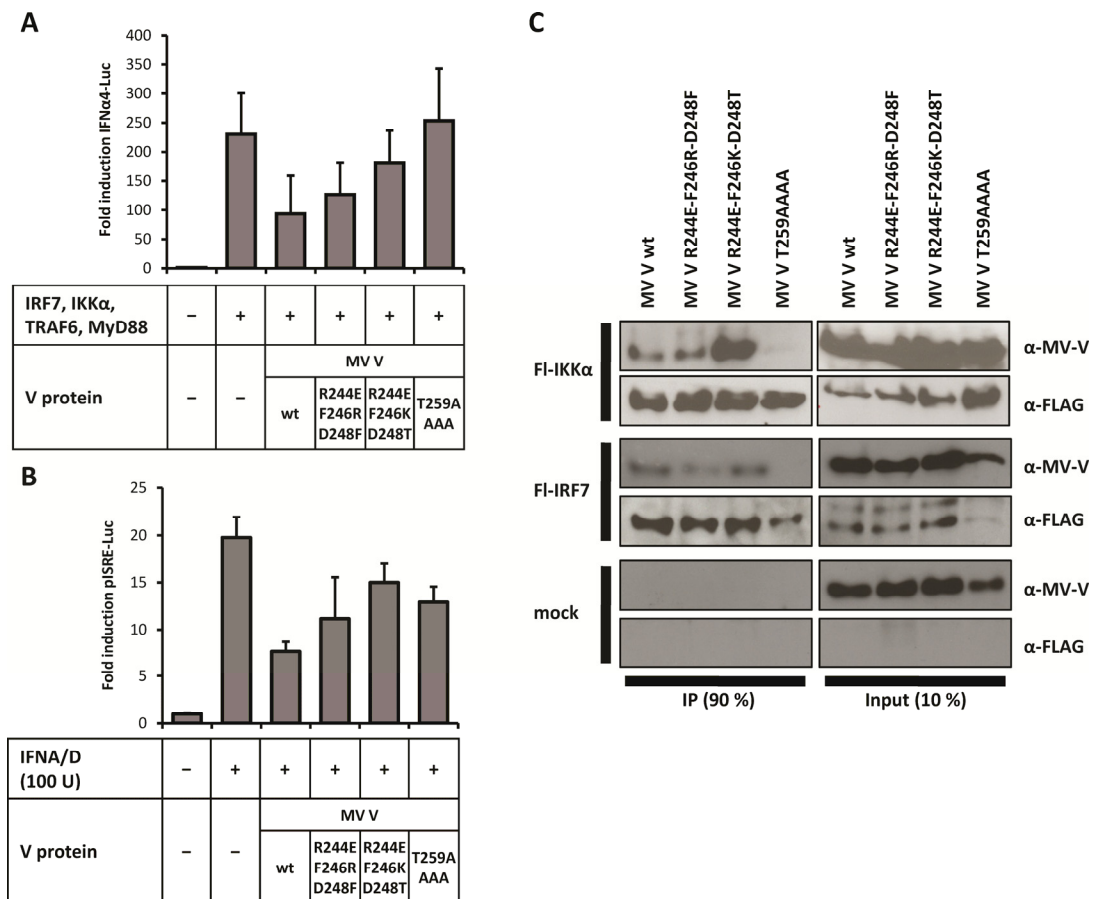


Figure 23: Inhibition of IFN α induction by Box1 and Box2 mutants of MV V.

(A) Luciferase reporter-gene assay with IRF7, MyD88, TRAF6 and IKK α , as well as luciferase under the control of the IFN α 4-promoter. Expression of the mutant MV V(T259A,L260A,G261A,T262A) (= T259AAAA; 125 ng expression vector) is no longer able to inhibit IFN α induction. The other mutants tested also show slight defectiveness compared to V wt. (B) Luciferase reporter-gene assay for type-I IFN signaling. ISRE-promoter driven luciferase expression is stimulated with 100 U /well of recombinant type-I IFN A/D. All mutants show slight decrease of inhibitory activity compared to wt V. All assays are normalized using co-transfection of CMV-promoter driven renilla luciferase. Mock transfection is set to 1. (C) Pull-down of FI-tagged IKK α or IRF7, (or empty vector) with Anti-FLAG[®] agarose beads. Co-expression of wt or mutant MV V. The mutant V(T259A,L260A,G261A,T262A) is unable to bind to IKK α , and also IRF7.

In summary, by comparing the sequences of the C-terminal domains of MV on the one side and MuV / hPIV2 / PIV5 on the other side, I was able to identify several amino acids that may influence the substrate specificity of MV V. These mutants were generated and tested in luciferase reporter gene assays and co-immunoprecipitation experiments and compared with wt MV V. The mutant MV V T259AAAA showed a clearly reduced inhibitory function and was unable to bind to IKK α or IRF7.

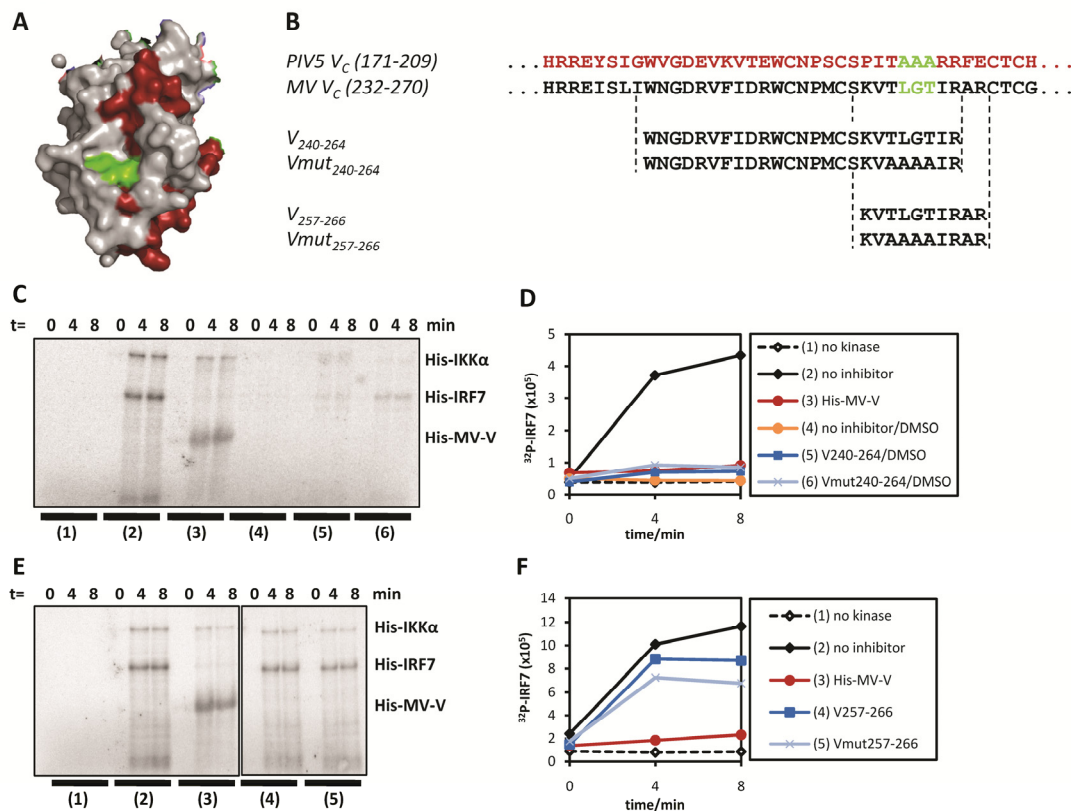


Figure 24: MV V peptides.

(A) Location of the Box2 amino acid analogs on the surface model of PIV5 V. Color code: gray: PV_N, red: V_C, green: A199,A200,A201 of Box2. The Box2 amino acids are located in a pocket at the surface of the protein. (B) Sequence alignment of PIV5 V_C and MV V_C. Color code for PIV5 V_C is analog to (A). Peptides were synthesized including Box1+2 (aa 240 – 264) of MV V or Box2 only (aa 257 – 266). Peptides were designed either with the MV V wt sequence or with the mutations equal to T259AAAA. (C and D) *In vitro* kinase assay with IKK α , IRF7, and full length His-MV-V (3) or peptides V₂₄₀₋₂₆₄ (5) and Vmut₂₄₀₋₂₆₄ (6). As peptides are dissolved in DMSO, a control with DMSO is included (4). Reactions with DMSO do not show kinase activity. (E and F) *In vitro* kinase assay with IKK α , IRF7, and full length His-MV-V (3) or peptides V₂₅₇₋₂₆₆ (4) or Vmut₂₅₇₋₂₆₆ (5). Both peptides show only minor effects on IKK α kinase activity in contrast to full length V. (D and F) Quantification of phospho-IRF7 bands.

In the next step, I was interested, whether peptides including the crucial amino acids 259-262 also could inhibit the activation of IRF7 by IKK α .

3.10 MV V peptides

Peptides were designed including either both Box1 and Box2 (V₂₄₀₋₂₆₄) or Box2 alone (V₂₅₇₋₂₆₆) as well as peptides with the T259AAAA mutation (Vmut₂₄₀₋₂₆₄ and Vmut₂₅₇₋₂₆₆; Fig. 24B). The peptides were synthesized and purified by HPLC (Metabion). Unfortunately, the peptides V₂₄₀₋₂₆₄ and Vmut₂₄₀₋₂₆₄ were not soluble in water and therefore could not be purified and were used as crude extracts dissolved in DMSO. I tested *in vitro* whether the peptides could block phosphorylation of IRF7 by IKK α . Surprisingly, a strong inhibition of IRF7-phosphorylation was found in presence of either V₂₄₀₋₂₆₄ or Vmut₂₄₀₋₂₆₄, which was comparable to full length His-MV-V (Fig. 24C and D). Unfortunately, when I added an equal volume of DMSO to the reaction instead of peptide solution, the kinase activity of IKK α was completely blocked (Fig. 24C, lane (4)) so that I conclude that the effect detected with the peptides is due to the solvent and not peptide specific. The peptides including Box2 (V₂₅₇₋₂₆₆ and Vmut₂₅₇₋₂₆₆) were also tested in the *in vitro* kinase assay system (Fig. 24E and F). These peptides are soluble in water and were pure up to 90 %. A weak decline of kinase activity was detected in the presence of V₂₅₇₋₂₆₆, but the effect was also detectable with Vmut₂₅₇₋₂₆₆, which should be unable to bind to IKK α .

From this data I conclude that small peptides including only the amino acids responsible for binding to IKK α and IRF7 are not able to act as inhibitors. Presumably, the formation of the whole binding pocket, which is composed of amino acids from the N-terminal domain (see Fig. 20A; shown in grey) as well as the C-terminal domain (shown in red and green) in case of PIV5 V (Fig. 24A) is necessary for a fully active V protein. This conclusion is coherent with the previous findings that the V C-terminus alone is not sufficient to inhibit the induction of IFN α , but may require also residues from the N-terminus.

3.11 Functions of MV V in NF- κ B activation

Not only IFN α , but also NF- κ B is activated via TLR-signaling, and, in addition, IKK α is also involved in this signaling process. So it was obvious to test, whether V is also able to inhibit activation of NF- κ B by IKK α . Luciferase reporter gene assays were performed using a NF- κ B promoter driven firefly luciferase. Induction of this gene was achieved by transfecting 300 ng of expression vectors for either IKK α (Fig. 25A) or its homologue IKK β (Fig. 25B), which are both involved in the formation of the IKK-complex consisting of IKK α , IKK β and IKK γ . In both cases some dose-dependent inhibitory effect of MV V could be detected, however, the inhibition was not as significant as in IFN α induction. As this result was not very clear, I decided to do confocal immunofluorescence experiments and tracked nuclear localization of the NF- κ B subunits p65/RelA (Fig. 25C) and RelB (Fig. 25D) upon stimulation of cells with TNF α in the presence or absence of transfected Fl-MV-V. HEp-2 cells were transfected with empty vector or Fl-MV-V, stimulated with 5 U of recombinant TNF α 24 h p. tr. or left untreated, and fixed and stained 30 min post stimulation. Without stimulation, nuclear localization of neither p65/RelA nor RelB could be detected (top lane). In case of stimulation with TNF α , a clear activation of both forms of NF- κ B could be detected, as nuclear accumulation of the transcription factors occurs (middle lane). In the presence of Fl-MV-V, nuclear localization of p65/RelA was inhibited in most of the cells, however, some showed nuclear localization (bottom lane). Also activation of RelB was inhibited by Fl-MV-V only to some extent. An *in vitro* kinase assay was performed using 100 ng of recombinant His-IKK α and 1 μ g of GST-I- κ B- α (Fig. 25E and F). In contrast to His-IRF7, phosphorylation of GST-I- κ B- α by IKK α was not inhibited by His-MV-V, and also His-MV-P did not influence the phosphorylation of GST-I- κ B- α .

In summary, these data suggest a substrate specific inhibition by MV V. Although NF- κ B activation is also mediated by IKK α – at least in parts – this function of IKK α is not inhibited as clearly as the activation of IRF7.

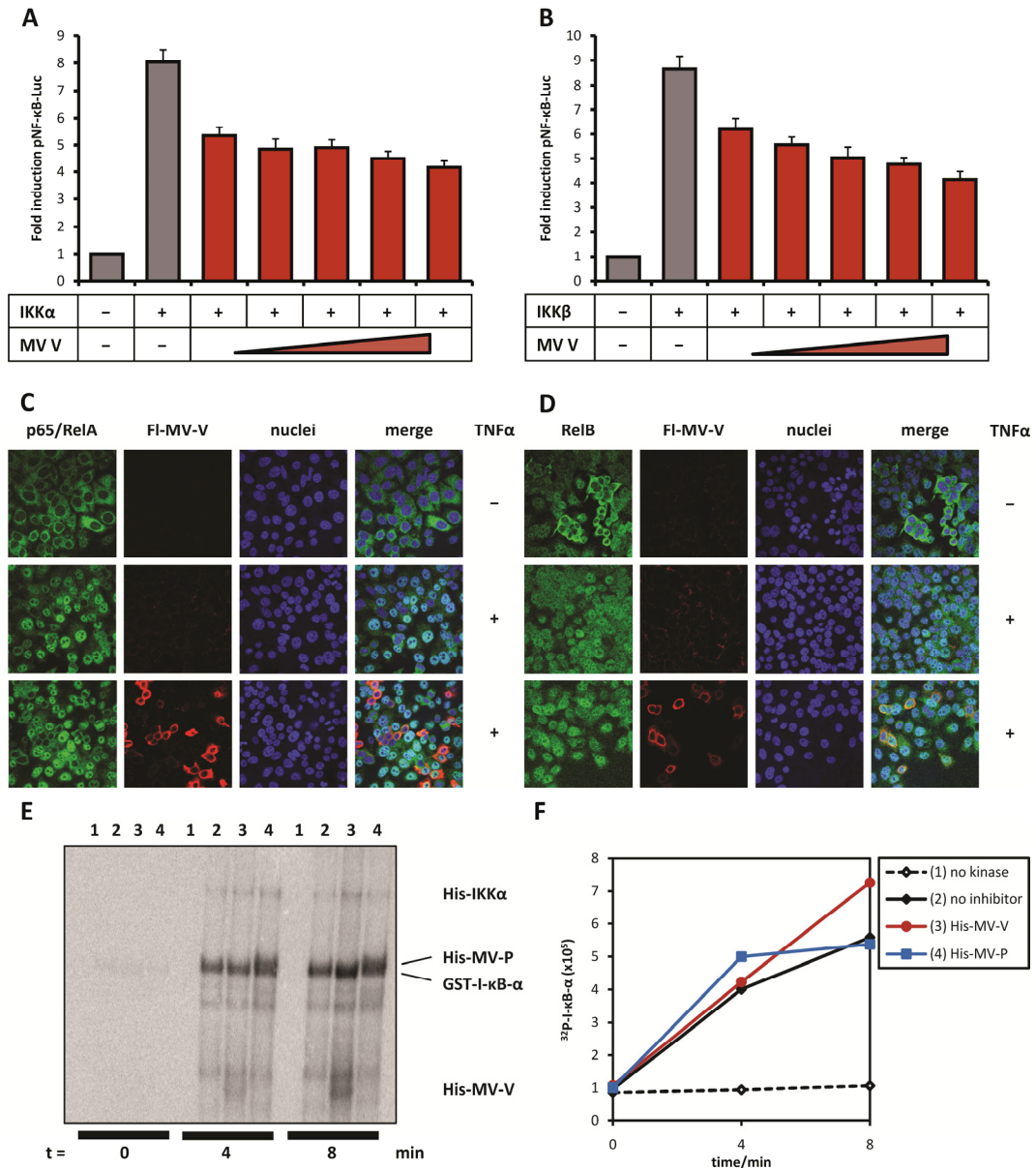


Figure 25: Effects of MV V on NF- κ B activation.

(A and B) Luciferase reporter-gene assays with overexpression of IKK α (A) or IKK β (B) to stimulate luciferase expression under the control of the NF- κ B-promoter. Co-expression of MV V (500 ng; 750 ng; 1000 ng; 1250 ng; 1500 ng) shows minor effects on the expression of NF- κ B promoter-driven luciferase. All assays are normalized using co-transfection of CMV-promoter driven renilla luciferase. Mock transfection is set to 1. (C and D) Confocal immunofluorescence of nuclear translocation the conventional NF- κ B subunit p65/RelA (C) or the alternative NF- κ B subunit RelB (D) upon stimulation of HEp-2 cells with 5 U of recombinant TNF α and effect of transfected FI-MV-V. Color code: green: p65/RelA, or RelB (stained with p65/RelA or RelB specific antibodies); red: FI-MV-V (stained with anti-FLAG[®] M2); blue: ToPro3 nuclear staining. Both p65/RelA and RelB are distributed in the cytoplasm (lane 1) and translocate to the nucleus upon stimulation (lane 2). In the presence of FI-MV-V, the translocation of both subunits is inhibited in some cells, but many still show full translocation of p65/RelA or RelB

into the nucleus (lane 3). (E and F) *In vitro* kinase assay with IKK α , GST-tagged I- κ B- α , and MV V (3) or MV P (4). Neither V nor P is able to inhibit the phosphorylation of I- κ B- α by IKK α . (F) Quantification of phospho-I- κ B- α bands.

3.12 Control of autophagy by Measles virus

Autophagy has been shown to be closely connected to TLR7 signaling. On the one hand, viral nucleic acids are transported via autophagy from the cytoplasm of infected pDCs to endosomal compartments, where TLRs are located (Lee et al., 2007). On the other hand, stimulation of TLR7 leads to increased formation of autophagosomes (Delgado et al., 2008). We addressed the question, whether MV is able to influence autophagy during infection and whether the V protein is also important in these mechanisms.

An experimental setting was designed to follow the induction of autophagy during MV infection. The results were with starvation conditions, a natural inducer of autophagy (Martinet et al., 2006). The autophagy-related protein light chain 3 beta (LC3B, or LC3) was chosen as readout for the induction of autophagy. This protein is exported from the nucleus and incorporated into autophagosomal membranes upon activation. U3A cells stably transfected with a plasmid encoding a GFP-LC3 fusion protein were used to visualize autophagy. The cells were treated with Bafilomycin (200 nM), an inhibitor of membrane fusion, which thereby inhibits the lysosomal degradation of autophagosomes. The cells were infected with MV (MOI = 1) at the time of Bafilomycin treatment, kept in starvation using EBSS medium without nutrients and serum, or left further untreated for 24 h, followed by fixation and staining of MV N as infection marker, as well as nuclear staining. The cells were analyzed using IF microscopy (Fig. 26A). In non infected and non starving cells, GFP-LC3 exists mostly in an inactive form, which is distributed in both cytoplasm and nucleus (top lane). In most cells some vesicular GFP-LC3 is visible, however, it has been shown that this is due to localization to the smooth endoplasmic reticulum, which is independent of autophagy (Korkhov, 2009). In both infected cells (middle lane) and starving cells (bottom lane) GFP-LC3 is activated within 24 h p. i. / p. treatment, which results in an accumulation of GFP-LC3 containing

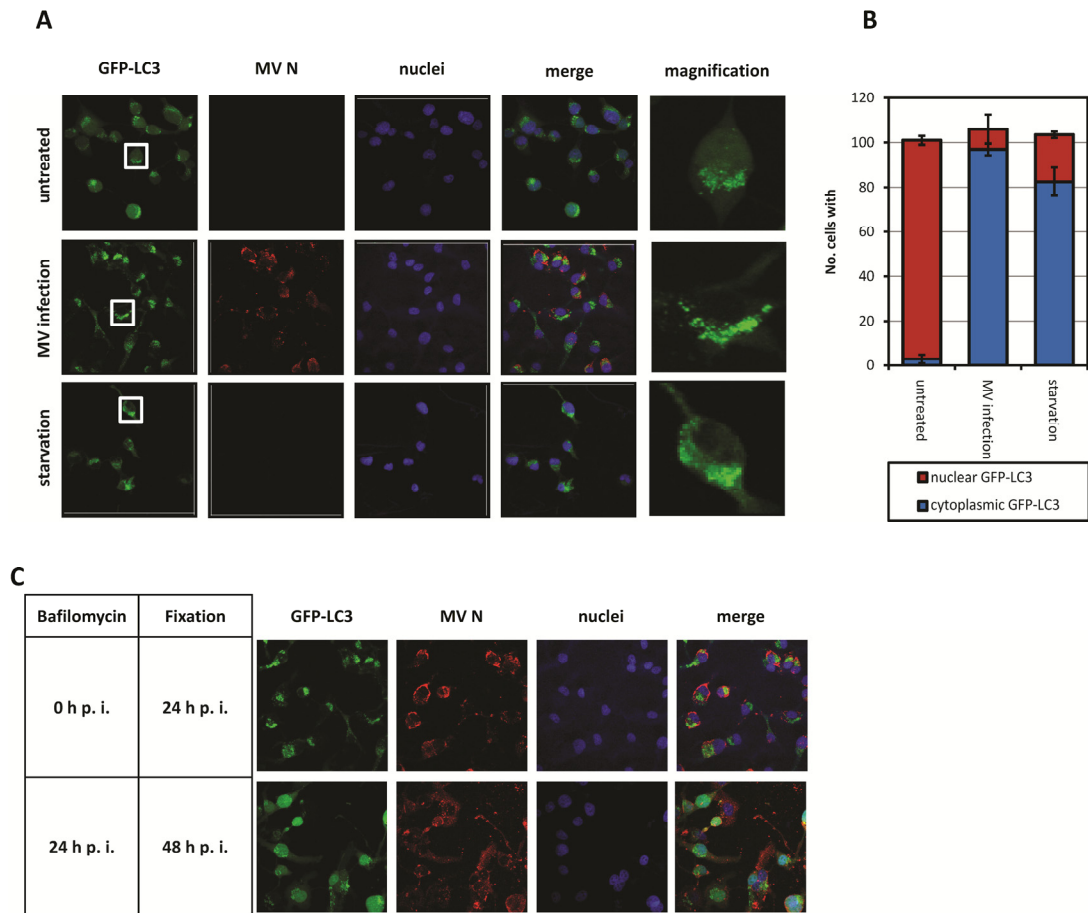


Figure 26: Effect of MV infection on the activation of autophagy.

U3A cells stably expressing GFP-LC3 (green) were analyzed for activation of autophagy. (A) Cells were treated with Bafilomycin (200 nM) and left further untreated (lane 1), were subsequently infected with MV at an MOI = 1 (lane 2), or were starved in EBSS medium (lane 3) for 24 h in each case. MV N was stained with anti-MV-N (red) and nuclei were stained with ToPro3 (blue). In untreated cells, GFP-LC3 appears to be distributed in both cytoplasm and nucleus, with few autophagosomes in the cytoplasm. In contrast, in both MV infected and in starving cells, GFP-LC3 is activated and incorporated into autophagosomes as indicated by the lack of nuclear GFP-LC3. (B) Cells were counted for GFP-LC3 localization in both cytoplasm and nucleus, or in cytoplasm only. Untreated cells mainly show inactive nuclear GFP-LC3, whereas GFP-LC3 is exported from the nucleus both in MV infection and in starvation. (C) Cells were infected with MV (MOI = 1) and treated with Bafilomycin (200 nM) either subsequently (lane 1) or 24 h p. i. (lane 2). Cells were fixed 24 h p. treatment in each case. Early upon infection (0 – 24 h; lane 1) MV induces the formation of autophagosomes. In contrast, at the later time point (24 – 48 h; lane 2) GFP-LC3 is not activated upon infection.

vesicles in the cytoplasm and a complete loss of nuclear GFP-LC3. Similar numbers of cells were counted and examined for activation of GFP-LC3 (Fig. 26B). In untreated cells, 97 % of all cells exhibited inactive GFP-LC3 in their

nuclei, whereas in only 3 % of the cells GFP-LC3 was cytoplasmic. In contrast, under starvation conditions, in 80 % of the cells GFP-LC3 was completely activated, whereas 20 % of the cells still showed nuclear GFP-LC3. Also during MV infection, the majority (92 %) of infected cells showed completely active GFP-LC3, whereas in 8 % of the infected cells nuclear GFP-LC3 was detectable. This indicates that autophagy is induced upon MV infection comparable to starvation of the cells.

Induction of autophagy by MV at different stages of infection can be followed by treating the cells with Bafilomycin at various time points p. i. Autophagosomes fuse with lysosomes after formation and undergo subsequent degradation. The fusion step is inhibited by Bafilomycin. As a consequence, induction of autophagy can be visualized from the time of treatment with Bafilomycin until fixation of the cells.

U3A cells stably expressing GFP-LC3 were infected with MV (MOI = 1) and treated with Bafilomycin either subsequently or 24 h p. i. (Fig. 26C). The cells were fixed 24 h p. treatment with Bafilomycin. In the case of simultaneous infection and Bafilomycin treatment, vesicular accumulation of active GFP-LC3 can be detected (top lane). In contrast, when cells are treated with Bafilomycin 24 h p. i., most GFP-LC3 appears in the inactive form in the nuclei of infected cells. GFP-LC3 that has been activated during the first 24 h of infection has already been degraded before the treatment with Bafilomycin. These results indicate that the virus performs a switch in the cell from induction of autophagy to inhibition during infection. This might be due to a viral factor that is expressed at later stages of infection. This factor could be one of the non structural proteins V or C.

4 Discussion

4.1 Mechanism of the inhibition of IFN α induction by MV V

In summary, the mechanism of the inhibition of TLR7/9 signaling by MV could be clarified on a molecular level (Fig. 27). The non-structural V protein was identified as the major antagonist of this signaling cascade involving MyD88, TRAF6, IKK α and IRF7. V acts as a decoy substrate for the crucial kinase IKK α and prevents activation of the transcription factor IRF7 by IKK α through a direct interaction with both the kinase (IKK α) and the substrate (IRF7).

Upon binding to IKK α , V inhibits the phosphorylation of IRF7 by IKK α , which leads to a strong downregulation of the levels of activated phospho-IRF7 (pIRF7) in the presence of V. I was able to show this effect both *in vitro* and in cell culture. Here, V acts as a decoy substrate for IKK α . N- and C-terminal deletion mutants of the protein were generated to identify phosphorylation sites of V. Notably, all mutants tested were phosphorylated by IKK α and other related kinases (IKK β , TBK1) *in vitro*, and also purified P was phosphorylated. This suggests a high degree of unspecific reactions *in vitro*. However, although both full length proteins V and P were phosphorylated, only V was able to compete with IRF7, but P did not. V was also unable to inhibit the phosphorylation of I- κ B- α by IKK α . This shows the specificity of V as an antagonist of IKK α /IRF7. The inhibition of phosphorylation of IRF7 by V is competitive and non-catalytic. Higher amounts of V are needed to inhibit activation of IRF7 for a longer period of time, whereas low amounts of V are suitable to fulfill their inhibitory function for a shorter period of time. Once all available V has undergone phosphorylation, it appears to be no longer available as a potential decoy factor *in vitro*.

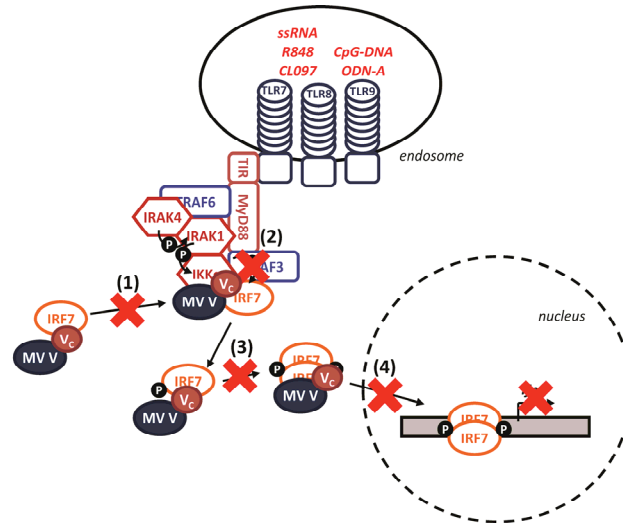


Figure 27: Model of the inhibitory mechanism of MV V.

Taking together the data obtained, we are able to create a model of the mechanism of inhibition of IFN α induction by MV V. This mechanism includes multiple steps, which are mediated by binding of MV V to IKK α and IRF7. (1) Binding to IRF7 inhibits the recruitment of the transcription factor to the activating signaling complex. (2) Binding to IKK α competes with IRF7 for the phosphorylation by IKK α . (3) Binding to phospho-IRF7 may inhibit the formation of pIRF7-dimers, or, in case of binding to pIRF7-dimers, (4) may inhibit the translocation of these dimers to the nucleus. In summary, all single steps of the mechanism may contribute to the downregulation of IFN α production by TLR7/9 signaling.

In parallel to its function as a decoy substrate for IKK α , V is also able to bind IRF7. This could prevent the recruitment of IRF7 to the signaling complex and thereby also would lead to the inhibition of the activation of IRF7. But V is also able to bind to IRF7-2D, a constitutive active form of IRF7 (Lin et al., 2000). Thus, V is able to prevent the last steps of the signaling cascade. It could not be clarified, whether V binds to pIRF7 monomers, thereby preventing the dimerization of pIRF7, or if it is able to bind also to active pIRF7 dimers, thereby preventing the translocation of the transcription factor to the nucleus. The first variant is certainly the more probable one, as the antagonistic functions of V in this pathway could be explained very simply assuming that V acts as an IRF7 mimic. V appearing as a “false IRF7” is able to bind to IKK α like IRF7, and it should also be able to form heterodimers with IRF7, thereby forming a complex that is unable to enter the nucleus and/or to act as a transcription factor for the expression of IFN α genes.

The interaction of V with the signaling proteins is mediated by the C-terminal V-specific Zn-finger domain (V_C). I could show that V_C is sufficient for binding to IKK α and also to IRF7. However, in the luciferase reporter gene assay, V_C fused to an Ig-tag (Ig-MV- V_C) did not inhibit the IFN α 6-promoter activity. Several tags were fused to V_C , among them FLAG®, His, myc, and DsRed. Fusion proteins with high MW tags (Ig-MV- V_C , DsRed-MV- V_C) were detectable on protein level, but did not influence the induction of IFN α . Fusion proteins with small tags (Fl-MV- V_C , myc-MV- V_C , His-MV- V_C) or untagged V_C also did not show inhibition of IFN α -promoter activation, but as they could not be detected by Western blot analysis of lysates of transfected cells, it is not clear whether these constructs were not functional or simply not expressed. This leads to the assumption that also parts of the PV N-terminus might be required to get a completely functional V protein. This is supported by the structure of the PIV5 V protein, which is highly homologous to MV V. Here, the Zn-finger domain functions as a scaffold for the formation of the tertiary protein structure.

The V_C domain is conserved among all V proteins in the family of *Paramyxoviridae*. However, it has been shown that specific V_C -domains of different viruses show different antagonistic functions. MV V binds and inhibits IKK α /IRF7, as shown here, whereas others have shown that the V proteins of *Rubulaviruses*, like MuV, hPIV2 or PIV5, inhibit TBK1/IKK ϵ /IRF3 dependent signaling via a mechanism that differs on the molecular level (Lu et al., 2008). Rubulavirus V proteins mainly interact with the kinases, but they are unable to interact with the involved transcription factor IRF3. The interaction of *rubulaviral* V proteins with IKK ϵ or TBK1 leads to the ubiquitinylation and degradation of TBK1 and IKK ϵ , which, in the end, inhibits the activation of IRF3. In addition, V is ubiquitinated and degraded. In both cases, V proteins act as decoy substrates for kinases of different signaling cascades in a competitive manner.

In contrast, it was shown that PIV5 V mediates the proteasomal degradation of STAT1, which plays a crucial role for IFN signaling (Precious et al., 2007). The MV V protein also inhibits IFN signaling by various mechanisms, as it was shown by several groups. MV V targets both STAT1 and STAT2 independently of each other. STAT1 is recruited by a domain including Y110 (Caignard et al.,

2007) and this function is shared with MV P (Devaux et al., 2007). In contrast to *rubulaviral* V proteins, MV V interaction with STAT1 does not involve the DDB1-Cul4A ubiquitin ligase and does not lead to the degradation of STAT1, as shown for PIV5 V (Precious et al., 2005). The interaction of V with STAT2 is mediated by the V C-terminus and inhibits also the phosphorylation of STAT2 (Ohno et al., 2004). The interaction surface of V with STAT2 could be further narrowed down to few amino acids of Box1 and Box2 (Ramachandran et al., 2008). Homology modeling indicated that the crucial amino acids form a pocket to which STAT2 could bind. Interestingly, I was able to locate the domain responsible for the inhibition of IFN α induction to the same pocket. By exchanging four amino acids in of MV V Box2 (T259, L260, G261, T262) to alanine (which represent the analogous PIV5 V sequence), I was able to generate a mutant V that lacks the ability to bind IKK α and IRF7. However, interference of this mutant with type-I IFN signaling (via STAT2 binding) is disturbed only to a minor extent. This becomes clear, considering that the MV sequence was exchanged mainly by the homologous sequence of PIV5 V, which also binds STAT2, but is unable to inhibit IKK α /IRF7 mediated IFN induction. With this study, the inhibitory functions of MV V regarding IFN signaling and IFN α induction could be separated from each other. So far it has not been tested, whether the generated mutants are still able to bind to MDA-5, another common target of *paramyxoviral* V proteins. This function is also mediated by the C-terminal domain of the V proteins. Considering that all V proteins among the *Paramyxovirinae* are able to bind MDA-5, it would not be surprising to see the MV mutants still being able to bind to MDA-5, thereby proving that this function is also independent of the ability to inhibit downstream signaling of either IKK α /IRF7 or IKK ϵ /IRF3.

The different evolution of V proteins of *Morbilliviruses* from other members of the *Paramyxoviridae* family was also shown by phylogenetic comparison of V protein sequences from a selection of viruses from all genera within the subfamily of *Paramyxovirinae*. Interestingly, sequence comparison revealed that the *Morbillivirus* V proteins form a branch in the phylogenetic tree different from *Rubulaviruses* and *Henipaviruses*. In contrast, comparison of N protein sequences showed that the genus *Rubulavirus* differs to a higher extent from

the *Morbilliviruses* and *Henipaviruses*. This indicates the special role of V proteins of the *Morbilliviruses*. However, it remains to be tested, whether the V proteins of RPV, CDV, PPRV and DMV also show the same phenotype like MV V. On the other hand, *Morbilliviruses* all share haematotropic characteristics, meaning that they predominantly infect and replicate in blood cells like lymphocytes and monocytes (Tatsuo et al., 2001). In case of MV it is clear that the virus infects pDCs, a DC subset which expresses TLR7/9 and is responsible for the production of large amounts of IFN α upon activation of this signaling pathway, although not many progeny virus is made.

Peptides of either Box2 alone or in combination with Box1 were generated based on the wt MV V sequence and also on the T259A-L260A-G261A-T262A mutant. Unfortunately, the peptides including Box1 and Box2 were not soluble in water, but DMSO and the solvent led to a drastic loss of functionality of *in vitro* kinase assays. The Box2-peptides were soluble in water so that they could be tested in the *in vitro* kinase assay to test whether the wt Box2-peptide was able to inhibit IRF7-phosphorylation by IKK α . I could show that both wt derived and mutant derived peptides led to only minor inhibition of kinase activity in comparison to full length His-MV-V. This result supports the theory that V_C alone or even smaller parts of the protein are not sufficient to inhibit the activation of IRF7 by IKK α . However, the peptides should also be tested in the cell culture system and in luciferase reporter gene assays. Liposomal transfection reagents are now available to introduce peptides into living cells as well as cell-penetrating arginine-rich fusion peptides like the HIV Tat-peptide (Schmidt et al., 2009). However, detection of the peptides is critical as no antibodies directed against the Box2 epitope are currently available.

4.2 Interaction of MV with pDCs

In order to study the antagonistic function of MV V in a natural system, i. e. pDCs, I established a rabies virus based vector system for the expression of MV P, V and C proteins. Recombinant RVs were generated expressing either MV protein from an additional gene. This was necessary as primary pDCs are hardly transfectable using lipofection or calciumphosphate protocols. As a

second reason, a reverse genetics system for MV is not yet established in the lab, which would allow the deletion of V expression in the virus context or the expression of mutant V proteins. Third, the source for primary pDCs of human origin is peripheral blood, however, the amount of pDCs per mL is very low and the purification procedure is difficult and time consuming. Therefore, I decided to extract precursor cells from murine bone marrow and differentiated them into a mixed culture containing pDCs. As the human pathogenic MV should not be able to infect cells of murine origin, the species barrier crossing zoonotic RV was used to infect the cells and thereby to induce the expression of the MV proteins. Surprisingly, I found MV infecting murine pDCs much better than RV. I could not figure out the reasons for this in detail, however, the expression of either MV P, V or C did not alter the RV phenotype. Therefore I conclude that induction of IFN α and its inhibition by MV V is not a crucial factor in the context of RV infection. Other factors different from IFN α induction must play a role in the inhibition of RV replication in murine pDCs. One possibility is that RV only very inefficiently enters the cells. However, pDCs exposed to RV (either wt or expressing MV proteins) did not respond to external stimulation of TLR9 with CpG ODN. This suggests that pDCs are inactivated or killed upon exposure to RV. This assumption could have been followed by performing a cytokine ELISA, e.g. against IL-6. Unfortunately, no other cytokine ELISA was available.

It has been shown *in vitro* that vaccine strains of MV are able to infect pDCs (Schlender et al., 2005), although the infection may not be productive (i.e. lead to production and release of new virus). However it still has to be clarified, whether wt strains are also able to do so *in vivo*. pDCs naturally do not express CD150 (reviewed in (Tahara et al., 2008)), the entry receptor for wt MV strains (de Swart et al., 2007), but they express CD46, which can be used in addition as a receptor by attenuated strains (Dörig et al., 1993). However it has been shown that MV is able to induce the expression of CD150 upon binding of the H protein to TLR2 (Bieback et al., 2002). Although TLR2 is expressed only weakly in pDCs (Hornung et al., 2002), this might give a hint that wt MV is also able to enter pDCs. There, TLR7 might be able to detect viral ssRNA. A third yet uncharacterized set of receptors mediates virus entry independent of CD150 or CD46 and is involved in entry of MV to epithelial cells (Tahara et al., 2008). We

and others were able to show that MV is able to infect even cells of non-primate origin, at least *in vitro* (BSR-T7/5; murine BMDCs; see also (Abdullah et al., 2009)). This receptor set may also play a role in the infection of human pDCs *in vivo*. The model of the infectious route of MV *in vivo* also admits a central role of DCs (either mDCs or pDCs) to the dissemination of the virus. Another option instead of infecting pDCs to migrate to lymph nodes is the attachment of the virus to the cell surface without entry, which is mediated by DC-SIGN (de Witte et al., 2006).

Another question to discuss is the kinetics of the activation of the antiviral immune response in pDCs and the inhibition by MV V. As V is a non-structural protein and therefore not incorporated into virus particles, replication has to take place before V is available. However, viral genomic RNA could be recognized by TLR7 even before the virus starts to replicate, i.e. following endocytosis of virus particles. This would lead to the production of IFN α and the immediate elimination of the virus. However, MV particles directly release their RNPs into the cytoplasm upon fusion of the viral and cellular membranes and are not endocytosed (Hashimoto et al., 2002) so that TLR7 will not be activated upon virus entry. This could argue against the involvement of TLR7 in the immune response to MV infection.

Recent studies provided evidence that nucleic acids of replicating viruses are transported from the cytoplasm to TLR-containing compartments via autophagy, as could be shown for vesicular stomatitis virus and Sendai virus (Lee et al., 2007). PDCs respond with the production of high amounts of IFN α upon autophagocytosis of viral RNA. This fact, and also the observation that the formation of autophagosomes is triggered by stimulation of TLR7 with ssRNA or R848 (Delgado et al., 2008), exhibit a direct connection of two antiviral mechanisms, i.e. TLR-signaling and autophagy (Fig. 28). In this case, it is necessary for the virus to express an antagonist as the replication rate increases (i.e. when high amounts of viral nucleic acids are found in the cytoplasm). This could be fulfilled exactly by the V protein.

MV V inhibits the activation of IRF7 and also – but to a minor extent – the activation of NF- κ B, as it was shown in this study. Both transcription factors are

activated upon stimulation of TLR7, which might be triggered by autophagy of cytoplasmic MV RNAs (Fig. 28).

It was shown in this study that MV induces autophagy in early steps of the infection, i.e. in the time up to 24 h p. i. The induction was comparable to autophagy processes induced by starvation. The GFP-LC3 marker protein was activated in both cases, which resulted in the export of inactive GFP-LC3 out of the nucleus and accumulation of autophagosomes in the cytoplasm. It still has to be clarified, whether this induction of autophagic processes is needed for virus replication or whether it is a cellular response to the infection. Notably, the induction of autophagy observed here is independent of the presence and functionality of the TLR7 signaling complex, as the cell lines used for this study (U3A; Vero) do not express TLR7 or IRF7 constitutively.

I was also able to show that autophagy is inhibited at later stages of infection. In the time 24 – 48 h p. i. GFP-LC3 was newly expressed, but remained in the inactive form mainly in the nuclei of infected cells. This indicates the involvement of a viral factor, which gains its functionality or which is expressed to required levels only after viral replication has started. The non-structural

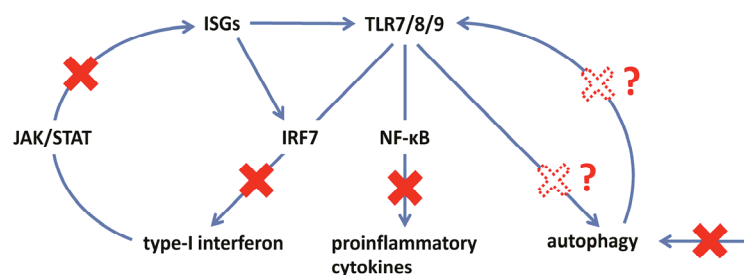


Figure 28: Model of TLR7/8/9 signaling, JAK/STAT signaling and autophagy.

Activation of TLR7/8/9 leads to the production of type-I IFN via IRF7 and of proinflammatory cytokines via NF-κB. IFN induction in turn activates JAK/STAT signaling, leading to the expression of ISGs, among which TLRs and IRF7 are upregulated. All three signal transduction pathways are modulated by the V protein of MV, leading to a block of cytokine production. Autophagy processes are also activated upon recognition of viral nucleic acids by TLR7/8/9, which leads to an increased uptake of viral PAMPs into endosomal compartments and thereby increased TLR activation. Induction of autophagy is inhibited by MV factors, but it is not clear, whether also the connection between TLR signaling and autophagy is affected.

proteins V and C perfectly fulfill these criteria and it has to be tested, which viral proteins are involved in the inhibition of autophagy. However, molecular targets of MV proteins in the autophagy process have to be identified. Also, it still remains unclear whether the signaling processes leading to the feedback mechanism of autophagy and TLR7 signaling are also directly modulated by MV proteins. The results obtained so far only show the modulation of TLR7-independent autophagy processes.

4.3 MV induced immunosuppression and impact of IFN α inhibition

MV causes a generalized immunosuppression upon infection of the host. This involves lymphopenia of B cells, monocytes, neutrophils, CD4+ and CD8+ T cells. Furthermore, MV causes a severe cytokine imbalance as well as silencing of PBMCs (reviewed in (Schneider-Schaulies and Schneider-Schaulies, 2009)). An initial Th1 cell activation is shifted to a prolonged Th2 cell response during MV infection. This leads to the suppression of the cellular immune response to secondary viral and bacterial infections. The interaction of MV with DCs seems to play a crucial role in these effects of immunosuppression. On the one hand, MV infection modulates DC maturation, cytokine production, antigen presentation, and T cell activation. Homing of infected DCs to local lymph nodes leads to the transfer of the virus to T cells either via direct infection, or by fusion of infected DCs with target cells (Fugier-Vivier et al., 1997). Modulated DC functions lead to the silencing of T cells. Proliferation of T cells is additionally inhibited by contact with MV infected cells (Schlender et al., 1996), which involves the viral glycoproteins H and F.

The findings provided in this study suggest a novel mechanism of modulation of the antiviral response by MV, which might contribute to the immunosuppressive phenotype of MV.

PDCs play a central role in the antiviral immune response (Fitzgerald-Bocarsly and Feng, 2007). They are described as major IFN α producing cells upon viral infections (Siegal et al., 1999; Cella et al., 1999), which leads to the activation of a Th1 biased adaptive immune response (Brinkmann et al., 1993). IFN of course also activates direct antiviral mechanisms of the innate immune response,

including the production of Mx (Horisberger and Hochkeppel, 1987) and 2'-5'-OAS (Baglioni and Maroney, 1980). It is therefore a major factor connecting both branches of the host immune response (reviewed in (Le Bon and Tough, 2002)). Thus it is surprising that MV may have chosen this cell type to invade the host. However, by the development of powerful tools to subvert pDC functions, MV is able to “hide” in or at the surface of these cells like in a Trojan horse to spread into the lymphatic sites of replication. The TLR7/9 mediated induction of IFN α is one of the central antiviral signaling processes performed by pDCs (and obviously plays in these cells a more important role than RLR signaling). By the inhibition of this signaling pathway by MV V, pDCs are strongly malfunctioning and this impairs the immune response to MV infection *in vivo*.

4.4 Components of the TLR7/9 signaling complex

To investigate the role of the MV V protein, the signaling complex recruited to TLR7/9 was reconstituted in cell lines. Naturally, TLR7 and 9 are constitutively expressed in immune cells like pDCs, but not in other cell types like epithelial cells. The same is true for IRF7. A functional signaling complex was reconstituted in epithelial cell lines (HEK-293T), hepatocytes (Huh7.5), and other non-immune cell lines, by transfection of expression vectors and overexpression of selected components of the complex. The adapter protein MyD88 is required as a scaffold protein, and also TRAF6 has been shown to play a crucial role (Kawai et al., 2004). TRAF3 was originally thought to play an important role in IFN β induction via TLR3 or RLRs and therefore was not tested in this study. However, it has also been described as a crucial factor in TLR7/9 signaling more recently (Oganesyan et al., 2006), but as I had already shown the interaction of the MV V protein with IKK α and IRF7 at that time, I did not follow the influence of TRAF3.

IRAK1, IRAK4 and IKK α have been described previously to play essential roles in the activation of IRF7 through signaling of TLR7/9 (Uematsu et al., 2005; Hoshino et al., 2006; Kim et al., 2007). However, when overexpressed in cell lines, only IKK α showed an increase in IFN α -promoter activity in the assay

established in this study. IRAK4 did not influence the IFN α -promoter activity, and IRAK1, as well as a splicing variant IRAK1c, strongly decreased the IFN α -promoter activity when overexpressed. This might give hint to a regulatory role of IRAK1 in the signaling complex. IRF7 is phosphorylated at multiple sites during the activation (Lin et al., 2000). Overexpression of IRAK1 might result in a deregulation of the kinetics of the activation of IRF7, which might lead to a premature proteasomal degradation of IRF7 and thereby loss of IFN α -promoter activation.

4.5 Inhibition of TLR7/9 signaling by the MV C protein

Here, I tested the proteins expressed from the MV P gene, namely MV P, V and C, for their ability to inhibit IFN α induction by the signaling complex of TLR7/9. I could show that both MV V and C are able to act as inhibitors for the activation of IFN α promoters and I was able to clarify the underlying mechanism for the V protein. However, the role of the C protein remains elusive and must be addressed in a separate project. MV C has been shown to be involved in the inhibition of protein kinase R (PKR) activity (Toth et al., 2009). This RNA helicase recognizes dsRNA and induces apoptosis and mitogen activated protein kinase (MAPK) signaling. PKR activation also leads to increased type-I IFN production and to the activation of NF- κ B (Williams, 2001). Moreover, PKR leads to the phosphorylation of the eukaryotic translation initiation factor 2 α (eIF2 α), which leads to a shut down in protein synthesis (reviewed in (Balachandran and Barber, 2007)). However, here I could show that MV C must have additional functions apart from the inhibition of PKR-dependent signaling.

I could show that C does not directly interact with components of the signaling complex. Others have described several functions of the C protein, which might be involved also in its ability to block IFN α induction. On the one hand, MV C possesses a nuclear localization signal (NLS) as well as a nuclear export signal (NES), which both contribute to the ability of the C protein to shuttle between cytoplasm and nucleus (Nishie et al., 2007). Thereby, signal transduction processes like the nuclear translocation of IRF7 might be disturbed by the C

protein. Similar results were found for the RPV C protein, which inhibits the induction of IFN β by IRF3 (Boxer et al., 2009).

4.6 Future perspectives

In this study I used the V protein of the Schwarz vaccine strain, which is derived from the original Edmonston wt isolate by several passages on different cell lines (Rota et al., 1994). Direct nucleotide comparison reveal only minor changes in the coding regions of parental and attenuated strains (Parks et al., 2001). Only one amino acid mutation (E225G) occurs within the V protein of MV(Schwarz) compared to the parental MV(Edmonston wt). The inhibitory function of V regarding TLR7/9 signaling was existent in the V protein of the attenuated Schwarz strain. It is assumed that also the V protein of wt MV should have the same function and probably should function even more effective than Schwarz strain V. However, this has to be clarified and therefore we will directly compare the functions of Schwarz strain V with the V protein of a wild type isolate (MVi/Berlin.DEU/04.08, genotype D5; RKI Berlin) on the molecular level as well as the ability to block IFN α induction in the virus context. It has been reported that the wt isolate of the G954 strain showed strong IFN α production in human pDCs, and passaging of the virus on Vero cells (G954-V13) did not change this phenotype, although the resulting virus was highly attenuated (Druelle et al., 2008). Comparing the V protein sequences of MV G954 and Schwarz revealed that in both G954-PBL and G954-V13 a mutation T259A was introduced. However, the mutation of Schwarz strain MV V T259A did not lead to a non-functional V protein in our study. Only by mutating also the subsequent amino acids led to a mutant (MV V T259A-L260A-G261A-T262A), which was unable to inhibit IFN α induction and did neither bind to IKK α , nor to IRF7.

Using a reverse genetics system for MV (Devaux et al., 2007), the biochemical data obtained in this study will be confirmed in the virus context in the future. Generation of recombinant V knock-out MV and recombinant MV expressing mutated forms of V instead of the original protein will further clarify the role of

V in infection studies. Chimeric recombinant MVs expressing V from wt strains will elucidate, whether wt V differs in its functions from Schwarz strain V.

The results described here may bring new aspects into the field of autoimmune disorders. Systemic lupus erythematosus (SLE; (Barrat et al., 2005)) and many other autoimmune disorders have been shown or are suspected to be dependent on the activation of TLR7/9. MV V is a specific antagonist of the MyD88-dependent induction of IFN α and therefore could be used to specifically block the TLR7/9 dependent signal transduction. Recombinant MV V could be used in murine SLE model organisms to study the effect *in vivo* (Christensen et al., 2006). By narrowing down the functional domain of V, smaller peptides could be generated to facilitate the local admission and agency of V.

5 Summary

Measles virus (MV) is a haematotropic member of the *Paramyxoviridae* family (order *Mononegavirales*, genus *Morbillivirus*) and an important human pathogen. It induces a generalized transient immune suppression as well as a specific immune response that provides life-long protection. This paradoxical effect is most likely due to early interactions of MV with immune cells, including conventional and plasmacytoid dendritic cells (cDCs and pDCs, respectively). A remarkable feature of MV is the ability to shut down interferon-alpha (IFN α) production in response to Toll-like receptor (TLR) 7 and TLR9 ligands in human pDCs, as shown previously in this laboratory. The MV proteins involved and the molecular mechanisms behind remained elusive.

To identify these proteins involved, the IFN-inducing TLR pathway of pDCs, which involves the adapter MyD88, the kinases IRAK1, IRAK4 and IKK α , and the transcription factor IRF7, was reconstituted in HEK-293T cells by expression of the recombinant proteins from transfected plasmids. Co-expression of individual MV proteins in reporter gene assays led to the identification of the MV V protein as a potent inhibitor. MV V was previously described to bind STAT1/2 and MDA-5, thereby interfering with other important immune signaling cascades as well.

MV V is expressed from the MV phosphoprotein (P) gene by mRNA editing and is composed of an N-terminal sequence identical to that of P and a unique 68-amino-acid Cys-rich and zinc-binding C-terminal domain. As shown by co-immunoprecipitation experiments, V specifically binds to both IKK α and IRF7 but not to the closely related IKK β , TBK1 and IKK ϵ or IRF3, respectively. Binding of MV V to IKK α resulted in phosphorylation of V on the expense of IRF7 phosphorylation both in living cells and *in vitro*, as illustrated by *in vitro* kinase experiments. In addition to interfering with activation of IRF7 by

preventing phosphorylation, MV V also binds to phosphomimetic IRF7 which contributes to preventing transcriptional activity of IRF7. The MV V-specific 68-amino-acid C terminal domain was identified as an autonomous targeting module directing V to IKK α and IRF7, while sequences of the common N-terminal domain were necessary for potent inhibition of IRF7-mediated IFN α promoter activation.

Among the V proteins of paramyxoviruses, which share organization as well as STAT-, and MDA-5-binding, MV V is unique in targeting MyD88-dependent IKK α /IRF7 activation, as exemplified by experiments using the V protein of parainfluenzavirus type 5 (PIV5; genus *Rubulavirus*). A mutant MV V protein carrying PIV5-like mutations at amino acids 259 – 262, lost the ability to bind both IKK α and IRF7 and therefore did not inhibit IFN α activation. In contrast, JAK/STAT signaling was not affected by this mutant, revealing independent inhibitory functions.

In addition to IFN α induction, MV V inhibited NF- κ B activation, which is also triggered by TLR-signaling. Activation of NF- κ B is partially dependent on IKK α . However, the efficiency of inhibition of NF- κ B activation was not as prominent as of IFN α induction. The exact mechanisms involved could not be clarified in this study.

Autophagy, which has recently been identified to be involved in the localization of viral nucleic acids to TLR-containing compartments, could be shown to be activated at early stages of MV infection, but it is blocked efficiently at later stages of infection. This gives hint that a viral factor is counteracting also this pathway involved in the innate immune response, but whether this factor is the MV V or a different protein still needs to be clarified.

The results provided here open the way for mutagenesis experiments to generate recombinant MV with specific defects in blocking either IKK α , JAK/STAT, or MDA-5 signaling, in order to appreciate the contribution of these individual functions to MV immune biology. Such studies will not only lead to recombinant vaccine viruses with abolished or reduced capacity to undermine the host immune response, but may also help to develop tools to specifically interfere with immunopathological TLR signaling.

5 Zusammenfassung

Das Masernvirus (MV) gehört zur Familie der *Paramyxoviridae* (Ordnung *Mononegavirales*, Genus *Morbillivirus*). Das hämatotrope Virus führt zu einer generalisierten Immunsuppression, löst aber auch eine spezifische Immunantwort aus, die einen lebenslangen Schutz gewährt. Dieses „Masern-Paradoxon“ lässt sich am ehesten durch eine Interaktion des Virus mit Zellen des Immunsystems früh nach Eintritt der Infektion erklären. Dies sind unter anderem konventionelle und plasmazytoide dendritische Zellen (cDCs und pDCs). Eine Besonderheit des MV besteht in der Inhibition der TLR7/9-abhängigen Produktion von Interferon-alpha ($IFN\alpha$) in pDCs. In dieser Arbeit konnte das virale Protein, das die Inhibition vermittelt, identifiziert und der zugrundeliegende molekulare Mechanismus aufgeklärt werden.

Zu diesem Zweck wurde der TLR7/9 abhängige Signaltransduktionskomplex, welcher zur Aktivierung von $IFN\alpha$ Promotoren führt, in HEK-293T Zellen rekonstituiert. Ausgewählte Proteine des Komplexes wurden transient überexprimiert, unter anderem das Adaptermolekül MyD88, die Serin-/Threoninkinasen IRAK1, IRAK4 und $IKK\alpha$, sowie der Transkriptionsfaktor IRF7. Darüber hinaus wurden verschiedene virale Proteine koexprimiert. Im Falle des V Proteins des MV (MV V) führte dies zu einer starken Reduktion der $IFN\alpha$ -Promotoraktivierung im Reportersystem. Aus anderen Studien war bereits bekannt, dass das V Protein auch die MDA-5-abhängigen und JAK/STAT Signaltransduktionswege des angeborenen Immunsystems inhibiert.

Das MV V Protein ist im Phosphoprotein (P) Gen des MV kodiert und entsteht durch kotranskriptionelle Editierung der mRNA. Dadurch besitzt das V Protein einen N-Terminus, der mit dem des P Proteins identisch ist und eine spezielle Cys-reiche und Zn-bindende C-terminale Domäne. Ko-Immunpräzipitations-

experimente zeigten, dass diese C-terminale Domäne für eine direkte Interaktion von V mit den Faktoren IKK α und IRF7 des Signaltransduktionskomplexes verantwortlich ist. Nahe verwandte Proteine, IKK β , TBK1, IKK ϵ und IRF3, werden jedoch nicht gebunden. *In vitro* Kinasestudien zeigten, dass die Bindung an IKK α zu einer Phosphorylierung des V Proteins führt und dadurch die Phosphorylierung von IRF7 verhindert wird. Dies konnte in lebenden Zellen bestätigt werden. Zusätzlich ist V in der Lage, an phosphomimetisches, konstitutiv aktives IRF7 zu binden und dadurch dessen transkriptionelle Aktivität zu inhibieren. Obwohl die C-terminale Domäne für die Bindung ausreichend war, bedurfte es des gesamten V Proteins, um die IFN α -Promotoraktivierung vollständig zu unterbinden.

Unter allen V Proteinen der Viren aus der Familie der *Paramyxoviridae*, welche als gemeinsame Funktionen die Inhibition von MDA-5-abhängiger und JAK/STAT-Signaltransduktion besitzen, ist das MV V Protein das Erste, welches die Aktivierung von IRF7 durch IKK α inhibiert. Aminosäureaustausche im MV V hin zur Sequenz des in dieser Hinsicht inaktiven V Proteins des Parainfluenzavirus Typ 5 (PIV5 V, Genus *Rubulavirus*) im Bereich der Aminosäuren 259 – 262 hatten zur Folge, dass weder IKK α oder IRF7 gebunden werden konnte. Auch die Aktivierung von IFN α -Promotoren konnte durch diese Mutante nicht mehr inhibiert werden. Im Gegensatz dazu war die Inhibition der JAK/STAT-Signaltransduktion unbeeinflusst, woraus sich schließen lässt, dass beides unabhängige Funktionen des MV V Proteins sind.

Darüber hinaus konnte gezeigt werden, dass MV V die Aktivierung von NF- κ B inhibiert, jedoch in einem geringeren Maß. NF- κ B wird ebenfalls durch TLR7/9 in einer Signaltransduktionskaskade aktiviert, welche teilweise von IKK α abhängig ist. Die molekularen Mechanismen dieser Inhibition sind allerdings bisher noch unklar.

Es konnte des Weiteren gezeigt werden, dass im frühen Verlauf einer Maserninfektion Autophagie induziert wird. Dadurch gelangen virale Nukleinsäuren aus dem Zytoplasma infizierter Zellen in endosomale Kompartimente, wo sie zur Aktivierung von TLR7 und zur IFN α Expression beitragen. Es konnte gezeigt werden, dass diese frühe Aktivierung von

Autophagie im späteren Verlauf der Infektion vom Virus blockiert wird. Ob das V Protein auch bei dieser Inhibition eine Rolle übernimmt muss weiter geklärt werden.

Die hier vorgelegten Ergebnisse eröffnen die Möglichkeit zu Studien mit rekombinanten MV, bei denen spezifisch eine oder mehrere inhibierende Funktionen des V Proteins ausgeschaltet werden. Dies wird zu einem tieferen Verständnis der Immunbiologie des MV beitragen und könnte zur Entwicklung rekombinanter Vakzinen mit reduzierten oder vollständig ausgeschalteten immunmodulatorischen Fähigkeiten führen. Andererseits könnte man diese Fähigkeiten des V Proteins zur Therapie von immunpathologischen Erkrankungen nutzen, bei denen TLR7/9-abhängige Signaltransduktion eine Rolle spielen.

6 References

- Abdullah,H., Earle,J.A., Gardiner,T.A., Tangy,F., and Cosby,S.L. (2009). PERSISTENT MEASLES VIRUS INFECTION OF MOUSE NEURAL CELLS LACKING KNOWN HUMAN ENTRY RECEPTORS. *Neuropathol. Appl. Neurobiol.*
- Andrejeva,J., Childs,K.S., Young,D.F., Carlos,T.S., Stock,N., Goodbourn,S., and Randall,R.E. (2004). The V proteins of paramyxoviruses bind the IFN-inducible RNA helicase, mda-5, and inhibit its activation of the IFN-beta promoter. *Proc. Natl. Acad. Sci. U. S. A* *101*, 17264-17269.
- Ank,N., West,H., Bartholdy,C., Eriksson,K., Thomsen,A.R., and Paludan,S.R. (2006). Lambda interferon (IFN-lambda), a type III IFN, is induced by viruses and IFNs and displays potent antiviral activity against select virus infections in vivo. *J. Virol.* *80*, 4501-4509.
- Baglioni,C. and Maroney,P.A. (1980). Mechanisms of action of human interferons. Induction of 2'5'-oligo(A) polymerase. *J. Biol. Chem.* *255*, 8390-8393.
- Balachandran,S. and Barber,G.N. (2007). PKR in innate immunity, cancer, and viral oncolysis. *Methods Mol. Biol.* *383*, 277-301.
- Bankamp,B., Hodge,G., McChesney,M.B., Bellini,W.J., and Rota,P.A. (2008). Genetic changes that affect the virulence of measles virus in a rhesus macaque model. *Virology* *373*, 39-50.
- Barrat,F.J., Meeker,T., Gregorio,J., Chan,J.H., Uematsu,S., Akira,S., Chang,B., Duramad,O., and Coffman,R.L. (2005). Nucleic acids of mammalian origin can act as endogenous ligands for Toll-like receptors and may promote systemic lupus erythematosus. *J. Exp. Med.* *202*, 1131-1139.
- Bieback,K., Lien,E., Klagge,I.M., Avota,E., Schneider-Schaulies,J., Duprex,W.P., Wagner,H., Kirschning,C.J., Ter,M., V, and Schneider-Schaulies,S. (2002). Hemagglutinin protein of wild-type measles virus activates toll-like receptor 2 signaling. *J. Virol.* *76*, 8729-8736.
- Black,F.L., Melnick,J.L., and Reissig,M. (1956). Formation of multinucleated giant cells in measles virus infected cultures deprived of glutamine. *Virology* *2*, 836-838.

- Borges,M.B., Caride,E., Jabor,A.V., Malachias,J.M., Freire,M.S., Homma,A., and Galler,R. (2008). Study of the genetic stability of measles virus CAM-70 vaccine strain after serial passages in chicken embryo fibroblasts primary cultures. *Virus Genes* 36, 35-44.
- Boxer,E.L., Nanda,S.K., and Baron,M.D. (2009). The rinderpest virus non-structural C protein blocks the induction of type 1 interferon. *Virology* 385, 134-142.
- Brinkmann,V., Geiger,T., Alkan,S., and Heusser,C.H. (1993). Interferon alpha increases the frequency of interferon gamma-producing human CD4+ T cells. *J. Exp. Med.* 178, 1655-1663.
- Brzózka,K., Finke,S., and Conzelmann,K.K. (2005). Identification of the rabies virus alpha/beta interferon antagonist: phosphoprotein P interferes with phosphorylation of interferon regulatory factor 3. *J. Virol.* 79, 7673-7681.
- Brzózka,K., Pfaller,C., and Conzelmann,K.K. (2007). Signal transduction in the type I interferon system and viral countermeasures. *Signal Transduction* 7, 5-19.
- Bunting,C.H. (1950). The giant-cells of measles. *Yale J. Biol. Med.* 22, 513-519.
- Caignard,G., Guerbois,M., Labernardiere,J.L., Jacob,Y., Jones,L.M., Wild,F., Tangy,F., and Vidalain,P.O. (2007). Measles virus V protein blocks Jak1-mediated phosphorylation of STAT1 to escape IFN-alpha/beta signaling. *Virology* 368, 351-362.
- Cella,M., Jarrossay,D., Facchetti,F., Alebardi,O., Nakajima,H., Lanzavecchia,A., and Colonna,M. (1999). Plasmacytoid monocytes migrate to inflamed lymph nodes and produce large amounts of type I interferon. *Nat. Med.* 5, 919-923.
- Chen,M., Cortay,J.C., and Gerlier,D. (2003). Measles virus protein interactions in yeast: new findings and caveats. *Virus Res.* 98, 123-129.
- Childs,K., Stock,N., Ross,C., Andrejeva,J., Hilton,L., Skinner,M., Randall,R., and Goodbourn,S. (2007). mda-5, but not RIG-I, is a common target for paramyxovirus V proteins. *Virology* 359, 190-200.
- Christensen,S.R., Shupe,J., Nickerson,K., Kashgarian,M., Flavell,R.A., and Shlomchik,M.J. (2006). Toll-like receptor 7 and TLR9 dictate autoantibody specificity and have opposing inflammatory and regulatory roles in a murine model of lupus. *Immunity.* 25, 417-428.
- Conzelmann,K.K., Cox,J.H., Schneider,L.G., and Thiel,H.J. (1990). Molecular cloning and complete nucleotide sequence of the attenuated rabies virus SAD B19. *Virology* 175, 485-499.
- Cui,S., Eisenacher,K., Kirchhofer,A., Brzozka,K., Lammens,A., Lammens,K., Fujita,T., Conzelmann,K.K., Krug,A., and Hopfner,K.P. (2008). The C-

- terminal regulatory domain is the RNA 5'-triphosphate sensor of RIG-I. *Mol. Cell* 29, 169-179.
- de Swart,R.L., Ludlow,M., de,W.L., Yanagi,Y., van,A.G., McQuaid,S., Yuksel,S., Geijtenbeek,T.B., Duprex,W.P., and Osterhaus,A.D. (2007). Predominant infection of CD150+ lymphocytes and dendritic cells during measles virus infection of macaques. *PLoS. Pathog.* 3, e178.
- de Witte,L., Abt,M., Schneider-Schaulies,S., van,K.Y., and Geijtenbeek,T.B. (2006). Measles virus targets DC-SIGN to enhance dendritic cell infection. *J. Virol.* 80, 3477-3486.
- Delgado,M.A., Elmaoued,R.A., Davis,A.S., Kyei,G., and Deretic,V. (2008). Toll-like receptors control autophagy. *EMBO J.* 27, 1110-1121.
- Devaux,P., von,M., V, Songsunthong,W., Springfield,C., and Cattaneo,R. (2007). Tyrosine 110 in the measles virus phosphoprotein is required to block STAT1 phosphorylation. *Virology* 360, 72-83.
- Dörig,R.E., Marcil,A., Chopra,A., and Richardson,C.D. (1993). The human CD46 molecule is a receptor for measles virus (Edmonston strain). *Cell* 75, 295-305.
- Druelle,J., Sellin,C.I., Waku-Kouomou,D., Horvat,B., and Wild,F.T. (2008). Wild type measles virus attenuation independent of type I IFN. *Virol. J.* 5, 22.
- Enders,J.F., Katz,S.L., and Holloway,A. (1962). Development of attenuated measles-virus vaccines. A summary of recent investigation. *Am. J. Dis. Child* 103, 335-340.
- Finke,S. and Conzelmann,K.K. (1999). Virus promoters determine interference by defective RNAs: selective amplification of mini-RNA vectors and rescue from cDNA by a 3' copy-back ambisense rabies virus. *J. Virol.* 73, 3818-3825.
- Fitzgerald-Bocarsly,P. and Feng,D. (2007). The role of type I interferon production by dendritic cells in host defense. *Biochimie* 89, 843-855.
- Fugier-Vivier,I., Servet-Delprat,C., Rivaller,P., Rissoan,M.C., Liu,Y.J., and Roubourdin-Combe,C. (1997). Measles virus suppresses cell-mediated immunity by interfering with the survival and functions of dendritic and T cells. *J. Exp. Med.* 186, 813-823.
- Goodbourn,S. and Randall,R.E. (2009). The regulation of type I interferon production by paramyxoviruses. *J. Interferon Cytokine Res.* 29, 539-547.
- Gotoh,B., Komatsu,T., Takeuchi,K., and Yokoo,J. (2001). Paramyxovirus accessory proteins as interferon antagonists. *Microbiol. Immunol.* 45, 787-800.
- Griffin,D.E. and Ward,B.J. (1993). Differential CD4 T cell activation in measles. *J. Infect. Dis.* 168, 275-281.

- Griffin,D.E., Ward,B.J., Jauregui,E., Johnson,R.T., and Vaisberg,A. (1990). Immune activation during measles: interferon-gamma and neopterin in plasma and cerebrospinal fluid in complicated and uncomplicated disease. *J. Infect. Dis.* *161*, 449-453.
- Griffin,D.E., Ward,B.J., Juaregui,E., Johnson,R.T., and Vaisberg,A. (1992). Immune activation during measles: beta 2-microglobulin in plasma and cerebrospinal fluid in complicated and uncomplicated disease. *J. Infect. Dis.* *166*, 1170-1173.
- Hashimoto,K., Ono,N., Tatsuo,H., Minagawa,H., Takeda,M., Takeuchi,K., and Yanagi,Y. (2002). SLAM (CD150)-independent measles virus entry as revealed by recombinant virus expressing green fluorescent protein. *J. Virol.* *76*, 6743-6749.
- Honda,K., Ohba,Y., Yanai,H., Negishi,H., Mizutani,T., Takaoka,A., Taya,C., and Taniguchi,T. (2005). Spatiotemporal regulation of MyD88-IRF-7 signalling for robust type-I interferon induction. *Nature* *434*, 1035-1040.
- Honda,K., Yanai,H., Mizutani,T., Negishi,H., Shimada,N., Suzuki,N., Ohba,Y., Takaoka,A., Yeh,W.C., and Taniguchi,T. (2004). Role of a transductional-transcriptional processor complex involving MyD88 and IRF-7 in Toll-like receptor signaling. *Proc. Natl. Acad. Sci. U. S. A* *101*, 15416-15421.
- Horisberger,M.A. and Hochkeppel,H.K. (1987). IFN-alpha induced human 78 kD protein: purification and homologies with the mouse Mx protein, production of monoclonal antibodies, and potentiation effect of IFN-gamma. *J. Interferon Res.* *7*, 331-343.
- Hornung,V., Ellegast,J., Kim,S., Brzozka,K., Jung,A., Kato,H., Poeck,H., Akira,S., Conzelmann,K.K., Schlee,M., Endres,S., and Hartmann,G. (2006). 5'-Triphosphate RNA is the ligand for RIG-I. *Science* *314*, 994-997.
- Hornung,V., Rothenfusser,S., Britsch,S., Krug,A., Jahrsdorfer,B., Giese,T., Endres,S., and Hartmann,G. (2002). Quantitative expression of toll-like receptor 1-10 mRNA in cellular subsets of human peripheral blood mononuclear cells and sensitivity to CpG oligodeoxynucleotides. *J. Immunol.* *168*, 4531-4537.
- Hoshino,K., Sugiyama,T., Matsumoto,M., Tanaka,T., Saito,M., Hemmi,H., Ohara,O., Akira,S., and Kaisho,T. (2006). IkappaB kinase-alpha is critical for interferon-alpha production induced by Toll-like receptors 7 and 9. *Nature* *440*, 949-953.
- Innis,C.A., Shi,J., and Blundell,T.L. (2000). Evolutionary trace analysis of TGF-beta and related growth factors: implications for site-directed mutagenesis. *Protein Eng* *13*, 839-847.

- Jansen,V.A., Stollenwerk,N., Jensen,H.J., Ramsay,M.E., Edmunds,W.J., and Rhodes,C.J. (2003). Measles outbreaks in a population with declining vaccine uptake. *Science* *301*, 804.
- Johnson,R.T. (1998). *Viral infections of the nervous system*. (Philadelphia: Lippincott-Raven).
- Johnson,R.T., Griffin,D.E., Hirsch,R.L., Wolinsky,J.S., Roedenbeck,S., Lindo,d.S., I, and Vaisberg,A. (1984). Measles encephalomyelitis--clinical and immunologic studies. *N. Engl. J. Med.* *310*, 137-141.
- Jurke, A. Zu den aktuellen Masernhäufungen in Nordrhein-Westfalen und Hamburg. 10/2009. 2009. Robert-Koch-Institut. *Epidemiologisches Bulletin*.
- Kadowaki,N. (2009). The divergence and interplay between pDC and mDC in humans. *Front Biosci.* *14*, 808-817.
- Kawai,T. and Akira,S. (2008). Toll-like receptor and RIG-I-like receptor signaling. *Ann. N. Y. Acad. Sci.* *1143*, 1-20.
- Kawai,T., Sato,S., Ishii,K.J., Coban,C., Hemmi,H., Yamamoto,M., Terai,K., Matsuda,M., Inoue,J., Uematsu,S., Takeuchi,O., and Akira,S. (2004). Interferon-alpha induction through Toll-like receptors involves a direct interaction of IRF7 with MyD88 and TRAF6. *Nat. Immunol.* *5*, 1061-1068.
- Kawai,T., Takahashi,K., Sato,S., Coban,C., Kumar,H., Kato,H., Ishii,K.J., Takeuchi,O., and Akira,S. (2005). IPS-1, an adaptor triggering RIG-I- and Mda5-mediated type I interferon induction. *Nat. Immunol.* *6*, 981-988.
- Kielian,M. and Rey,F.A. (2006). Virus membrane-fusion proteins: more than one way to make a hairpin. *Nat. Rev. Microbiol.* *4*, 67-76.
- Kim,T.W., Staschke,K., Bulek,K., Yao,J., Peters,K., Oh,K.H., Vandenburg,Y., Xiao,H., Qian,W., Hamilton,T., Min,B., Sen,G., Gilmour,R., and Li,X. (2007). A critical role for IRAK4 kinase activity in Toll-like receptor-mediated innate immunity. *J. Exp. Med.* *204*, 1025-1036.
- Klagge,I.M., Ter,M., V, and Schneider-Schaulies,S. (2000). Measles virus-induced promotion of dendritic cell maturation by soluble mediators does not overcome the immunosuppressive activity of viral glycoproteins on the cell surface. *Eur. J. Immunol.* *30*, 2741-2750.
- Kolakofsky,D., Roux,L., Garcin,D., and Ruigrok,R.W. (2005). Paramyxovirus mRNA editing, the "rule of six" and error catastrophe: a hypothesis. *J. Gen. Virol.* *86*, 1869-1877.
- Korkhov,V.M. (2009). GFP-LC3 labels organised smooth endoplasmic reticulum membranes independently of autophagy. *J. Cell Biochem.* *107*, 86-95.
- Kumar,H., Kawai,T., and Akira,S. (2009). Toll-like receptors and innate immunity. *Biochem. Biophys. Res. Commun.* *388*, 621-625.

- Larkin, M.A., Blackshields, G., Brown, N.P., Chenna, R., McGettigan, P.A., McWilliam, H., Valentin, F., Wallace, I.M., Wilm, A., Lopez, R., Thompson, J.D., Gibson, T.J., and Higgins, D.G. (2007). Clustal W and Clustal X version 2.0. *Bioinformatics*. *23*, 2947-2948.
- Le Bon, A. and Tough, D.F. (2002). Links between innate and adaptive immunity via type I interferon. *Curr. Opin. Immunol.* *14*, 432-436.
- Lee, H.K., Lund, J.M., Ramanathan, B., Mizushima, N., and Iwasaki, A. (2007). Autophagy-dependent viral recognition by plasmacytoid dendritic cells. *Science* *315*, 1398-1401.
- Li, T., Chen, X., Garbutt, K.C., Zhou, P., and Zheng, N. (2006). Structure of DDB1 in complex with a paramyxovirus V protein: viral hijack of a propeller cluster in ubiquitin ligase. *Cell* *124*, 105-117.
- Lin, R., Lacoste, J., Nakhaei, P., Sun, Q., Yang, L., Paz, S., Wilkinson, P., Julkunen, I., Vitour, D., Meurs, E., and Hiscott, J. (2006). Dissociation of a MAVS/IPS-1/VISA/Cardif-IKKe epsilon molecular complex from the mitochondrial outer membrane by hepatitis C virus NS3-4A proteolytic cleavage. *J. Virol.* *80*, 6072-6083.
- Lin, R., Mamane, Y., and Hiscott, J. (2000). Multiple regulatory domains control IRF-7 activity in response to virus infection. *J. Biol. Chem.* *275*, 34320-34327.
- Liston, P. and Briedis, D.J. (1994). Measles virus V protein binds zinc. *Virology* *198*, 399-404.
- Littmann, M. Masern: Zu einer Häufung in Mecklenburg-Vorpommern. 13/2008. 2008. Robert-Koch-Institut. *Epidemiologisches Bulletin*.
- Loo, Y.M. and Gale, M., Jr. (2007). Viral regulation and evasion of the host response. *Curr. Top. Microbiol. Immunol.* *316*, 295-313.
- Lu, L.L., Puri, M., Horvath, C.M., and Sen, G.C. (2008). Select paramyxoviral V proteins inhibit IRF3 activation by acting as alternative substrates for inhibitor of kappaB kinase epsilon (IKKe)/TBK1. *J. Biol. Chem.* *283*, 14269-14276.
- Martinet, W., De Meyer, G.R., Andries, L., Herman, A.G., and Kockx, M.M. (2006). Detection of autophagy in tissue by standard immunohistochemistry: possibilities and limitations. *Autophagy*. *2*, 55-57.
- Michallet, M.C., Meylan, E., Ermolaeva, M.A., Vazquez, J., Rebsamen, M., Curran, J., Poeck, H., Bscheider, M., Hartmann, G., König, M., Kalinke, U., Pasparakis, M., and Tschopp, J. (2008). TRADD protein is an essential component of the RIG-like helicase antiviral pathway. *Immunity*. *28*, 651-661.

- Minagawa,H., Tanaka,K., Ono,N., Tatsuo,H., and Yanagi,Y. (2001). Induction of the measles virus receptor SLAM (CD150) on monocytes. *J. Gen. Virol.* *82*, 2913-2917.
- Naniche,D. (2009). Human immunology of measles virus infection. *Curr. Top. Microbiol. Immunol.* *330*, 151-171.
- Naniche,D., Varior-Krishnan,G., Cervoni,F., Wild,T.F., Rossi,B., Raboutin-Combe,C., and Gerlier,D. (1993). Human membrane cofactor protein (CD46) acts as a cellular receptor for measles virus. *J. Virol.* *67*, 6025-6032.
- Naniche,D., Yeh,A., Eto,D., Manchester,M., Friedman,R.M., and Oldstone,M.B. (2000). Evasion of host defenses by measles virus: wild-type measles virus infection interferes with induction of Alpha/Beta interferon production. *J. Virol.* *74*, 7478-7484.
- Nishie,T., Nagata,K., and Takeuchi,K. (2007). The C protein of wild-type measles virus has the ability to shuttle between the nucleus and the cytoplasm. *Microbes. Infect.* *9*, 344-354.
- Oganesyan,G., Saha,S.K., Guo,B., He,J.Q., Shahangian,A., Zarnegar,B., Perry,A., and Cheng,G. (2006). Critical role of TRAF3 in the Toll-like receptor-dependent and -independent antiviral response. *Nature* *439*, 208-211.
- Ohno,S., Ono,N., Takeda,M., Takeuchi,K., and Yanagi,Y. (2004). Dissection of measles virus V protein in relation to its ability to block alpha/beta interferon signal transduction. *J. Gen. Virol.* *85*, 2991-2999.
- Palosaari,H., Parisien,J.P., Rodriguez,J.J., Ulane,C.M., and Horvath,C.M. (2003). STAT protein interference and suppression of cytokine signal transduction by measles virus V protein. *J. Virol.* *77*, 7635-7644.
- Parks,C.L., Lerch,R.A., Walpita,P., Wang,H.P., Sidhu,M.S., and Udem,S.A. (2001). Comparison of predicted amino acid sequences of measles virus strains in the Edmonston vaccine lineage. *J. Virol.* *75*, 910-920.
- Pestka,S., Krause,C.D., and Walter,M.R. (2004). Interferons, interferon-like cytokines, and their receptors. *Immunol. Rev.* *202*, 8-32.
- Pichlmair,A. and Reis e Sousa (2007). Innate recognition of viruses. *Immunity.* *27*, 370-383.
- Pichlmair,A., Schulz,O., Tan,C.P., Naslund,T.I., Liljestrom,P., Weber,F., and Reis e Sousa (2006). RIG-I-mediated antiviral responses to single-stranded RNA bearing 5'-phosphates. *Science* *314*, 997-1001.
- Precious,B., Childs,K., Fitzpatrick-Swallow,V., Goodbourn,S., and Randall,R.E. (2005). Simian virus 5 V protein acts as an adaptor, linking DDB1 to STAT2, to facilitate the ubiquitination of STAT1. *J. Virol.* *79*, 13434-13441.

- Precious,B.L., Carlos,T.S., Goodbourn,S., and Randall,R.E. (2007). Catalytic turnover of STAT1 allows PIV5 to dismantle the interferon-induced anti-viral state of cells. *Virology* 368, 114-121.
- Ramachandran,A., Parisien,J.P., and Horvath,C.M. (2008). STAT2 is a primary target for measles virus V protein-mediated alpha/beta interferon signaling inhibition. *J. Virol.* 82, 8330-8338.
- Reis e Sousa (2004). Activation of dendritic cells: translating innate into adaptive immunity. *Curr. Opin. Immunol.* 16, 21-25.
- Rima,B.K. and Duprex,W.P. (2009). The measles virus replication cycle. *Curr. Top. Microbiol. Immunol.* 329, 77-102.
- Rota,J.S., Wang,Z.D., Rota,P.A., and Bellini,W.J. (1994). Comparison of sequences of the H, F, and N coding genes of measles virus vaccine strains. *Virus Res.* 31, 317-330.
- Rota,P.A., Featherstone,D.A., and Bellini,W.J. (2009). Molecular epidemiology of measles virus. *Curr. Top. Microbiol. Immunol.* 330, 129-150.
- Ryzhakov,G. and Randow,F. (2007). SINTBAD, a novel component of innate antiviral immunity, shares a TBK1-binding domain with NAP1 and TANK. *EMBO J.* 26, 3180-3190.
- Schlender,J., Hornung,V., Finke,S., Gunthner-Biller,M., Marozin,S., Brzózka,K., Moghim,S., Endres,S., Hartmann,G., and Conzelmann,K.K. (2005). Inhibition of toll-like receptor 7- and 9-mediated alpha/beta interferon production in human plasmacytoid dendritic cells by respiratory syncytial virus and measles virus. *J. Virol.* 79, 5507-5515.
- Schlender,J., Schnorr,J.J., Spielhoffer,P., Cathomen,T., Cattaneo,R., Billeter,M.A., Ter,M., V, and Schneider-Schaulies,S. (1996). Interaction of measles virus glycoproteins with the surface of uninfected peripheral blood lymphocytes induces immunosuppression in vitro. *Proc. Natl. Acad. Sci. U. S. A* 93, 13194-13199.
- Schmidt,N., Mishra,A., Lai,G.H., and Wong,G.C. (2009). Arginine-rich cell-penetrating peptides. *FEBS Lett.*
- Schneider-Schaulies,S. and Schneider-Schaulies,J. (2009). Measles virus-induced immunosuppression. *Curr. Top. Microbiol. Immunol.* 330, 243-269.
- Schnell,M.J., Mebatsion,T., and Conzelmann,K.K. (1994). Infectious rabies viruses from cloned cDNA. *EMBO J.* 13, 4195-4203.
- Schultheiss,U., Puschner,S., Kremmer,E., Mak,T.W., Engelmann,H., Hammerschmidt,W., and Kieser,A. (2001). TRAF6 is a critical mediator of signal transduction by the viral oncogene latent membrane protein 1. *EMBO J.* 20, 5678-5691.
- Schwarz,K. (1964). IMMUNIZATION 1964. *Nurs. Times* 60, 1315-1316.

- Shingai,M., Ebihara,T., Begum,N.A., Kato,A., Honma,T., Matsumoto,K., Saito,H., Ogura,H., Matsumoto,M., and Seya,T. (2007). Differential type I IFN-inducing abilities of wild-type versus vaccine strains of measles virus. *J. Immunol.* *179*, 6123-6133.
- Siedler, A. and Santibanez, S. Masern im Jahr 2005 und Ausbrüche in Baden-Württemberg und Nordrhein-Westfalen in der ersten Hälfte des Jahres 2006. 27/2006. 7-7-2006. Robert-Koch-Institut. Epidemiologisches Bulletin.
- Siegel,F.P., Kadowaki,N., Shodell,M., Fitzgerald-Bocarsly,P.A., Shah,K., Ho,S., Antonenko,S., and Liu,Y.J. (1999). The nature of the principal type 1 interferon-producing cells in human blood. *Science* *284*, 1835-1837.
- Song,M.M. and Shuai,K. (1998). The suppressor of cytokine signaling (SOCS) 1 and SOCS3 but not SOCS2 proteins inhibit interferon-mediated antiviral and antiproliferative activities. *J. Biol. Chem.* *273*, 35056-35062.
- Tahara,M., Takeda,M., Shirogane,Y., Hashiguchi,T., Ohno,S., and Yanagi,Y. (2008). Measles virus infects both polarized epithelial and immune cells by using distinctive receptor-binding sites on its hemagglutinin. *J. Virol.* *82*, 4630-4637.
- Takaoka,A. and Yanai,H. (2006). Interferon signalling network in innate defence. *Cell Microbiol.* *8*, 907-922.
- Takasu,T., Mgone,J.M., Mgone,C.S., Miki,K., Komase,K., Namae,H., Saito,Y., Kokubun,Y., Nishimura,T., Kawanishi,R., Mizutani,T., Markus,T.J., Kono,J., Asuo,P.G., and Alpers,M.P. (2003). A continuing high incidence of subacute sclerosing panencephalitis (SSPE) in the Eastern Highlands of Papua New Guinea. *Epidemiol. Infect.* *131*, 887-898.
- Takeda,M., Tahara,M., Hashiguchi,T., Sato,T.A., Jinnouchi,F., Ueki,S., Ohno,S., and Yanagi,Y. (2007). A human lung carcinoma cell line supports efficient measles virus growth and syncytium formation via a. *J. Virol.* *81*, 12091-12096.
- Takeuchi,K., Kadota,S.I., Takeda,M., Miyajima,N., and Nagata,K. (2003). Measles virus V protein blocks interferon (IFN)-alpha/beta but not IFN-gamma signaling by inhibiting STAT1 and STAT2 phosphorylation. *FEBS Lett.* *545*, 177-182.
- Tatsuo,H., Ono,N., Tanaka,K., and Yanagi,Y. (2000). SLAM (CDw150) is a cellular receptor for measles virus. *Nature* *406*, 893-897.
- Tatsuo,H., Ono,N., and Yanagi,Y. (2001). Morbilliviruses use signaling lymphocyte activation molecules (CD150) as cellular receptors. *J. Virol.* *75*, 5842-5850.

- Toth,A.M., Devaux,P., Cattaneo,R., and Samuel,C.E. (2009). Protein kinase PKR mediates the apoptosis induction and growth restriction phenotypes of C protein-deficient measles virus. *J. Virol.* *83*, 961-968.
- Uematsu,S., Sato,S., Yamamoto,M., Hirotani,T., Kato,H., Takeshita,F., Matsuda,M., Coban,C., Ishii,K.J., Kawai,T., Takeuchi,O., and Akira,S. (2005). Interleukin-1 receptor-associated kinase-1 plays an essential role for Toll-like receptor (TLR)7- and TLR9-mediated interferon- α induction. *J. Exp. Med.* *201*, 915-923.
- Uphoff, H. and Hauri, A. Zum Auftreten von Masern in Hessen im bisherigen Verlauf des Jahres 2005. 13/2005. 1-4-2005. Robert-Koch-Institut. *Epidemiologisches Bulletin*.
- van Binnendijk,R.S., Poelen,M.C., Kuijpers,K.C., Osterhaus,A.D., and Uytdehaag,F.G. (1990). The predominance of CD8+ T cells after infection with measles virus suggests a role for CD8+ class I MHC-restricted cytotoxic T lymphocytes (CTL) in recovery from measles. Clonal analyses of human CD8+ class I MHC-restricted CTL. *J. Immunol.* *144*, 2394-2399.
- van Treeck, U. Masern: Zu den aktuellen Ausbruchsgeschehen in Nordrhein-Westfalen und Niederbayern. 17/2007. 27-4-2007. Robert-Koch-Institut. *Epidemiologisches Bulletin*.
- Vidalain,P.O., Azocar,O., Lamouille,B., Astier,A., Raboutin-Combe,C., and Servet-Delprat,C. (2000). Measles virus induces functional TRAIL production by human dendritic cells. *J. Virol.* *74*, 556-559.
- WHO. Fact sheet on measles. WHO Fact sheet no.286 . 2008.
- WHO. Fact sheet on smallpox. WHO Fact sheet . 2009.
- WHO/UNICEF Joint Statement. GLOBAL PLAN FOR REDUCING MEASLES MORTALITY 2006-2010. WHO . 2006.
- Wild,T.F., Malvoisin,E., and Buckland,R. (1991). Measles virus: both the haemagglutinin and fusion glycoproteins are required for fusion. *J. Gen. Virol.* *72 (Pt 2)*, 439-442.
- Williams,B.R. (2001). Signal integration via PKR. *Sci. STKE.* *2001*, re2.
- Yin,H.S., Wen,X., Paterson,R.G., Lamb,R.A., and Jardetzky,T.S. (2006). Structure of the parainfluenza virus 5 F protein in its metastable, prefusion conformation. *Nature* *439*, 38-44.
- Yoneyama,M., Suhara,W., Fukuhara,Y., Fukuda,M., Nishida,E., and Fujita,T. (1998). Direct triggering of the type I interferon system by virus infection: activation of a transcription factor complex containing IRF-3 and CBP/p300. *EMBO J.* *17*, 1087-1095.
- Young,V.A. and Rall,G.F. (2009). Making it to the synapse: measles virus spread in and among neurons. *Curr. Top. Microbiol. Immunol.* *330*, 3-30.

7 Appendices

A Complete sequence alignment of paramyxoviral N proteins

Beilong	MSRLG PAL DEFRSFKNN PPRR GALTTAI QGI KKNVIVLVP--TMK QPAKR	48
J-virus	MSKLN KVL DEFRDFKNN PPKKV GPVTAL QGF KKNVVVPV--MMK DTVKR	48
Measles	MATLLRSLALF KRNKDKPP ITSGSGGAI RGI KHIIIVIP--GDSS ITTR	48
Rinderpest	MASLLKSLALF KRNKDKPP LAAGSGGAI RGI KHVIVIP--GDSS ITTR	48
Dolphin	MATLLRSLALF KRNKDR TPLIAGSGGAI RGI KHVIVVPV--GDSS IVTR	48
Peste-des-petits-ruminants	MATLLKSLALF KRNKDKAP TASGSGGAI RGI KNVIVIP--GDSS ITTR	48
Canine	MASLLKSLTLF KRTRDQ PLASGSGGAI RGI KHVIVLIP--GDSS IVTR	48
Mossman	MS GVLS ALREFKDARLASK GEGL TRGAT GIK QKIAV IIP --Q QEG SKVR	48
Tupaia	MADLF SKV ND FQKY R TNLGR Q GLT V KLV GV RST V VLV P--STK DHRLR	48
Hendra	MSD IFDE AASFRSY SKLGR DGRASAAT ATL TKIRIF VP --ATNS PELR	48
Nipah	MSD IFDE AASFRSY SKLGR DGRASAAT ATL TKIRIF VP --ATNS PELR	48
Human	MSS VLK TFERFT IQE EL QEQ SDDT PV LET IK PTIR VFV I--NNND PVVR	48
Simian	MSS VLK TFERFT IQE EL QD HEED PV LET IR PLIR VFV --NSND PALR	48
Parainfluenzavirus	MSS VLK AYERFT LTE EL QD QSEEG TIP PT LK PVIR VFI L--TSNN PELR	48
Mapuera	MSS VL SMFERFT ME EL QDR GAEG TL PP ET IK ST IK VFI L--NSDD PRLR	48
Porcine	MSS VL TAFERFT IE EL QDR GAEG SIP PE LK TR IQ V FV L--NDED PHLR	48
Mumps	MSS VL KAFERFT IE EL QDR GEEG SIP PE LK SA VK V FV I--N TNP TR	48
Menangle	MSS V FR AF EL FT LE EQ NEHGND IEL PP ET LR TN IK VC IL--NN QEP QAR	48
Tioman	MSS V FR AF EL FT LE EQ ELGND IEI PP ET LR SN IK VC IL--NS QDP QTR	48
Newcastle	MSS V FE DE Y QL LA ATR PN GA HGGG EK GS LK VD V P V FT L --NSDD PEDR	48
Fer-de-lance	-MEL FDI AD GF AD H C IN LRSS KQ AT GS L SA IK DQ IL VL IP--GT QD SDIL	47
Sendai	MAGLL ST FD T FSSRR SE SINK SG GA VIP Q R ST V S V FL GPS V T DD AD K	50
	1.....10.....20.....30.....40.....50	



Beilong	FQ FMT L IL Q IA WS AKS SA AFIT G AFF S LLS MFAD NP G AM LR N LVND PD ID	98
J-virus	F HF IT F CL Q L V W SD L SG AFIT G AFL L LS IFA EN PA MLR S LLND PD ID	98
Measles	S RL LD RL V RL IGN PD V SG PK L T G AL I G IL SL F V ES PG Q L I OR IT DD PD VS	98
Rinderpest	S RL LD RL V K M V GD PD IS G PK L T G AL I S IL SL F V ES PG Q L I OR IT DD PD IS	98
Dolphin	S RL LD RL V RL LAG DP Y IS G PK L T G AL I S IL SL F V ES PS Q L I OR IT DD PD VS	98
Peste-des-petits-ruminants	S RL LD RL V RL LAG DP D ING SK L T G V M I S ML SL F V ES PG Q L I OR IT DD PD VS	98
Canine	S RL LD RL V RL V GD PE ING PK L T G IL I S IL SL F V ES PG Q L I OR IT DD PD VS	98
Mossman	W Q LL R LL L L G VI W S Q E AS PG VIT G A FL S L IS L ISE SP GN M V R RL LN ND PD LA	98
Tupaia	W K L I R L L L AV Y ND SL P DS IS IG ALL SL L AI S FE Q PA AV IR GL L SD PD LE	98
Hendra	W E L L F AL D V IR S PS A ES M K IG A AF T L IS MY S ER PG AL IR S LL ND PD IE	98
Nipah	W E L L F AL D V IR S PS A ES M K IG A AF T L IS MY S ER PG AL IR S LL ND PD IE	98
Human	S R LL FF N L R I IMS NT ARE GH RAG ALL SL L SL PS A AM SN H IK L AM HS PE AS	98
Simian	A Q LL L F N L R I IMS NT ARE SH K T G ALL SM F SL P AA AM GN H L KL AT RS PE AS	98
Parainfluenzavirus	S R LL L F CL R IV LS NG ARD SH R F G ALL TM F SL PS AT ML N H V K L AD RS PE AD	98
Mapuera	W K MM N F CL R L IMS DA AK IS R K V G AM IT LF SL P AS GM Q N H VR L ADR S PD AQ	98
Porcine	W R MF N F CL R L IL S PA IT RT ARK IG AM IT LF SL P AA AM Q N H V RL ADR S PD AI	98
Mumps	Y H ML N F CL R I IC S Q N AR ASH R V G AL IT LF SL P S AG M Q N H IR L ADR S PE AQ	98
Menangle	H D MM C F CL R L IAS NS ARA A H K T G A IL T L SL PT AM M Q N H L R I ADR S PD AD	98
Tioman	H D MM C F CL R L IAS NS ARA A H K T G A IL T L SL PT AM M Q N H L R I ADR S PD AD	98
Newcastle	W N FA V F CL R I AV S ED ANK PL R Q G AL IS LL CS H S Q V MR N H V AL AG K Q NE AT	98
Fer-de-lance	S N LL I ALL SL IF N AG CP EP IC AG A FL SL LL VL FT NN PT A AL G TH A K D SD L V	97
Sendai	L F I AT T L FL A HS L DT D K Q HS Q RG G FL V SL L AM A Y SS PE L Y L T T NG V N AD V K	100
60.....70.....80.....90.....100	



Beilong	VQIAEVSVDVNSR--ITLATRGRGMERYEEEEIVQMVETPPKGRDKAYPYA	146
J-virus	VQLAEIADIDNDK--LKLATRKGEMSRYENDMMRMASAGPSKGPSPYPYV	146
Measles	IRLLEVQSQDQSQSGLTFASRGTNMEDEADQYFSHDDPISSDQSRFGWFG	148
Rinderpest	IKLVEVVQSKTQSGSLTFASRGTSMDDDEADRYFTYDEPNDEERQSYWFE	148
Dolphin	IRLVEVIQSEKSLSGSLTFASRGANMEDEADDYFSIQAGEEGDTRGTHWFE	148
Peste-des-petits-ruminants	IRLVEVVQSTRSQSGLTFASRGADLDNEADMYFSIEGFPSSGGKKRINWFE	148
Canine	IKLVEVIQSPINSVCGLTFASRGASLDSAEDEFFKIVDEGSKAQQLGWLE	148
Mossman	ITIIIEFTIGPDSE--YKFAARGMSVYEEQMAHYLHLRDTPPQSAFDDPFPE	146
Tupaia	VQMIIEVSLDDQGE--IRFAARGDILTRYKDAYFEKIRDFPNPDDDLAIFE	146
Hendra	AVIIDVGSMLNGIP--VMERRGDKAQEEMEGLMRILKTARESSKGGKTPFV	146
Nipah	AVIIDVGSVMVNGIP--VMERRGDKAQEEMEGLMRILKTARDSSKGGKTPFV	146
Human	IDRVEITGFENNSFRVIPDARSTMSRGEVLAFAEALAEIDPDLNHNQTPFV	148
Simian	IDRVEITGFEGRSFRVVPDARSTMSRAEVLAYEAIAEDIPTLNHNKTPFV	148
Parainfluenzavirus	IERVEIDGFEEGFSFRLIPNARSGMSRGEINAYAAALAEIDLPTLNHNATPFV	148
Mapuera	IERIEIEGFAPDSFKLIINERSSMTQEEINSLDFMARELPKGFQKTVYL	148
Porcine	IERVEINGFVDGTWRLLIPNDRAILPDATNALNVADELPPDLVNRTPFV	148
Mumps	IERCEIDGFEPGTYRLIPNARANLTANEIAAYALLADDLPPTINNGTPFV	148
Menangle	IERLEIDGFEPGTFRLRANARTPMTNGEVTALNLMAQDLPTYSNDTPFL	148
Tioman	IERIEVDGFEPGTYRLRNPARTPLTNGEITALSMLANDLPDITYNDTPFT	148
Newcastle	LAVLEIDGFANG--MPQFNRRSGVSEERAQRFAMIAGSLPRACNSNGTPFV	146
Fer-de-lance	ISTYITITEFSGMGPVLMNRDQ-----VEEFMTNKLNDLIRVIKFPDLFV	141
Sendai	VVIYINIEKDKPKRTKTDGFIKTRDMEYERTTEWLFQPMVNKS--PLFQGG	148
110.....120.....130.....140.....150	



Beilong	ESDYVKIIPRSIEDLQIAIQIVTAQLWILLTKAVTAIDTARDSENRRRWIK	196
J-virus	RQEYQELCPKSTEELQLCVQSITTLQWILLTKAVTAIDTARDSSEKRRWGK	196
Measles	NKEISDIEVQDPEGFNMLIGTILAQIWVLLAKAVTAPDTAADSSELRRWIK	198
Rinderpest	NREIQDIEVQDPEGFNMLLATILAQIWILLAKAVTAPDTAADSSELRRWVK	198
Dolphin	NKEIIEVQDPEEFNILLASILAQIWILLAKAVTAPDTAADSSETRRWIK	198
Peste-des-petits-ruminants	NREIIDIEVQDPEEFNMLLASILAQVWILLAKAVTAPDTAADSSELRRWVK	198
Canine	NKDIDVIEVDDAEQFNILLASILAQIWILLAKAVTAPDTAADSSEMRRWIK	198
Mossman	ESEAWRQDDMPMDEFLVANMTVQVQLWTLLIKAVTAPDTARDGEQRRWLK	196
Tupaia	DPELGDYSDITQDEYQAMITITITIQWILLTKAVTAPDTAHDSEQRFFIK	196
Hendra	DSRAYGLRITDMSTLVSAVITIEAQIWILLAKAVTAPDTAESETRRWAK	196
Nipah	DSRAYGLRITDMSTLVSAVITIEAQIWILLAKAVTAPDTAESETRRWAK	196
Human	NNDVEDDIFDETEKFLDVCYSVLMQAWIVTCKCMTAPDQPPVSAK-MAK	197
Simian	NADVEQGDYDETEGFLELCYSVLMQAWIVTCKCMTAPDQPPVSAK-MAK	198
Parainfluenzavirus	DSEVEGTAWDEIETFLDMCYSVLMQAWIVTCKCMTAPDQPAASIEKRLQK	198
Mapuera	NVDAEGLVCDEVEQFLDRAYTVLLQVWILACKCMTAYDQPAASIKKRTDK	198
Porcine	VQGGEDLPCDEVEIFLQRAYSVLIQAWIMVCKCMTAYDQPAASIEHRIAK	198
Mumps	HADVEGQPCDEIEQFLDRCYSVLIQAWVMVCKCMTAYDQPAASADRRFAK	198
Menangle	NPNTETEQCDEMEQFLNAYSVLVQVWVTVCKCMTAHDQPTGSDERRLAK	198
Tioman	NHRAEGENCDETEQFLNAYSVLVQVWVTVCKCMTAHDQPTGSDERRLAK	198
Newcastle	TAGAEDDAPEDITDILERILSIQAQVWVTVAKAMTAFETANESKTRRIIK	196
Fer-de-lance	RSNKADALFNGPVEFKVALNSILIQVWVLLAKSITASNTAEGSEDRRTER	191
Sendai	RDAADPTLLQIYGYPAICLGAIIQVWVIVLVAITSSAGLRKGFNRLEA	198
160.....170.....180.....190.....200	



Beilong	YEQRRADADYRLDEGWLNFARVRIAADLAVRRYMVEILLIDANRAPSPKA	246
J-virus	FLOQRRALEEYQLVDAWLDRARVRVASDLAIRRYMITILLETKGKMTGPKP	246
Measles	YTQQRVVGFEFRLERKWL DVVRNRIAEDLSLRRFMVALILDIKRTPGNKP	248
Rinderpest	YTQQRVIGFEFRLDKGWLDTVRNRIAEDLSLRRFMVALILDIKRTPGNKP	248
Dolphin	YTQQRVVGFEFRLDKGWLDAVRNRIAEDLSLRRFMVALILDIKRTPGNKP	248
Peste-des-petits-ruminants	YTQQRVVGFEFRLDKGWLDAVRNRIAAGGLFLRFMVSLILDIKRTPGNKP	248
Canine	YTQQRVVGFEFRMNKIWL DIVRNRIAEDLSLRRFMVALILDIKRSPGNKP	248
Mossman	FVQQRVRESFYKLTVMMDRARMHIAASLSIRRYMVKTLIEIQRMGQKKG	246
Tupaia	YLOQRKAYAAFKFTTIFTERVRRKIAQSL SIRKFMV SIMLEVRKSGSAKG	246
Hendra	YVQQRVNPFFALTQQWLTEMRNLLSQSLSVRKFMVEILMEVKKGGSAKG	246
Nipah	YVQQRVNPFFALTQQWLTEMRNLLSQSLSVRKFMVEILLIEVKKGGSAKG	246
Human	YQOQGRINARVYLQPEAQLIQNAIRKSMVVRHFMTYELQLSQRSLLAN	247
Simian	YQOQGRINPRFILQPEARRIIQNNAIRKAMVVRHFMTYELQMAQSKTLLAN	248
Parainfluenzavirus	YRQOGRINPRVYLLQPEARRIIQNNAIRKGMVVRHFMTFELQLARAQSLVSN	248
Mapuera	YKQOGRFLATYTLQAQAQATLQNVIROSLIVRQFMAYELQTSRHHQGTITN	248
Porcine	YRQOGRLEARVYLQPEAQLIQNAIRKSMVVRHFMTYELQLSQRSLLAN	248
Mumps	YQOQGRLEARYMLQPEAQLIQNAIRKSMVVRHFMTYELQLSQRSLLAN	248
Menangle	YQOQGRILDQRYALQPELRRQIQTCIRSLTIRQFLTHELQ TARKQGAITG	248
Tioman	YQOQGRILDQRYALQPELRRQIQACIRGSLTIRQFLTHELQ TARKQGAITG	248
Newcastle	YLRQGRVQKVIYLPVCRNTIQLTIRQSLAVRIFLVSSELKRGNTAGGTS	246
Fer-de-lance	FEQEGRIASIVYELSKNMKKRLRETLRKHMIKKTMV SIMQESVAMGSNGG	241
Sendai	FRDGTGTVK GALVFTGETVEGIGSVMRSQQSLVSLMVETLVTMNTARSDLT	248
210.....220.....230.....240.....250	



Beilong	RVLELICDIGNYISEAGLAGFHLTIKYGIETRYPALALNELQADLGTILA	296
J-virus	RVVELIADIIGNYISETGMAGFFLTIKYGIETKYPVLAMSEFAADLATVLS	296
Measles	RIAEMICDIDTYIIVEAGLASFILTIKFGIETMYPALGLHEFAGELSTLES	298
Rinderpest	RIAEMICDIDTYIIVEAGLASFILTIKFGIETMYPALGLHEFAGELSTIES	298
Dolphin	RIAEMICDIDTYIIVEAGLASFILTIKFGIETMYPALGLHEFAGELTTVES	298
Peste-des-petits-ruminants	RIAEMICDIDNYIIVEAGLASFILTIKFGIETMYPALGLHEFAGELSTIES	298
Canine	RIAEMICDIDNYIIVEAGLASFILTIKFGIETMYPALGLHEFAGELTTIES	298
Mossman	RLLEVIADIIGNYIEESGLAGFQLTIRFGIETKYAALALNEFQGDIA TIER	296
Tupaia	RISECIADVSAIIEEAGLSGFILTLKYGITRFPVLALNAFQSDL SVIRN	296
Hendra	RAVEIISDIGNYVEETGMAGFFATIRFGLTRYPALALNEFQSDLNTIKG	296
Nipah	RAVEIISDIGNYVEETGMAGFFATIRFGLTRYPALALNEFQSDLNTIKS	296
Human	RYYAMVGDIGKYIEHSGMGGFFLTLKYGLGTRWPTLALAAFSGELQKLKA	297
Simian	RYYAMVGDVIGKYIEHSGMGGFFLTLKYGLGTRWPTLALAAFSGELQKLKA	298
Parainfluenzavirus	RYYAMVGDVIGKYIENCGMGGFFLTLKYALGTRWPTLALAAFSGELTKLKS	298
Mapuera	RYYALVGDIGKYIENAGMSAFFLTIKYALGTRWQPLALAAFSGELTKIKS	298
Porcine	KYYAIVGDIGKYIENAGLSAFFLTVKFAFGTKWQPLALSAFSGELTKLKS	298
Mumps	RYYAMVGDIGKYIENSGLAFFLTLKYALGTKWSPSLAAFTGELTKLRS	298
Menangle	KYYAMVGDIGKYIDNAGMSAFFMTMRFALGTRWPPALALAAFSGELLKLS	298
Tioman	RYYAMVGDIGKYIDNAGMSAFFMTMRFALGTRWPPALALSAFSGELLKLS	298
Newcastle	TYYNLVGDVDSYIRNTGLTAFFLTLKYGINTKTSALALSSLSGDIQKMKQ	296
Fer-de-lance	ELVKTI AVISHYVVNAGLTGFFQTIKYGINTRSAALAVSDIQAE LGKIK A	291
Sendai	TLEKNIQIVGNVIRDA GLASFMTIKYGVETKMAALTLNLRFPDINKLRS	298
260.....270.....280.....290.....300	



Beilong	LMKCYVELGERAPFMVILEDSVQTKFSPGSYPLLWSYAMGVGSMLDRAVN	346
J-virus	LMKMYTTLGKAPYMVILEESIQTGFAPGNYPILWSYAMGVASVLDRSVS	346
Measles	LMNLYQQMGETAPYMVILENSIQNKFSAGSYPLLWSYAMGVGVELENSMG	348
Rinderpest	LMNLYQQMGELAPYMVILENSIQNKFSAGAYPLLWSYAMGVVKLKNSMG	348
Dolphin	LMNLYQQMGETAPYMVILENSIQNKFSAGSYPLLWSYAMGVGVELENSMG	348
Peste-des-petits-ruminants	LMTLYQQLGAVAPYLVILENSIQNKFSAGAYPLLWSYAMGVGVELENSMG	348
Canine	LMMLYQQMGETAPYMVILENSIQNKFSAGSYPLLWSYAMGVGVELENSMG	348
Mossman	LMKLYLELGPAPFMVILEDSIQTRFAPGNYPPLLWSYAMGVGSALDRAMA	346
Tupaia	LIDLYKSMGTIAPFMVLIEDATQVKFAPGNYSLLWSFAMGVGTALDHAMN	346
Hendra	LMLLYREIGPRAPYMVILEESIQTGFAPGGYPLLWSFAMGVATTIDRSMG	346
Nipah	LMLLYREIGPRAPYMVILEESIQTGFAPGGYPLLWSFAMGVATTIDRSMG	346
Human	LMLHYQSLGPMAYMALLESPKLMDFVPSYPLDYSYAMGIGTVLDTNMR	347
Simian	LMLHYQSLGPMAYMALLESPKLMDFAPEYPLMYSYAMGIGTVIDTNMR	348
Parainfluenzavirus	LMALYQTLGQARYLALLESPHLMDFAAANYPLLWSYAMGIGTVLVDNMR	348
Mapuera	LMMLYRDLGENARYLALLEAPQMMEFAPANYPLLWSYAMGIGTVLDAQMR	348
Porcine	LMMLYRDLGQARYLALLEAPQAMDFAPANYPLIYSYAMGIGTVLDPQMR	348
Mumps	LMMLYRDLGQARYLALLEAPQIMDFAPGGYPLIFSYAMGVGTVLDVQMR	348
Menangle	LMQLYRSLGDRARYMALLESEMMEFAPANYPLCYSYAMGIGSVQDPMMR	348
Tioman	LMQLYRNLGKARYMALLEPEMMEFAPANYPLCYSYAMGIGSVQDPMMR	348
Newcastle	LMRLYRMKGDNAPYMTLLGSDQMSFAPAEYAQLYSFAMGMASVLDKGTG	346
Fer-de-lance	LMQLYKKKGENAPYMVILDDSDASYFAPAAYPMIWSFAMGYGTAVDTALA	341
Sendai	LIDTYLSKGPAPFICILKDPVHGFEFAPGNYPALWSYAMGVAVVQNKAMQ	348
310.....320.....330.....340.....350	



Beilong	NLNRYARNYLEQPFYNLGVGMVEKMEGSVNRHVAEELGLTGEQIAQIKDLV	396
J-virus	NLNRYTRYLENAFFRLGESMVQNMGFTVKNKAEDLGFSEEQVAAVREIL	396
Measles	GLNFGRSYFDPAYFRLGQEMVRRSAGKVSSTLASELGITAEADARLVSEIA	398
Rinderpest	GLNFGRSYFDPAYFRLGQEMVRRSAGKVSSENLAELGITEEEARLVSEIA	398
Dolphin	GLNFGRSYFDPAYFRLGQEMVRRSAGKVSSSLAAELGITAEADAKLVSEIA	398
Peste-des-petits-ruminants	GLNFGRSYFDPAYFRLGQEMVRRSAGRVSSVIAAELGITAEAAKLVSEIA	398
Canine	GLNFGRSYFDPAYFRLGQEMVRRSAGKVS SALAAELGITKEEAQLVSEIA	398
Mossman	NLNFNRSYLDYGYFRLGYRIVRQSEGSVDRMARELGITDEEQQLRRLRV	396
Tupaia	NLNINRDYLEPSYFRLGQEVVRLSESTVDRSMAQELGIDPTESEDLIMRAV	396
Hendra	ALNINRGYLEPMYFRLGQKSARHHAGGIDQNMANKLGLNSDQVAELAAAV	396
Nipah	ALNINRGYLEPMYFRLGQKSARHHAGGIDQNMANKLGLNSDQVAELAAAV	396
Human	NYAYGRSYLNPQYFQLGVETARKQQGAVDNRTAEDLGMTAADKADLTATI	397
Simian	NYAYGRSYLNPQYFQLGVETARKQQGAVDNRTAEDLGMSQADKVELAATL	398
Parainfluenzavirus	NYAFSRSYMNKTYFQLGMETARKQQGAVDMRMAEDLGLTQAEERTEMANTL	398
Mapuera	NYKYGRDFLNPVFFQFQGVETARKQQSAVDVKMAAELGVTITDKEEMAQTL	398
Porcine	NYNFARPFNLNAMYFQFQGVETARRQQGAVDTKMAEELGLTQADKQEMTETL	398
Mumps	NYTYARPFNLNGYFQIGVETARRQQGTVDNRVADDLGLTPEQRTEVTQLI	398
Menangle	NYTFARPFNLNAMYFQFQGVETANRQQGSVDKAMAAELGLTEDEKRDMSAAV	398
Tioman	NYTFARPFNLNAMYFQFQGVETANRQQGSVDKMAEELGLTEERRDMSATV	398
Newcastle	KYQFARDFMSTSFWRLLGVEYQAQGSINEDMAAELKLTAAARRGLAAAA	396
Fer-de-lance	GVNRYNRSFLDSKWFAGKMAVESGSKVNVGMLKTLGLTEQQGQTLATIL	391
Sendai	QYVTGRITYLDMEMFLLGQAVAKDAESKITSALEDELGLTDTAKGRLRHHL	398
360.....370.....380.....390.....400	



Beilong	KQEAHSGAVPKHTSRITGVGSAKFNPAASVDELI	PSDEDNQDDDDATTSYG	446	
J-virus	KSEANMNSNGPQGPKANQSS	TKSLDIKNADSIIPESDDETDAPEDVKARL	446	
Measles	MHTTEDKISRAGVPRQAQVSFLHGDQSENEL	PRLGGKEDRRVKQSRGEAR	448	
Rinderpest	AYTGDDRNRTSGPKQAQVSFLRTDQGGETQNN	ASKRDEARAPQIRKEAR	448	
Dolphin	AQANDDRANRAIGPKQNQISFLHPDRGDAST	PGNILRANEQDGGSTR-MKR	447	
Peste-des-petits-ruminants	SQAGDERTARGTGPRQAQVSFLQHKTGE	GESSAPATREGVRAAIPNGSEE	448	
Canine	SKTTEDRTIRTAGPKQSQITFLHSE	RSEVNTNQPPPTINKRSENQGGDKYF	448	
Mossman	ADLGNRGSSEAAAYQGGAFQLANI	QDFENDDAFAANPQAPRNRRNR	446	
Tupaia	QAAGVGSRDPAARTRGRFQVADIQIDE	GPVDLATEAEDQTTKDNEQRIK	446	
Hendra	QETS	VGQDNMQAREAKFAAGGVLVGGGEQDIDEEEP	PIEHSGRQSVTF	446
Nipah	QETS	AGRQESNVQAREAKFAAGGVLVGGSDQDIDEGEEP	PIEQSGRQSVTF	446
Human	SKLSLSQLPRGRQPI	SDFAGANDREMGGQAND-----	TPVYNFNPIDT	441
Simian	AKLTI	GGGRGRQLDDPFAGAAGDYQGAAGG-----	AQGFYASRRV	442
Parainfluenzavirus	AKLTTANRGADTRGGVNF	SSVTGTTQVPAAT-----	GDYLESYMAAD	442
Mapuera	TRLGAARRDASAYAATP	SGPAQQAQAMPAPQAIDS--	RDSTAQPAAP	445
Porcine	NRLGAAGARGAAPAA	PNPFNAAPPAPAPIPVAQPAQDGP	-HDNAAAAAPAP	447
Mumps	DRLARGRGAGIPGGV	PNPVPVQQQQPAAYEDI	PALEESDDDGDEDGG	448
Menangle	TRLTTGRGGNQAQELINVMGARQGRDQ	RRGNR-----	DYDVVEENE	440
Tioman	TRLTTGRGAGQAQD	MINIMGARQAAGGRGAQGR-----	ALRIVEEDE	440
Newcastle	QRVSEENSSIDMPT	QVLTGLSEGGSQLQG-----	GSNRSQG	436
Fer-de-lance	EESKDARAAMISGIS	SSNIKDGESFELEPNMSP-----		425
Sendai	ANLSGGDGAYRKPTGGG	AIEVALDNADIDLETKAHADQ	DARWGGDSGER	448
410.....420.....430.....440.....450			

Beilong	KP-----YR	PQIELAEK	PDSVP	INEHLARKYADAD	T	DAMRGQVAGILRK	490
J-virus	DA-----EKEASR	KKREASMRKRQSKQDKSRADST	I	RDIEDELNDIISK			490
Measles	ES-----YRET	GPSRASDARAHLPTGT	PLDIDTATESSQD	PQDSRRSA			492
Rinderpest	TS-----SKSDKY	KEDTDKEPMS	PSVKTLIDVDTT	PEVDTDPLGSKKSA			492
Dolphin	GG-----NIAT	PKGTSIDQTSTT	LSKDT-LDIDEQSDNTDD	FISIQKSA			490
Peste-des-petits-ruminants	RD-----RKQTR	PGRPKGETPGQLL	PEIMPEDEV	PRESGQNPREAQRSA			492
Canine	IH-----FNDR	FPGYTPDVNSSEWSESRYD	TQTIQDDGND--	DDRKSM			490
Mossman	GQPD----QGDDDD	SDEGDDQGGSGYAAAVHAVLHSS	GDGGDDLTS	GADG			492
Tupaia	VDPD----RGSIG	SNAQFQPPKPLRGRVMP	PERKPTDQK	NLQDQRP			492
Hendra	KREMS	SLADSV	PSSSVSTSGG	TRLTNSLLNLRSLAAKA	IKESTAQSS		496
Nipah	KREMS	ISSLANSVP	PSSSVSTSGG	TRLTNSLLNLRSLAAKA	AKEAASSNA		496
Human	RRYD----NYDS	GEDRIDNDQQAIRENR	GEPGQP	PNNQTS	SDNQQRFP	PP	487
Simian	RKYN----DYES	DEEAGMDDDYEQEAREGR	GYDDDDARQ	IGGQSG	FDFS		488
Parainfluenzavirus	RLRQ----RYAD	A-----	THDEM	PLEEEEEED	TSAGPRTG-----	PT	478
Mapuera	DPVP----DDS	-----	FSSKYQSYLIMQEKMKD	PALIDGIR---	ANLLS		482
Porcine	APGA----DAP	PGPAGLHIP	PGPEPGFEP	QEYYRQPG	MMDMVK---	NRLRI	490
Mumps	AGFQ----NGAQ	APAAARQGGQ	NDFRVQPLQDF	PIQAQLF	PLYPQVSNIP	N	494
Menangle	ETES----DSDN	DEEQEIQNRPLPP	IPQMPQ	NIDWEVR-----	LAE		477
Tioman	TTDD----ESVDD	QADDIQGRPLPPV	PAP	IREIDWEAR-----	IAE		477
Newcastle	QPEA----GDGK	TQFLDLMGAVANS	MREAPNSA	QGT	PQ-----		470
Fer-de-lance	-----	SIYSESTTKLDRIK	LAK	EVRETAITAED	NI	G-----	458
Sendai	WAR----QVSG	GHFVTLHGAER	LEETNDEDV	SDIERIAMRLA	ERRQE		493
460.....470.....480.....490.....500						

Beilong	-----ERKKKKHSENA--PGVVLPSQSTG	514
J-virus	-----TKNLSSKPKGSS--NTTDTFKQSDM	514
Measles	-----DALRLQAMAGISEEQGSDTTPIVY	518
Rinderpest	-----EALIRLQAMASILEDSTLGNDSPRAY	518
Dolphin	-----EALAKMRAMAKLLENQGPRDVTAHVY	516
Peste-des-petits-ruminants	-----EALFRLQAMAKILEDQEEGEDNSQVY	518
Canine	-----EAIAKMRMLTKMLSQPGTSEESSPVY	516
Mossman	-----SIDPPTSGLGANRYRSPGLNDSKPKF	518
Tupaia	PSATPRLTKDAEDNIDQLFAQYDSGVAAPEDVTLVTSSTSPARSSGTG	542
Hendra	-----SERNPNNRPQADSGRKDDQEPKPAQ	522
Nipah	-----TDDPAISNRTQGSEKKNNQDLKPAQ	522
Human	IPQRTSGMSSEEFQHSMNQYIRAMHEQYRGSQDDDANDATDGNDISLELV	537
Simian	VPQRAPGMSDEEFQAQMTKYIQHVQQHYQEAQEGAEDGGYNQTTDDQGAG	538
Parainfluenzavirus	LEQVALDIQN-----AAVGAPIHTDDLNAAL	504
Mapuera	DPNCPEDISASDLQGAVERYVHEVIERVQQGDTYGIWPSAGATAAEDAI	532
Porcine	ASGGAPGVLPHELDAAAQIYVDEVVTGLRRPNDFAGILEAMFQQLAEEQK	540
Mumps	HQNHQINRI GGMEHQDLLRYNENGDSQQDARGEHGNTFPNNPNQNAQSQV	544
Menangle	IERNQQMAARDRPAVVT-----ADVHQEPADARVDEQDML	514
Tioman	IEEQGQMRDQGVGRLVN-----QAPNVQNTFRQNTQDNQAL	514
Newcastle	-----SGPPPTLGFSQSNQTD	486
Fer-de-lance	-----SLDDESKVI	467
Sendai	-----DSATHGDEGRNNGVDHDEDDTAAV	518
510.....520.....530.....540.....550	


Beilong	GDSLVIDS--	522
J-virus	SDLSAING--	522
Measles	NDRNLLD---	525
Rinderpest	NDRDLLS---	525
Dolphin	NDKDLG---	523
Peste-des-petits-ruminants	NDKDLG---	525
Canine	NDRELLN---	523
Mossman	NDADLLGLGD	528
Tupaia	SDMDLINQSP	552
Hendra	NDLDFVRADV	532
Nipah	NDLDFVRADV	532
Human	GDFDS-----	542
Simian	GDFDT-----	543
Parainfluenzavirus	GDLDI-----	509
Mapuera	GDFQS-----	537
Porcine	GDLED-----	545
Mumps	GDWDE-----	549
Menangle	LDLDM-----	519
Tioman	LDLDI-----	519
Newcastle	WGY-----	489
Fer-de-lance	AGMS-----	471
Sendai	AGVGGI-----	524
560	



B Complete sequence alignment of paramyxoviral V proteins


Beilong	---MSDYNPDVLOQLVKDG-----IKTIELLQOSPEDFQKTYGRSAIQ	40
J-virus	---MNSYSVQALEQLVNDG-----IKTAQFFQKNQENIQKTYGRSAIG	40
Hendra	-----MDKLDLVNDG-----LDIIDFIQKNQKEIQKTYGRSSIQ	34
Nipah	-----MDKLELVNDG-----LNIIDFIQKNQKEIQKTYGRSSIQ	34
Human	-MAEETPTYTEQVDELHAG-----LGTVDFFLSRPIDAQSSLGKGSIP	43
Simian	-MAEETPTTAEQVNDVHAG-----LGTVDFFLSRPVDGQSSLGKGSVP	43
Parainfluenzavirus	MDPTDLSFSFDEINKLIETG-----LNTVVEYFTSQQVGTSSSLGKNTIP	44
Mumps	---MDQFIKQDEITELLETG-----MNVANHFLSAPIQGTNSLSKATII	41
Menangle	---MDNPPSDAEISAWIDKG-----LDTVEHFSLVATDPARSLGKSTIK	41
Tioman	---MDPSPSDAEISAWIDKG-----LDTVEHFSLASTQSVRSLGKSTIK	41
Mapuera	---MDLTFSPSEIDDLFGTG-----LDTIQFITDQKSKQNDAGHSAKDS	41
Porcine	MASSSLFSFDGEITELLETG-----LGTIESIERMVAAKGGVDDGGIDPE	44
Measles	-MAEEQARHVKNGLCEIRALKAEPISLAIEEAMAAWSEISDNPGQERAT	49
Rinderpest	-MAEEQAYHVKNGLCEIKALRARPLDPLVVEEALAAWVETSEGQTLDRMS	49
Peste-des-petits-ruminants	-MAEEQAYHVKNGLCEIKSLKASPPDLSTIRDTIESWREGLSPSGRATPN	49
Dolphin	-MAEEQAYHVKNGLCEIKSLRENPPDAVEIKEAQIIRSKAACGESSESHH	49
Canine	-MAEEQAYHVSKGLECKALRENPPDIEETQEVSSIRDQTRNPSQANGTA	49
Newcastle	---MATSTDAETDDTLETSG-----TVIDSIIITAQKSAETVGRSAIP	40
Fer-de-lance	---MANFNGFEASSLIDQGLDDIEAIGQMT CIRPSEESPYVEIPDTGIV	46
Tupaia	MNNTETIENASKVLEAIDAAKEE--ELRNLSLIVQPRAPLNAGSTPGEII	48
Mossman	-METNCQDKIKNALQILAVAKETQ--SPKSEELRERLDISGVTTTASTD	47
Sendai	--MDQDALISKEDSEVEREASGGRESLSDVIGFLDAVLSSPEPTDIGGDRS	48

1.....10.....20.....30.....40.....50



Beilong	EPSTRARIQSWESRNPDHDYTGKNKNQRSEGAKERANKSESAGTASADGGH	90
J-virus	LPTTKERISAWEAVAETPYGEQIQLGGGNGEDQRGEQAEQDNPPGGHGHG	90
Hendra	QPSIKDRTRAWEDFLQSTSGEHEQAEGGMPKNDGGTEGRNVEDLSSVTSS	84
Nipah	QPSIKDQTKAWEDFLQCTSGESEQVEGGMSKDDGDVERNLEDLSSTSP	84
Human	PGVTAVLTSAAEK-SKPVAAAGPVKPRR---KKVISNTTPVTIADNIPPE	89
Simian	PGITAVLTNAAEK-AKTAAPVVKPKR---KKIQHMTPAVTIADNGDPN	89
Parainfluenzavirus	PGVTGLLTNAAEAK-IQESTNHQKGSVG---GGAKPKKPRPKIAIVPADD	90
Mumps	PGVAVPLIGNPEQKNIQYPTASNQGSKS---KGRGSGARPTMVS---SSE	85
Menangle	PGKTQELIRSAEKLAGAVVQGGEGKDRD---NAKKEVTTA-----APE	81
Tioman	PGNTEELVAAAEKVAANTAKGILSGVRC---TNPDPATR-----PK	79
Mapuera	PPQTQNGPDSGSPDPTQVQGAK-----PKSHGIYPPIPTAPPVPT	81
Porcine	SQPGQRLPTPTPTRTTSTPTAAGSASATLELSPEGGAIKKAPRAHPTLPN	94
Measles	CREEKAGSGLSKPCLSAIGSTEGGAPRIRGQGPGE--SDDAETLGIPT	97
Rinderpest	SDEAEADHQDISKPCFPAAAGPGKSSMSRCHDQGLRG--SNSCDEELGAFI	97
Peste-des-petits-ruminants	PDMSEGDHQINQPCSPAIGPNKVYLSPEDNLGFREITSNDYEAELGGVQ	99
Dolphin	QDNEKDLDFDESCSSAIRPETYRMLLGGDTGFRAPGYIPNEGEP--EP	97
Canine	SMQEEVVSQDLDESHEPAKGSNYVGHVLQNNPSSGE--SNALVEAEQPA	97
Newcastle	QGKTKALSTAWEKHGIAQPHASQDNPDQ---QVRLDKQSSPEQVTPHNT	87
Fer-de-lance	PGIVGKAIGEIESKTINGDHTSAPTPHN---TIKGNADKVKKSGETIPD	92
Tupaia	NEIKHLSLRD-QEGGTSKDEEESGAGRTVAEGAATRDHKVSKSRPKKQP	97
Mossman	TVEAESQDRSEKEPGSGRSGEEQQSSASSSSVGFQTQYAEQDGDGVSDGGA	97
Sendai	WLHNTINLQRPGPSSTRAKGEGEGEVSTSSQTQNRSGEESVGGTSEPE	98

.....60.....70.....80.....90.....100



Beilong	GDKP SNNGGDSQNEYQGS SDQVWDAAYNDGNSGGAWGGPTGGLPTAGERG	140
J-virus	GEEIPTGANPSALQLQGSYNQVWDGPNVATYSGGE-GGDTGNQHGRTDSG	139
Hendra	DGTIGQRVSNTRAWAEDPDDIQLDPMVTDVVYHDHGGECTGHGPPSSSPER	134
Nipah	DGTIGKRVSNTRDWAEGSDDIQLDPVVTDVVYHDHGGECTGYGFTSSPER	134
Human	KLPINTPIPNPLLP LARPHGKMTDIDIVT-----	118
Simian	RLPANPIANPLIPIERPPGRMTDLDLAT-----	118
Parainfluenzavirus	KTVPGKPIPNPLLGLDSTPSTQTVLDSLGS-----	119
Mumps	GGTGGIQIPEPLFAQTGGGIVSTVYQDP-----	114
Menangle	PAVRGKVRPIDVEPSDNTYEEVIPSNSK-----	110
Tioman	EKQKGS PVKMQHQEQESVYEEV IPTESAP-----	108
Mapuera	ARHPGSRVDDPVLVDYPRRGKVTTHEPKE-----	110
Porcine	PLGQEEFPGNPLSTFTFVRGSSSTHDPLP-----	123
Measles	RNLQASSTGLQCYVVDHSGEAVKGIQDADSIMVQSGLDGDSTLSGGDNE	147
Rinderpest	GDSSMHSTE VQHYHVYDHSGEKVEGVEDADSLVQSGADDGVEVWGGDEE	147
Peste-des-petits-ruminants	G--KGSNSQVQRYYVYSHGEEIEGLEADADSLVVQADPPVANIFNGGEDG	147
Dolphin	GDIGKEEFVAVRCYHVYDHGGQAVEGVKDADLLVVPTGSDDDAEFRDGDSE	147
Canine	KDDIQPGPGIRCYHVYDHSGEVVKI EDADSLVVPAGAVSNRGFEGGEGS	147
Newcastle	PLVTPTEFSPPTQATGEAGDTQLKTGASNS-----	116
Fer-de-lance	KAEEPQPVQQDRSKVKESNITMNP-----	117
Tupaia	RSGLQGAAGKNPTPDGEGGDTCNRELDQHSDDGHSNTEGASSDLASIQ	147
Mossman	NGSISR VFYSTVCENNPDES LGRSSCYVMLGKAGGIEPVNTAGDREEST	147
Sendai	AEA HARNVDKQNIHWATGRGASTDSVPQDLGNRDSGILEDFPNEG GYPR	148
110.....120.....130.....140.....150	

Beilong	-----	140
J-virus	-----	139
Hendra	GWSYHMSGTHDGNVRAVPDTKVLPNAPKTTVPEEVREIDLIGLEDKFASAG	184
Nipah	GWSDYTS GANNGNVCLVSDAKMLSYAPEIAVSKEDRETDLVHLENKLSTT	184
Human	-----	118
Simian	-----	118
Parainfluenzavirus	-----	119
Mumps	-----	114
Menangle	-----	110
Tioman	-----	108
Mapuera	-----	110
Porcine	-----	123
Measles	-----	147
Rinderpest	-----	147
Peste-des-petits-ruminants	-----	147
Dolphin	-----	147
Canine	-----	147
Newcastle	-----	116
Fer-de-lance	-----	117
Tupaia	P-----	148
Mossman	R-----	148
Sendai	SCAEDENREMAANPDKREGEDQAEG-----	172
160.....170.....180.....190.....200	

Beilong	-----YPITTC-NQEFEGYHPDGPVDARE	163
J-virus	-----SAADTGGSNQSDGSSYSTVDAGD	163
Hendra	GLNPAAVPFVFKNQSTPTTEPPVPIEYYYSGRRGDLSKSPFRGNVNLDS	234
Nipah	GLNPTAVPFILRNLSDPKADSPVIAEHYYGLGVKEQNVGPQTSRNVNLDS	234
Human	-----	118
Simian	-----	118
Parainfluenzavirus	-----	119
Mumps	-----	114
Menangle	-----	110
Tioman	-----	108
Mapuera	-----	110
Porcine	-----	123
Measles	-----	147
Rinderpest	-----	147
Peste-des-petits-ruminants	-----	147
Dolphin	-----	147
Canine	-----	147
Newcastle	-----	116
Fer-de-lance	-----	117
Tupaia	-----CQTDDA	154
Mossman	-----SN	150
Sendai	-----LPEEIRRSAPLPDEGEGRADNNGRGVESCSPHSARVTIGVLV	213
210.....220.....230.....240.....250	

Beilong	YNQISSMDHEMS---AAETLGSSTQLTMRNATDDFAKIFEEGTPKVH	209
J-virus	LRQMMIFDHEHS---AIEVGASKNNTMKIRNATEEDLGNVMSEGTSKIH	209
Hendra	IKIYTSDEEDENQLEYEDEFAGSSSEVIDTTPEDNDSINQEEVVGDFSD	284
Nipah	IKLYTSDEEADQLEFEDEFAGSSSEVIVGISPEDEEPSVGGKPNESIG	284
Human	-----GNITEGSYKGVELAKLGKQTLTTRFTSNEPVSSA	152
Simian	-----GTVTQGTYKGVELAKAGKNALLTRFSSGSLTDQ	152
Parainfluenzavirus	-----KTLFSGSYKGVKLAIFGKENLMTRFIEEPRENPI	153
Mumps	-----TIQPTGSYRSVELAKIGKERMINRFVEKPRSTPT	148
Menangle	-----LIPPVTPKK---PPRHKDRIMSMMPLQSDKQLT	140
Tioman	-----LIPKTTPKK---PPRNKEKVMMSMALSPPDES	138
Mapuera	-----SSQADGYEYDSYLAQNAKTNILKRWTDVSGDVEP	144
Porcine	-----GSRPGSEVYEGDLMARARSELVTRWSDEEGDPVP	157
Measles	---SENSDVDIGEPDTEGYAITDRGSAPISMGFRASDVETAEGGEIHELL	194
Rinderpest	---SENSDVDSGEPDPEGSAPADWGSSPISPATRASDVETVEGDEIQKLL	194
Peste-des-petits-ruminants	---SDDSDVDSGPDPPGRDTLYDRGSVASNDVARSTDVEKLEGADIQEV	194
Dolphin	---SLESDDGESGTVDIRGNSSSNRGSAPRIKVERSDDVETISSEELQGLI	194
Canine	---LDDSTEDSGEDYSEGNASSNWGYSFGLKPDRAADVSMIMEEELSALL	194
Newcastle	-----LLYMLDKLSNKSSNAKKGPKDRPPRRTPPTPGPTTR	152
Fer-de-lance	-----DSSGFKQLFNRDELKINSWKNTIAGSMM	146
Tupaia	PCSSTSYLDEEDEPAVRPKTQCKQSGLIESKEDEDGMLSELHEQHKGRSK	204
Mossman	QLGEDDDAGOSGLTSARALESGTQSDEPVVKPKRKNKKSPPNESAVDENM	200
Sendai	IPSPLEEAVALQRNKRPPANSRSRSLTPVVVPSTRSPPPDHDNSTRSPPR	263
260.....270.....280.....290.....300	



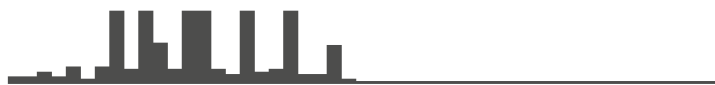
Beilong	RRLRG	-----	214
J-virus	KRLRG	-----	214
Hendra	QGLEHPPFLGKFPEKEETPDVRRKDSLMDSCKRGGVPKRLPMLSEEFEC	-----	334
Nipah	RTIEGQSIRDNLQAKDNKSTDVPGAGPKDSAVKKEEPPQKRLPMLAEFEFC	-----	334
Human	GSAQD	-----	157
Simian	ASSKD	-----	157
Parainfluenzavirus	ATSSP	-----	158
Mumps	VTEFK	-----	153
Menangle	ESMES	-----	145
Tioman	DETHE	-----	143
Mapuera	IPMNP	-----	149
Porcine	TRVLQ	-----	162
Measles	RLQSR	-----	199
Rinderpest	EDQSR	-----	199
Peste-des-petits-ruminants	NSQKG	-----	199
Dolphin	RSQSQ	-----	199
Canine	RTSRN	-----	199
Newcastle	EPVEP	-----	157
Fer-de-lance	NHKDE	-----	151
Tupaia	RLSALG	-----	210
Mossman	REEDIKEAFG	-----	210
Sendai	KPPTTQDEHTNPRNTPAVRIK	-----	284
310.....320.....330.....340.....350		

Beilong	-----	214
J-virus	-----	214
Hendra	SGSDDPITIQELEREGSHPGGS-LRLREPPQSSGNSRNC-PDRQLKTGDAA	382
Nipah	SGSEDPITIRELLKENS LIN CQQGKDAQPPYHWSIERSISDPKTEIVNGAV	384
Human	-----	157
Simian	-----	157
Parainfluenzavirus	-----	158
Mumps	-----	153
Menangle	-----	145
Tioman	-----	143
Mapuera	-----	149
Porcine	-----	162
Measles	-----GNNFPKLGK	208
Rinderpest	-----IRKMTKAGK	208
Peste-des-petits-ruminants	-----RGRFQGGK	208
Dolphin	-----KHNGFGVDR	208
Canine	-----VGIQKRDGK	208
Newcastle	-----	157
Fer-de-lance	-----	151
Tupaia	-----	210
Mossman	-----MNPQFRARRL	220
Sendai	-----DRRPPTGTRS	294
360.....370.....380.....390.....400	

Beilong	--ITAVVPAQKQPGAVGGPVKKGHRREYCIDTFGGRTIIREWCNPOCAPL	262
J-virus	--VAAMTDLPVPRRTGGPVKKGHRREFCIDNFGGKTYIREWCNPOCAPI	262
Hendra	SPGGVQRPPTMPKSRIMP IKKGHRREVSICWDGRRRAWVEWCNPOVCSRI	432
Nipah	QTADRQRPPTMPKSRGIP IKKGHRREISICWDGKRAWVEWCNPOACSRI	434
Human	---PNFKRGGANRERAR----GNHRREWSIAWVGQVRFVFEWCNPRCAPV	200
Simian	---PNFKRGGGEIDGRHK----GRHRREWSIAWVGDEVKVVFEWCNPTCAPV	200
Parainfluenzavirus	---IDFKRGRDTG-----GFHRREYSIGWVGDEVKVFTEWCNPFSCSPI	197
Mumps	---RGAGSGCSRFDNPR----GGHRREWSLSWVQGEVRFVFEWCNPFCSPI	196
Menangle	---QVFKRGKGFETWPKRHRTGGHRREIAIDWIGGRPRVTEWCNPFICHPI	192
Tioman	---AVFKRGSTSTTWPRRHRTGGHRREIASWATGTPRVTEWCNPFICHPI	190
Mapuera	---EVFKRGADLTKPTNPN--PGHRREWSIGWVGSTVKVLEWCNPTCSPI	194
Porcine	---SIFKRGADRKGANPGE--PGHRREYSIGWVCGTVRFVFEWCNPFCSPI	207
Measles	TLNVPPPDPGRASTSGTPIKKGHRREISLIWNGDRVDFIDRWCPMCSKV	258
Rinderpest	TLVVPPPIPSQERPTASEKPIKKGHRREIDLWNGDRVDFIDRWCPMCSKV	258
Peste-des-petits-ruminants	TLRVPEIPDVKHSRPSAQSIKKGHRRELSLIWNGDRVDFIDRWCPMCSKV	258
Dolphin	FLKVPPPIPTSVPLDPAKSIKKGHRREISLIWNGDRVDFIDRWCPMCSRI	258
Canine	TLQFPHNPEGKTRVPECGSIKKGHRRELSLWNGDSCWIDRWCPMCSRI	258
Newcastle	----WKQPGKAAAPGQGRPWKPGHRREHSISWTAEGVTIISWCNPFSCAPV	203
Fer-de-lance	----NKLGRGASSEGRPPSRGHRREISLSTIDGIFEVWFECNPMCSRI	196
Tupaia	---RVNSSIPSPRDELKKGHRREYSMVWSNDGVFIEWCNPMCSRI	256
Mossman	TGLEAAASTLPSIVVHKEQTKRGHRREYNFVWTDGFRVEAWCPMCSRI	270
Sendai	APDRPITDGYPTHGPPETDAIKKGHRREHIIYERDGYIVNEWCNPOVCSRI	344
410.....420.....430.....440.....450	



Beilong	TVTPTQKEKSCGECPRQCARCIDDRGYWPK-----	292
J-virus	TVTPTQSRCTCGECPKVCARCIKDRIYVPK-----	292
Hendra	TPQPRQEQCYCGECPTECSQCCHEE-----	457
Nipah	TPLPRRQEQCCGECPTFCFG-----	456
Human	TASARKFTCTCGSCPSICGEGEGDH-----	225
Simian	TATDRKFSCTCGTCDPRCGEGEDN-----	225
Parainfluenzavirus	TAAARFECTCHQCPVTCSECRDT-----	222
Mumps	TAAARFHSCKCGNCPAKCDQCERDYGPP-----	224
Menangle	SQSTFRGSCRCGNCPCGICSLCERDYTLTDSGSD-----	227
Tioman	SQFTYRGTCTRCGCCPDVCSLCERDYALLADIRDPCES-----	228
Mapuera	TATSRYEVCVCGICPKICPRCVGDYGHVETAGRKDWLSRGGSDSSSRG	244
Porcine	SMEPRYQCTCGTCTPAKCPQCAGDNGIVESNRGP-----HDGAGNES--	249
Measles	TLGTIRARCTCGECPRVCEQCRTDTGVDTRIWHNLPEIPE-----	299
Rinderpest	TVGTVRAKICGECPRVCEQCITDSGIENRIWHNLADIPE-----	299
Peste-des-petits-ruminants	KMGVIRAKCVCGECPQVCGECKDDPGVDTRIWHYSITDSA-----	298
Dolphin	KMGIVRVKCTCGECPVFCDECREDPETPTRIWHYSLPEIPEQWPF-----	303
Canine	NWGIIRAKCVCGECPPTCNECKDDPEMQTRVWYATPSQDLK-----	299
Newcastle	RAEPRQYSCTCGSCPATCRLCAGDDVYDGGIITEGR-----	239
Fer-de-lance	TPDFKPKICVCGECPRYCPRCKEQGGIRVPE-----	227
Tupaia	RPLPIREICVCGRCPLKCSKCLLDPE-----	282
Mossman	RNLPRREKCRCGWCPKECPICALGN-----	295
Sendai	RVISRRELVCVCKACPKICKLCRDDI-----	369
460.....470.....480.....490.....500	



Beilong	-----	292
J-virus	-----	292
Hendra	-----	457
Nipah	-----	456
Human	-----	225
Simian	-----	225
Parainfluenzavirus	-----	222
Mumps	-----	224
Menangle	-----	227
Tioman	-----	228
Mapuera	DCESDQE	251
Porcine	-----	249
Measles	-----	299
Rinderpest	-----	299
Peste-des-petits-ruminants	-----	298
Dolphin	-----	303
Canine	-----	299
Newcastle	-----	239
Fer-de-lance	-----	227
Tupaia	-----	282
Mossman	-----	295
Sendai	-----	369
	

8 Curriculum vitae

Personal data

Full name:	Christian Karl Pfaller
Birth date:	August, 24 th , 1980
Place of birth:	Berching, Bavaria, Germany
Citizenship:	German

Education

2005 – 2009	PhD thesis in the lab of Prof. Dr. Karl-Klaus Conzelmann at the Max von Pettenkofer-Institut & Gene Center, LMU Munich Title of the thesis: <i>"Subversion of Toll-like receptor 7/9 signaling by Measles virus – V holds the key"</i>
2005	Diploma in chemistry at the LMU Munich
2004 – 2005	Diploma thesis in the lab of Prof. Dr. Karl-Klaus Conzelmann at the Max von Pettenkofer-Institut & Gene Center Title of the thesis: <i>"Rekonstituierung der MyD88-abhängigen Induktion von Interferon Alpha in Zelllinien und Modifikation der Signaltransduktion durch virale Proteine"</i>
2000 – 2005	Studies of chemistry at the LMU Munich
1999	Abitur at the Gymnasium Hilpoltstein

Publications

- 2008 Pfaller,C.K. and Conzelmann,K.K. *Measles virus V protein is a decoy substrate for IkappaB kinase alpha and prevents Toll-like receptor 7/9-mediated interferon induction.* J. Virol. 82, 12365-12373.
- 2007 Brzózka,K., Pfaller,C., and Conzelmann,K.K. *Signal transduction in the type I interferon system and viral countermeasures.* (Review) Signal Transduction 7, 5-19.
- 2005 Westerhausen,M., Rotter,T., Pfaller,C., Kneifel,A.N., and Schulz,A. *NMR spectroscopy and crystal structure of [Me2GaP(H)SitBu3]2 and theoretical investigations of the model compounds.* Inorganica Chimica Acta 358, 4253-4260.

Awards

- 2006 – 2008 Scholarship of the Graduiertenkolleg 1202 "Oligonukleotide in Zellbiologie und Therapie" (German Research Foundation, DFG)

Conference Presentations

- 2009 4th IFN workshop "IFN and Infection" in Bern
- 2008 14th International Congress of Virology of the International Union of Microbiological Societies (IUMS) in Istanbul
- 2008 18th Annual Retreat of the German Society for Virology (GfV) in Heidelberg
- 2007 3rd European Congress of Virology & 17th Annual Retreat of the German Society for Virology (GfV) in Nuremberg

Poster Presentations

- 2009 19th Annual Retreat of the German Society for Virology (GfV) in Leipzig